BOTSWANA INTERNATIONAL UNIVERSITY OF SCIENCE AND TECHNOLOGY



Long Range Wide Area Network (LoRaWAN) Propagation Model Performance in Botswana

Author:
Lone Godfrey Future KOLOBE

Supervisor:
Dr. Caspar K. LEBEKWE
DR. BOYCE SIGWENI

A research thesis Submitted to the Faculty of Engineering to a Study leading to a Thesis In Partial fulfilment of the Requirements for the Award of the Degree of Master of Computer and Telecommunication Engineering

September 2, 2021

"If we knew what it was we were doing, it would not be called research, would it?"

Albert Einstein

BOTSWANA INTERNATIONAL UNIVERSITY OF SCIENCE AND TECHNOLOGY

Abstract

Faculty of Engineering and Technology
Department of Electrical, Computer and Telecommunications Engineering

Long Range Wide Area Network (LoRaWAN) Propagation Model Performance in Botswana

by Lone Godfrey Future KOLOBE

Long Range (LoRa) is a leading low power wide area network under the IEEE 802.15.4 designation. The technology has been used extensively in wireless sensor network applications (WSN) and studies are shifting to investigate the technology's viability when used for navigation. However, the problem of planning and deployment of LoRa in navigation as well as the repeatable accuracy of such a system based on known timing errors has not been done.
The first chapter of this thesis presents a background into the LoRa technology and introduce some of the metrics of interest in navigation as well as in WSN applications, in which LoRa has traditionally been used. Additionally, the objectives and problem statement are presented. In the second chapter of the thesis, a closed form of the variance in time of arrival (TOA), a way to determine pseudo-range for LoRa and introduce the sources of error in the ranging function, namely path-loss and noise are derived. Furthermore, the contribution of geometry in the navigation solution is determined. By investigating the contribution of geometry, assessments of the ideal gateway placement technique are performed. The gateway placement techniques under assessment are random placement, naive placement and imaginary triangular tessellation. These gateway placement techniques are then validated statistically against one another using effect size, statistical significance and the Z-statistic.
The findings of this research show that LoRa is viable to use in navigation applications. It was observed through simulations that LoRa is capable of attaining repeatable accuracy below 20m. Moreover, the imaginary tessellation technique is the best placement technique based on statistical analysis as well as practical analysis of the results. It was also determined that the Ericsson 9999 model is able to produce simulation results which are more consistent with experimental findings compared to the COST 231- Walfish Ikagami path-loss model and the free space path-loss model. In conclusion, this work investigated the use of LoRa in a navigation application and found the technology viable. A gateway placement technique which is ideal for navigation, reduces geometry based errors and assured a low horizontal dilution of precision (HDOP) in a desired coverage area therefore increasing the accuracy of the position solution for LoRa was also determined. The work also proposes that LoRa be considered as a signal of opportunity (SoOP) in future works given the documented performance.

Acknowledgements

First and foremost I am extremely grateful to my supervisors, Dr. C.K. Lebekwe and Dr. B. Sigweni for their invaluable advice, continuous support, and patience during my MEng study. Their immense knowledge and plentiful experience have encouraged as well as informed my academic research and daily life. I would like to thank all the members in the department of Electrical, Computer and Telecommunications engineering. It is their kind help, and support that have made my study and life in the BIUST a wonderful time. Finally, I would like to express my gratitude to my parents, my partner and my siblings. Without their tremendous understanding and encouragement over the past two years, it would have been impossible for me to complete my research.

Contents

Abstract ii

Acknowledgements iii

Declaration of Authorship xiii

1 Introduction and Background 1
- 1.1 Background . . . 2
- 1.2 Introduction . . . 3
  - 1.2.1 LPWAN Technology . . . 3
  - 1.2.2 LoRa and LoRaWAN . . . 4
  - 1.2.3 LPWAN Propagation Models . . . 5
  - 1.2.4 Horizontal Dilution of Precision . . . 6
- 1.3 Problem Statement . . . 7
  - 1.3.1 Research Rational . . . 7
  - 1.3.2 Research Goal . . . 7
  - 1.3.3 Research Objectives . . . 8
- 1.4 Masters Thesis Outline . . . 8
- 1.5 Chapter Summary . . . 8

2 Literature Review 9
- 2.1 Low Power Wide Area Networks: The LoRa signal . . . 10
- 2.2 Low Power Wide Area Networks: LoRaWAN protocol . . . 11
- 2.3 Horizontal Dilution of Precision . . . 13
  - 2.3.1 Deriving HDOP . . . 14
  - 2.3.2 Geolocation in LoRa . . . 16
- 2.4 Taxonomy of Propagation Models . . . 22
  - 2.4.1 Statutory Regulations . . . 25
  - 2.4.2 Propagation Metrics . . . 26
- 2.5 Propagation Models for the 915MHz ISM Band . . . 27
  - 2.5.1 Free space pathloss model . . . 27
  - 2.5.2 COST 231- Walfish Ikagami pathloss model . . . 27
  - 2.5.3 Ericsson 9999 pathloss model . . . 28
- 2.6 Systematic Literature Review . . . 29
  - 2.6.1 Research Questions . . . 30
  - 2.6.2 Search Strategy . . . 30
  - 2.6.3 Search Terminology . . . 30
  - 2.6.4 Search Process . . . 31
  - 2.6.5 Results of the Systematic Literature Review . . . 31
    - Intra-scheme metrics of comparison . . . 33
    - LoRa Performance metrics and test-beds . . . 34
- 2.7 Chapter Summary . . . 35

3 Methodology **36**
3.1 Receiver sensitivity analysis . . . 37
3.2 Gateway placement Techniques . . . 40
3.2.1 Random placement . . . 40
3.2.2 Naive placement . . . 41
3.2.3 Placement with imaginary triangular tessellation . . . 43
3.3 Statistical Tests: Statistical significance and Effect size . . . 45
3.3.1 Statistical significance . . . 45
3.3.2 Effect size . . . 45
3.3.3 Simulation Data . . . 46
3.4 Empirical propagation model performance . . . 47
3.4.1 Performance comparison . . . 48
3.4.2 Deployment of the gateways in the coverage area . . . 48
3.5 Chapter Summary . . . 49

4 Results and Analysis **50**
4.1 Receiver Sensitivity analysis . . . 51
4.1.1 Random gateway placement . . . 51
4.1.2 Naive gateway placement . . . 52
4.1.3 Guided HDOP gateway placement . . . 53
4.2 Statistical Analysis of Placement methods . . . 55
4.2.1 Statistical tests:Naive placement VS Random Placement . . . 56
4.2.2 Statistical tests:HDOP guided placement VS Random Placement 57
4.2.3 Statistical tests:HDOP guided placement VS Naive Placement . 58
4.3 Propagation Model Ranking . . . 59
4.3.1 Coverage area Repeatable accuracy . . . 62
4.3.2 Repeatable accuracy summery . . . 62
4.4 Chapter Summary . . . 66

5 Conclusion **67**
5.1 Receiver sensitivity grid . . . 68
5.1.1 Placement technique . . . 68
5.2 Propagation model performance . . . 68
5.3 Research Contributions . . . 68
5.4 Future Work . . . 68
5.5 Chapter Summary . . . 69

A Appendix A **70**
A.1 Effect Size . . . 70
A.2 Statistical significance . . . 71
A.3 Statistical Significance Formulae . . . 71

B Appendix B **73**
B.1 Pathloss Table . . . 73

C Appendix C **75**
C.1 LoRa Deployments Signal Strength . . . 75
C.2 FSPL Repeatable Accuracy in the coverage area . . . 81
C.3 COST 231 WI Repeatable Accuracy in the coverage area . . . 84
C.4 Ericsson 9999 Repeatable Accuracy in the coverage area . . . 87

List of Figures

2.1 Start of an up-chirp in the time domain . . . 10
2.2 LoRaWAN packet with an explicit header . . . 12
2.3 LoRaWAN packet with an implicit header . . . 12
2.4 LoRa packet as a transmitted signal in the time domain [30] . . . 13
2.5 HDOP . . . 14
2.8 LoRa and Sigfox comparison . . . 34

3.1 The proposed experimental methodology based on the work of Lebekwe et al, the LoRa alliance strategy committee, Sigweni el al and Milankovich et al. . . . 36
3.2 BIUST coverage area . . . 37
3.3 HDOP gateway placement algorithm . . . 38
3.4 Possible gateway sites around the BIUST geographical area indicated by the blue mark points . . . 39
3.5 Triangularly tessellated gateway placement in proposed locations from 3.1 . . . 40
3.6 Placed gateways . . . 43
3.7 HDOP guided method, placed gateways . . . 44

4.1 4 Randomly placed gateways . . . 51
4.2 5 Randomly placed gateways . . . 51
4.3 8 Randmoly placed gateways . . . 52
4.4 9 Randomly placed gateways . . . 52
4.5 11 Randomly placed gateways . . . 52
4.6 8 Naively placed gateways arrangement 1 . . . 53
4.7 8 Naively placed gateways arrangement 2 . . . 53
4.8 8 Naively placed gateways arrangement 3 . . . 53
4.9 8 Naively placed gateways arrangement 4 . . . 53
4.10 3 HDOP guided gateway placements . . . 54
4.11 Unweighted HDOP map with HDOP guided placed gateways . . . 54
4.12 4 HDOP guided gateway placements . . . 54
4.13 5 HDOP guided gateway placements . . . 54
4.14 8 HDOP guided placed gateways . . . 55
4.15 Box and Whisker plot for random placement (1), naive placement (2) and HDOP guided placement (3) . . . 56
4.16 Random placement coverage results . . . 57
4.17 Naive placement coverage results . . . 58
4.18 HDOP guided placement coverage results . . . 59
4.20 COST WI SNR graph . . . 61
4.21 Ericsson 9999 SNR graph . . . 61
4.22 Free Space Path Loss SNR graph . . . 61
4.23 FSPL repeatable accuracy: 400 m, 1000 m, 1500 m gateway separation at SF 8,10,12 and BW 125kHz . . . 62

4.24 COST 231 WI repeatable accuracy: 400 m, 1000 m, 1500 m gateway separation at SF 8,10,12 and BW 125kHz 63
4.25 Ericsson 9999 repeatable accuracy: 400 m, 1000 m, 1500 m gateway separation at SF 8,10,12 and BW 125kHz 64

A.1 Mann Whitney U one tailed test critical values [71] 71

C.1 FSPL Signal Strength: 1500 m gateway separation at SF12 75
C.2 FSPL Signal Strength: 1500 m gateway separation at SF10 75
C.3 FSPL Signal Strength: 1500 m gateway separation at SF8 75
C.4 FSPL Signal Strength: 1000 m gateway separation at SF12 75
C.5 FSPL Signal Strength: 1000 m gateway separation at SF10 76
C.6 FSPL Signal Strength: 1000 m gateway separation at SF8 76
C.7 FSPL Signal Strength: 400 m gateway separation at SF12 76
C.8 FSPL Signal Strength: 400 m gateway separation at SF10 76
C.9 FSPL Signal Strength: 400 m gateway separation at SF8 76
C.10 COST 231 Signal Strength: 1500 m gateway separation at SF12 76
C.11 COST 231 Signal Strength: 1500 m gateway separation at SF10 77
C.12 COST 231 Signal Strength: 1500 m gateway separation at SF8 77
C.13 COST 231 Signal Strength: 1000 m gateway separation at SF12 77
C.14 COST 231 Signal Strength: 1000 m gateway separation at SF10 77
C.15 COST 231 Signal Strength: 1000 m gateway separation at SF8 77
C.16 COST231 Signal Strength: 400 m gateway separation at SF12 77
C.17 COST 231 Signal Strength: 400 m gateway separation at SF10 78
C.18 COST 231 Signal Strength: 400 m gateway separation at SF8 78
C.19 ERICSSON 9999 Signal Strength: 1500 m gateway separation at SF12 . 78
C.20 ERICSSON 9999 Signal Strength: 1500 m gateway separation at SF10 . 78
C.21 ERICSSON 9999 Signal Strength: 1500 m gateway separation at SF8 . . 79
C.22 ERICSSON 9999 Signal Strength: 1000 m gateway separation at SF12 . 79
C.23 ERICSSON 9999 Signal Strength: 1000 m gateway separation at SF10 . 79
C.24 ERICSSON 9999 Signal Strength: 1000 m gateway separation at SF8 . . 79
C.25 ERICSSON 9999 Signal Strength: 400 m gateway separation at SF12 . . 80
C.26 ERICSSON 9999 Signal Strength: 400 m gateway separation at SF10 . . 80
C.27 ERICSSON 9999 Signal Strength: 400 m gateway separation at SF8 . . 80
C.28 FSPL Signal Strength: 400 m gateway separation at SF8 BW 125kHz . . 81
C.29 FSPL Signal Strength: 400 m gateway separation at SF10 BW 125kHz . 81
C.30 FSPL Signal Strength: 400 m gateway separation at SF12 BW 125kHz . 81
C.31 FSPL repeatable accuracy: 1000 m gateway separation at SF8 BW 125kHz 81
C.32 FSPL repeatable accuracy: 1000 m gateway separation at SF10 BW 125kHz 82
C.33 FSPL repeatable accuracy: 1000 m gateway separation at SF12 BW 125kHz 82
C.34 FSPL repeatable accuracy: 1500 m gateway separation at SF8 BW 125kHz 82
C.35 FSPL repeatable accuracy: 1500 m gateway separation at SF10 BW 125kHz 82
C.36 FSPL repeatable accuracy: 1500 m gateway separation at SF12 BW 125kHz 83
C.37 COST 231 WI repeatable accuracy: 400 m gateway separation at SF10 BW 125kHz 84
C.38 COST 231 WI repeatable accuracy: 400 m gateway separation at SF12 BW 125kHz 84

C.39 COST 231 WI repeatable accuracy: 400 m gateway separation at SF12 BW 125kHz 84
C.40 COST 231 WI repeatable accuracy: 1000 m gateway separation at SF8 BW 125kHz 84
C.41 COST 231 WI repeatable accuracy: 1000 m gateway separation at SF10 BW 125kHz 85
C.42 COST 231 WI repeatable accuracy: 1000 m gateway separation at SF12 BW 125kHz 85
C.43 COST 231 WI repeatable accuracy: 1500 m gateway separation at SF8 BW 125kHz 85
C.44 COST 231 WI repeatable accuracy: 1500 m gateway separation at SF10 BW 125kHz 85
C.45 COST 231 WI repeatable accuracy: 1500 m gateway separation at SF12 BW 125kHz 86
C.46 Ericsson 9999 repeatable accuracy: 400 m gateway separation at SF8 BW 125kHz 87
C.47 Ericsson 9999 repeatable accuracy: 400 m gateway separation at SF10 BW 125kHz 87
C.48 Ericsson 9999 repeatable accuracy: 400 m gateway separation at SF12 BW 125kHz 87
C.49 Ericsson 9999 repeatable accuracy: 1000 m gateway separation at SF8 BW 125kHz 87
C.50 Ericsson 9999 repeatable accuracy: 1000 m gateway separation at SF10 BW 125kHz 88
C.51 Ericsson 9999 repeatable accuracy: 1000 m gateway separation at SF12 BW 125kHz 88
C.52 Ericsson 9999 repeatable accuracy: 1500 m gateway separation at SF8 BW 125kHz 88
C.53 Ericsson 9999 repeatable accuracy: 1500 m gateway separation at SF10 BW 125kHz 88
C.54 Ericsson 9999 repeatable accuracy: 1500 m gateway separation at SF12 BW 125kHz 89

List of Tables

2.1 SNR and TOA variance in metres . . . 19
2.2 LoRa navigation or geolocation articles . . . 20
2.3 LoRa navigation or geolocation articles continued . . . 21
2.4 Propagation models classification by [40] . . . 24
2.5 Continuation of propagation models classification by [40] . . . 25
2.6 BOCRA documented ISM bands [41] . . . 26
2.7 Ericsson 9999 model parameters . . . 28
2.8 Systematic Literature Review Summary . . . 29
2.9 LoRa and LoRaWAN use cases [35] . . . 32
2.10 LoRa and LoRaWAN performance metrics, validation . . . 34

3.1 Possible BIUST gateway sites coordinates . . . 39
3.2 LoRa naive deployment articles . . . 42
3.3 Simulation data characteristics . . . 46
3.4 Use case table for terrestrial navigation/positioning . . . 47
3.5 Transmission characteristics 1 . . . 48
3.6 Transmission characteristics 2 . . . 48

4.1 Mann-Whitney U Test Result: Naive placement VS Random Placement 57
4.2 Mann-Whitney U Test Result: HDOP guided placement VS Random Placement . . . 57
4.3 Mann-Whitney U Test Result: HDOP guided placement VS Naive Placement . . . 58

A.1 Interpretation of effect sizes [66] . . . 70

B.1 Gateway and transmitter heights above ground . . . 73
B.2 Gateway and transmitter heights above ground . . . 74

List of Abbreviations

ADR	**A**daptive **D**ata **R**ate
BIUST	**B**otswana **I**nternational **U**niversity of **S**cience and **T**echnology
BPSK	**B**inary **P**hase **S**hift **K**eying
BW	**B**andwidth
C/R	**C**oding **R**ate
CF	**C**arrier **F**requency
CR	**C**ognitive **R**adio
CSS	**C**hirp **S**pread **S**spectrum
FEC	**F**orward **E**rror **C**orrection
FSPL	**F**ree **S**pace **P**ath **L**oss
GPS	**G**lobal **P**ositioning **S**ystem
GSA	**G**lobal **S**ensitivity **A**nalysis
GSM	**G**lobal **S**ystem for **M**obile communication
HDOP	**H**orizontal **D**ilution **o**f **P**recision
IBM	**I**nternational **B**usiness **M**achines
IoL	**I**nternet **o**f **L**ife
IoT	**I**nternet **o**f **T**hings
ISM	**I**ndustrial **S**cientific and **M**edical
ITM	**I**regular **T**errain **M**odel
LoRa	**Lo**ng **Ra**nge
LoRa-Sim	**Lo**ng **Ra**nge **Sim**ulator
LoRaWAN	**Lo**ng **Ra**nge **W**ide **A**rea **N**etwork
LOS	**L**ine **o**f **S**ight
LPWAN	**L**ow **P**ower **W**ide **A**rea **N**etwork
MAC	**M**edia **A**ccess **C**ontrol
MANETS	**M**obile **A**dhoc **N**etworks
NB-IoT	**N**arrow **B**and **I**nternet **O**f **T**hings
NLOS	**N**on **L**ine **o**f **S**ight
OSI	**O**pen **S**ystems **I**nterconnection model
PER	**P**acket **E**rror **R**ate
PHY	**P**hysical layer
PRR	**P**acket **R**eception **R**ate
QOS	**Q**uality **o**f **S**ervice
RF	**R**adio **F**requency
SDR	**S**oftware **D**efined **R**adio
SCR	**S**oftware **C**ontrolled **R**adio
RSSI	**R**ecived **S**ignal **S**trength **I**ndictor
SADC	**S**othern **A**frican **D**evelopment **C**ommunity
SF	**S**preading **F**actor
SLR	**S**ystematic **L**iterature **R**eview
SNR	**S**ignal to **N**oise **R**atio
TNS	**T**errestrial **N**avigation **S**ystem
TP	**T**ransmission **P**ower

WSN **W**ireless **S**ensor **N**etwork

List of Symbols

A_{bm}	free space attenuation	dB
A_{fs}	pathloss due to a medium city	dB
d	distance	m
f_c	transmission frequency	Hz
G_b	transmitter antenna gain	dB
G_m	receiver antenna gain	dB
G_{re}	gateway gain factor	dB
G_{te}	receiver gain factor	dB
h_b	height of gateway	m
h_m	height of transmitter	m
P_r	received signal power	dB
P_t	transmitted signal power	dB

BOTSWANA INTERNATIONAL UNIVERSITY OF SCIENCE & TECHNOLOGY

FORM PGS - 330

POSTGRADUATE SCHOOL

Declaration Regarding the Work and Copyright

DECLARATION REGARDING THE WORK AND COPYRIGHT

Candidate (please write in caps or type) LONE GODFREY FUTURE KOLOBE

Student ID: 13000492

Thesis Titled: Long Range Wide Area Network (LoRaWAN) Propagation Model

I, the **Candidate**, certify that the Thesis is all my own original work and that I have not obtained a degree in this University or elsewhere on the basis of any of this work.

(If the thesis is based on a group project, then the student must indicate the extent of her / his contribution, with reference to any other theses submitted or published by each collaborator in the project, and a declaration to this effect must be included in the thesis)

This dissertation/thesis is copyright material protected under the Berne Convention, the Copyright and Neighbouring Rights Act, Act. No. 8 of 2000 and other international and national enactments, in that behalf, on intellectual property. It must not be reproduced by any means, in full or in part, except for short extracts in fair dealing; for researcher private study, critical scholarly review or discourse with an acknowledgement, without the written permission of the office of the Postgraduate School, on behalf of both the author and the BIUST.

Signed: ---------- Date: ----------

Primary Supervisor (please write in caps or type) DR C.K. LEBEKWE

I, the Candidate's **Primary Supervisor**, hereby confirm that I have inspected the above titled thesis and, to the best of my knowledge, it is based on the original work of the candidate.

Signed: ---------- Date: ----------

N.B. This declaration should follow the Table of Contents).

Chapter 1

Introduction and Background

This chapter consists of four (4) sections namely: background, introduction, problem statement and the thesis outline. The purpose of the section is to give the reader a brief overview on the area being researched, provide summaries of key concepts and principles which guide this research study, state the problem and lastly the outline of this document.

1.1 Background

The area of mobile ad hoc networks (MANETS) have existed in multiple forms since the early 1970s [1]. The intent behind MANETS is to create optimal non-centralized personal networks at times utilizing multiple hop techniques [2] to relay information between nodes. However, the use of multi-hop techniques introduces technical difficulties with developing energy efficient routing algorithms and quality of service schemes [3].

An alternative technology to MANETs when transmitting non-priority bits over large distances with limited to no physical infrastructure is low power wide area networks (LPWANs). The latter technologies utilize narrowband/spread spectrum communication over licensed and unlicensed bands [4] [5] [6]. Technologies of interest in this regard are Sigfox and LoRa which both work in the industrial scientific and medical (ISM) sub GHz band. Radio-waves propagating in this band, are able to penetrate air, rock and water with little to no attenuation [6] [7]. As a result of this ability as well as long ranges of connectivity, these technologies have been deployed in areas such as mining, research and development, logistics, fleet management, tracking, internet of life (IoL) and internet of things (IoT) applications to name a few [8] [9]. Unlike typical MANETs, LPWANs often utilize very low power levels in transmission. This is primarily due to two (2) functional requirements:

- To utilise devices in the ISM band, that are limited to a transmission power of 17dB or less [3],
- To deploy nodes with long life spans using only a battery power source in wireless sensor network deployment areas (WSN) [7].

Additionally, LPWAN propagation is susceptible to large scale fading (shadowing and path loss) phenomenon as a result of large transmission distances between the nodes: typically greater than a kilometre [10] [11]. However, LPWAN models especially LoRa are based on empirical data, where model calibrations are done to ensure a better fit for a new/given area. This has driven research into radio-wave propagation models used by these technologies, with the intent to improve upon the accuracy of these models, so that they can used in planning and setting up such networks.

1.2 Introduction

This section, lays the foundations of some major concepts which guide the study into LoRa, its propagation models as well as the state of the research field.

1.2.1 LPWAN Technology

Mekki et al. projects that there will be over 50 billion devices online by 2020 [6]. While similarly Sinha et al proposed that there would be least 25 billion devices,by the same year [12]. In response to this projected increase in wireless communication, LPWAN communication schemes have been developed as an alternative to multi-hop systems, GSM and other wideband schemes, promising:

- Low start-up or maintenance cost of nodes and/or sink nodes/gateways,
- Low bandwidth and low noise sensitivity,
- Ultra low power throughput,
- Wide area coverage,
- Very good penetration: they can be used underground, underwater and terrestrially in LOS or NLOS scenarios [13].

All the above requirements are attained all the while trading off a high data transmission rates, [14] as well as having a high packet latency when using higher spreading factors and little to no quality of service (QoS) [6] [15] [8]. This can be visualised using figure 1.1. Nonetheless, technologies which have dominated in the long range IoT communication landscape are: Sigfox, LoRa and NB-IoT [6] [12]. The two former schemes, Sigfox and LoRa, both transmit over the sub 1GHz ISM bands while the latter (NB-IoT) utilizes LTE and 3GPP technology transmitting in the licensed band [13]. Figure 1.2 illustrates the typical network architecture of a LPWAN. As a result of LoRa's high level of usage, as well as its significant lower start-up costs, this thesis will focus on its propagation model(s), and ranging application capabilities in any given geographical area.

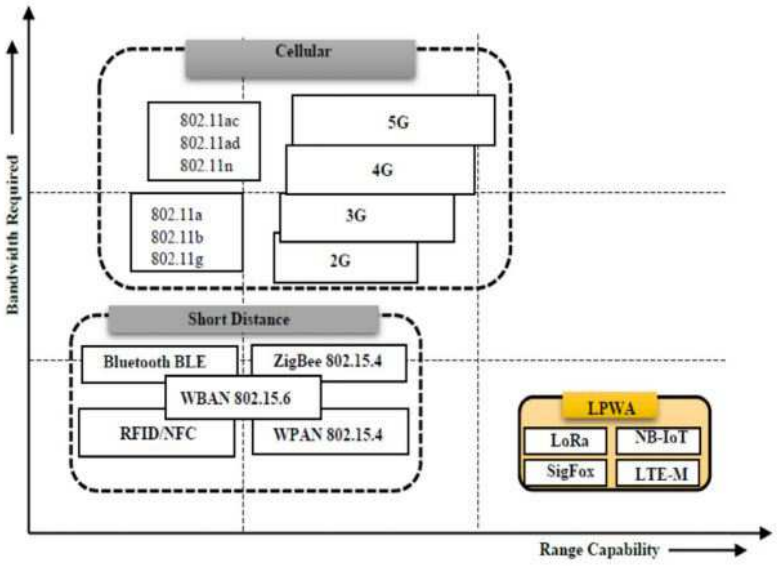


FIGURE 1.1: LoRa bandwidth versus range comparisons [16]

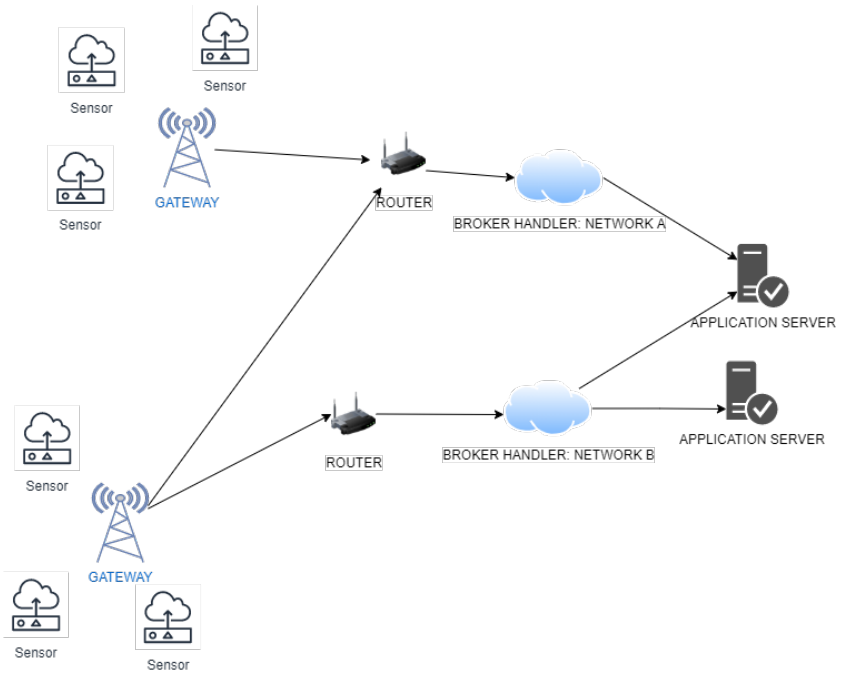


FIGURE 1.2: LPWAN Architecture [16]

The next section describes LoRa and LoRaWAN technologies.

1.2.2 LoRa and LoRaWAN

"LoRa is a proprietary spread spectrum modulation scheme that is derivative of chirp spread spectrum (CSS) and which trades data rate for sensitivity within a fixed channel bandwidth"[17]. LoRa utilizes proprietary CSS modulation [3] to modulate signals. As result of this modulation scheme LoRa has high resilience to interference, as well as noise [7] [6]. LoRa utilizes six spreading factors (SF7,SF8,SF9,SF10,SF11 and SF12), to allow the scheme to adapt the data rate and range [6]. However, latency is gained in employing higher spreading factors [3] [5]. It is worth noting that the LoRa technology like many others in the LPWAN class utilizes a “wait and listen” scheme [13] [18] making it half duplex. Using the LoRaWAN protocol, LoRa has a message payload of up to 243bytes [6]. As a means of addressing numerous potential use cases in IoT communication, LoRa has three classes of communication which all keep the core characteristics of LPWANS while adding flexibility for different use cases. The classes are A, B and C [6] [13]. The classes are expanded upon in chapter 2.

LoRa also has a MAC protocol (LoRaWAN) developed by SEMTEC and IBM that specifies the connection properties of the LoRa modulation scheme while also allowing the automatic or manual setting of connection parameters [3]. More to this, LoRaWAN uses a scheme - adaptive data rates (ADR) - to set the connection parameters and data transfer rates. LoRa PHY layer uses a series of up and down chirp signals to modulate and transmit signals over the air [3]. Spread spectrum techniques have enjoyed significant attention due to their resistance to jamming [19]. A technique is considered spread spectrum if the transmission bandwidth is larger than the minimum required information transmission bandwidth [19][20]. Furthermore, the following criteria were outlined by [19] as the properties of spread spectrum modulation:

- The bandwidth used for transmission is much greater than the minimum bandwidth required to transmit information
- The "spreading" process is done by a "spreading signal or code signal". This signal is independent of the data being transmitted.
- At the receiver, signal recovery is performed through correlation of the spread signal with a replica of the coding signal used to spread the transmitted data.

The benefit of increasing channel bandwidth is the improved overall system performance. However, this is not guaranteed as the bandwidth is increased to infinity as increasing bandwidth lead to increased channels hence leading to higher bit error rate (BER).

$$T_s = \frac{2^{SF}}{BW}, \text{ seconds,} \tag{1.1}$$

$$R_c = R_s 2^{SF}, \text{ Chips per second,} \tag{1.3}$$

$$R_s = \frac{1}{T_s} = \frac{BW}{2^{SF}} \text{ Symbols per second,} \tag{1.2}$$

$$R_b = \frac{4BW}{4+CR} \text{ Bits per second.} \tag{1.4}$$

[17]

Where:

- T_s - Symbol time,
- R_s - symbol rate,
- R_c - chip rate,
- R_b - nominal bit rate,
- SF - spreading factor, ranging from 7-12. Spreading factors denote the number of chirps used to encode data bits [16]. Where the number of chirps will be = 2^{SF} [16].
- CR - coding rate, ranging from 1-4. This is specifically used by LoRa for FEC. FEC is used to protect transmissions from error bursts [3]. Coding rate can be set to 4/5, 4/6, 4/7 or 4/8, in doing this higher CR will give better protection while increasing the packet time on air [3].
- BW - modulation bandwidth [17].

1.2.3 LPWAN Propagation Models

Milankovich et al, described a model as a mathematical means of predicting the performance of a RF wave [21]. Models by their nature will often be a simplification of natural phenomenon, with it being possible for multiple different models to be compatible with the same natural phenomenon. The authors in [22] described this paradox as "...equifinality..." or "...model interdeterminancy". As a result of the former, models will often not be described as "proven true" as they are limited in the variables they can take in, they are thus deemed "extensively corroborated" . The same authors further proposed that this should be done after subjecting models to some formal internal consistency tests. These tests will assess a model according to some or all of the following metrics:

- Past usage,
- Status of its proponents,
- Degree of acceptance by peers.

Based on the above metrics, not all models are created equal, this because different applications will require varying levels of accuracy, these being the following:

- "In applied science", where a model is used by specific set of experts in a given field. The model will typically work to simply qualify a phenomenon theoretically. An example may be a biological model to describe population growth within given constraints.
- "In consultancy", where a model has to survive scrutiny on at least a cost-benefit analysis level. This is the simplest form of assessment to determine legitimacy of the model in the real world .
- "In a context of global change", in this instance a model has a significant impact on the ways and means of daily life for people across all walks of life. For instance a climate change/sensitivity model.

Therefore, the propagation models in the context of LPWAN, specifically LoRa will need to check all three metrics used for model assessment. This is because the technology, depending on the usecase, may have far reaching implications whether financially, or in terms of quality of life when planning LoRa network deployments [21].

The next subsection, describes the Horizontal Dilution of precision (HDOP), a metric which informs on optimised gateway placement in order to guarantee good LoRa coverage everywhere in the area of interest.

1.2.4 Horizontal Dilution of Precision

The oldest forms of navigation systems were deployed as terrestrial systems employing the use of hyperbolas to attain the location of a receiver [23]. Systems such as Loran and Omega used the hyperbolic location principle. Using this method, three or more transmitters [24] will have hyperbolas drawn from a radius equivalent to the distance between the transmitter and the receiver [23]. This is repeated for all transmitters with the point where the hyperbolas intersect being considered the approximate receiver's location. The position solution is influenced by -node-gateway geometry. However, when a weighting matrix is applied the position solution will be influenced by other factors such as the variance in the signal time of arrival (TOA) variance, signal to noise ratio (SNR) and multipath [25] [26]

Generally, a metric of interest is the position uncertainty, and this may be due to poor node-gateway geometry in 2D and is termed horizontal dilution of precision (HDOP). HDOP is a unit-less ratio of position error to range error. A good receiver-transmitter geometry will result in a good HDOP, $HDOP \leq 1$, while poor geometry will result in bad HDOP, $HDOP > 1$ [27]. The practical implication is that low HDOP values will not amplify the position error and it will therefore be a affected by SNR, multipath or TOA variance more than the receiver-gateway geometry. Table 1.1 shows the ratings of HDOP values.

TABLE 1.1: HDOP ratings [24]

HDOP Value	**Rating**
0-1	Ideal
2-4	Excellent
4-6	Good
6-8	Moderate
8-20	Fair
20-50	Poor

The next section provides the research project problem statement, research rationale, the research goal and the specific objectives of the project.

1.3 Problem Statement

The increased use and relevance of LoRa in scientific, medical and industrial applications warrants an investigation into the implementation as well as performance of LoRa as a terrestrial navigation. This could be of benefit in localisation, IoL and IoT applications or if LoRa is ever considered as a signal of opportunity (SoOP).

1.3.1 Research Rational

This work will use propagation models to produce weighting matrices to assess the performance of LoRa when used for navigation. Propagation models in this context is interchangeable with path loss models. Their purpose being to estimate the most probable behaviour of a link, most probable is the operative word due to the fact that the data gathered to create a model will often be limited, this prevents models from being able to 'perfectly' model link behaviour. However, modern telecommunications has introduced a flexibility in the form of software defined radio (SDR) or cognitive radio (CR) where hardware can be programmed and re-programmed to perform optimally in a given scenario, which is key as the range of transmission is often related to the transmission power as well as frequency of operation [21] [28]. The relevance of propagation models lies in the fact that they are essential in the cellular planning process, ensuring that designers can maximize the coverage to clients when designing a network and its topology.

Additionally, propagation models have real world fiscal implications as they determine where transmission equipment are placed in a given geographical area. In view of this, improved understanding of propagation models and gateway geometries in a given area directly leads to lower network deployment cost, and fewer instances of catastrophic network failure. This will prove vital in future novel deployments of LoRa in various industrial and scientific applications.

1.3.2 Research Goal

The main goal of this research project, is to simulate the LoRa performance in Botswana using relevant/appropriate propagation models. Specifically propagation models suitable for LoRa applications in the 915MHz band. Finally, this research aims to

determine a means to predict LoRa coverage in rural Botswana for terrestrial navigation purposes.

1.3.3 Research Objectives

- To review pathloss/propagation models viable to model LoRa in the 915MHz bands in Botswana,
- To determine the performance of applicable propagation models in rural Botswana for ranging or localisation applications using a software platform written using MATLAB.

1.4 Masters Thesis Outline

Chapter 2 will outline the literature review for the research project. The technical background of LoRa, its previous applications and the suitability of the technology in navigation. Furthermore, the metrics of interest in terrestrial navigation are outlined and viable propagation models for the 915Mhz ISM band. Chapter 3 details the experimental methodology used to accomplish the project objectives. The chapter explores the methods of LoRa gateway placement for navigation purposes as well as determining the statistical methods used to assess the gateway placement methods used in the study. Chapter 4 explains the experimental results of the research project. The chapter analyses the performance of the gateway placement techniques from chapter 3 using the statistical tests, namely statistical significance and effect size, as well as the HDOP score which is the total number of grid points with a HDOP score of 1 or less. The section also assesses LoRa repeatable accuracy, and as a result the suitability of the technology for navigation applications. Chapter 5 gives the project conclusion, as well as recommendations on the potential future work based on project findings.

1.5 Chapter Summary

Chapter 1 provided an introduction into the LoRa technology, and its relevance in the LPWAN area. The chapter also provides insight into concepts of interest for the study namely;LoRa, propagation models and HDOP. The chapter also provided the research problem statement, the overall project goal and objectives.

Chapter 2

Literature Review

Chapter 2 provides detailed literature review of LoRa, LoRaWAN, HDOP, geolocation in LoRa and propagation models applicable to the technology. The chapter also includes details and results of a systematic literature review conducted, to ascertain the use-cases of LoRa, identify metrics as well as techniques used to determine validity of results obtained.

2.1 Low Power Wide Area Networks: The LoRa signal

LoRa exists in two parts; first, an Open System for Interconnection (OSI) model physical layer transmission scheme which uses CSS modulation to transmit signals through a wireless channel. The second part is the LoRaWAN protocol, operating at the OSI datalink and network layers [5]. A Lora radio signal is susceptible to induced channel fading and additive white noise when propagating through a wireless channel. Specifically, a wave that propagates through a wireless channel over a distance between 100m and 1000m, is susceptible to large scale fading or path-loss fading. Small scale fading, will occur in distances within the order of the wavelength of the signal [29] [11].

Within the wireless channel, scatterers (eg. Trees, buildings etc) result in the transmitted signal being split into multiple components while on route to the receiver . These components are the line of sight (LOS) and none line of sight (NLOS) components which arrive at the receiver at time (t) and $t + \tau_n$ respectively. Where n is the multipath component number. The variable τ represents the time delay between the reception of the LOS component and the other delayed multipath/NLOS components. Mathematically, a received signal $y(t)$ will be the product of the modulated transmitted signal $x(t)$ and channel response $h(t) = \delta(t - \tau)$ summed with the random noise n [11] [30]. The signal characterisation is shown in equation 2.1.

LoRa is a chirp modulated signal, this chirp can be modelled in continuous time as shown in figure 2.1. Mathematically a LoRa chirp maybe modelled as 2.1.

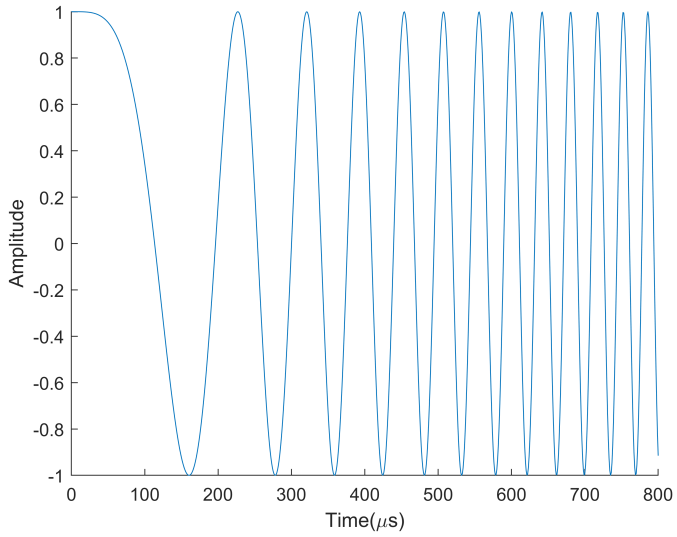


FIGURE 2.1: Start of an up-chirp in the time domain

$$x(t) = e^{j\mu t^2}, \tag{2.1}$$

$$\mu = \frac{BW^2}{2^{SF}} 0 \leq t \leq T_{sym}, \tag{2.2}$$

A LoRa modulated signal in the time domain is modelled as:

$$x(kT_c) = \frac{1}{\sqrt{2^{SF}}} e^{j2\pi[(N_{shift}+k)_{mod(2^{SF})}]\frac{k}{2^{SF}}}, \tag{2.3}$$

where $k = 0, 1, 2, ...(2^{SF} - 1)$, and $0 \leq N_{shift} \leq 2^{SF} - 1$ [31],

The transmitted signal will therefore be:

$$s(t) = \sum_{k=0}^{SF-1} x(t - kT_c), \tag{2.4}$$

$$s(t) = \sum_{k=0}^{SF-1} \frac{1}{\sqrt{2^{SF}}} (e^{j\mu t^2 - 2\pi[(N_{shift}+k)_{mod(2^{S_F})}]\frac{k}{2^{SF}}},) \tag{2.5}$$

The channel response $h(t)$ can be modelled as a sum of delays multiplied by some attenuation of amplitude a_m, and possessing a phase difference ϕ:

- where the attenuation amplitude is g_m and phase ϕ is $-2\pi F_c \tau_m$,
- F_c is the carrier frequency,
- the complex channel response reduces to 2.1,
- **M** is the number of resolvable multipaths.

$$h(t) = \sum_{m=0}^{M-1} a_m \delta(t - \tau_m), \tag{2.6}$$

$$a_m = g_m e^{-j2\pi F c \tau_m}, \tag{2.7}$$

$$h = \sum_{m=0}^{M-1} g_m e^{-j2\pi F_c \tau_m}, \tag{2.8}$$

$$h = \sum_{m=0}^{M-1} g_m cos(2\pi F_c \tau_m) - j \sum_{m=0}^{M-1} g_m sin(2\pi F_c \tau_m). \tag{2.9}$$

The received LoRa signal when applying narrowband assumption is,

$$y(t) = \sum_{n=0}^{M-1} a_m s(t) + n(t). \tag{2.10}$$

The next section explains the LoRaWAN protocol specifically the packet structure and its features.

2.2 Low Power Wide Area Networks: LoRaWAN protocol

The underlying technology (protocols) of LoRa were developed by the LoRa alliance, a group of the most influential companies in the global computer and telecommunications industry including but not limited to IBM and SEMTEC [12] [16] [4]. Additionally, LoRa utilizes six spreading factors (SF7, SF8, SF9, SF10, SF11 and SF12), allowing the scheme to adapt the data rate and range [6], this allows the data packet being sent to be padded making it more resilient to noise. Latency is gained in employing higher spreading factors [32] [4]. It is worth noting that the LoRa technology like many others in the LPWAN class utilizes a "wait and listen" scheme basically it is half duplex [13] [6].

Using the LoRaWAN protocol LoRa, has a message payload of up to 243 bytes . As a means of addressing numerous potential use cases in IoT communication, LoRa has three classes of communication which all keep the core characteristics of LPWANS while adding a dimension of flexibility for applications where constant communication is needed these are classes A, B and C [6] [13].

LoRaWAN MAC protocol specifies the connection properties of the LoRa connection while also allowing the automatic or manual setting of connection parameters. The LoRaWAN protocol uses an adaptive data rate (ADR) to set the connection parameters. Despite the existence of an ADR scheme, it is unable to explicitly determine the order, manner or even instance during which the relevant transmission parameters should be used given channel conditions [32] [4]. Transmission settings used in a usecase are either the default settings, or specified via the use of the link header or manually set by the user based on empirical data or some calculation [33].

The LoRaWAN packet format may have a header being explicit or implicit, as illustrated in figure 2.2 and 2.3. An explicit header will contain information on the payload length and CR. However, the implicit header will not contain the former details resulting in default settings being assumed by the receiver. Within the packet, the preamble is used to detect the start of the packet on the receiver side. The presence of a header, in the explicit header mode, will add details on the payload size in bytes as well as the Forward Error Correction (FEC) and Coding Rate (CR). A cyclic redundancy check for the payload will also be specified with a dedicated 16 bits at the end of the payload. The payload is a variable field that holds the actual data of the application. Figure 2.4 shows a LoRa packet as it is transmitted as a series of chirps, where the preamble is a series of 8 consecutive up chirps followed by 2 down chirps, before the payload is received [34] [30].



FIGURE 2.2: LoRaWAN packet with an explicit header

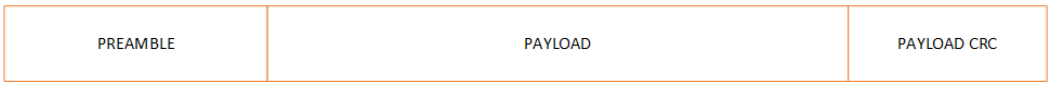


FIGURE 2.3: LoRaWAN packet with an implicit header

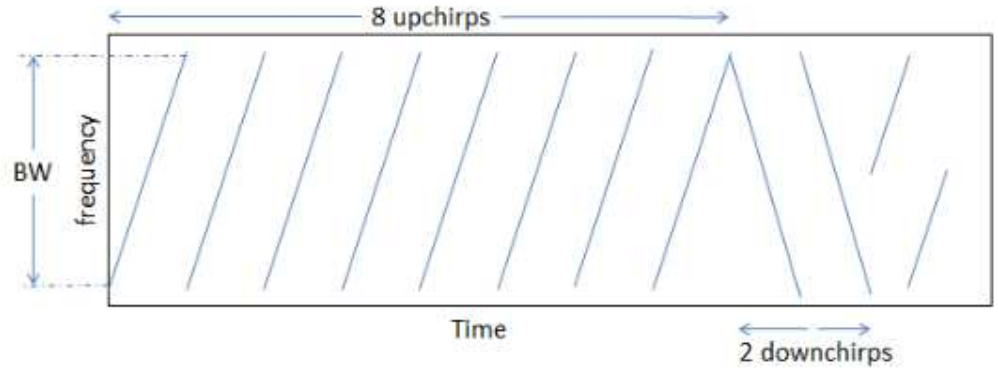


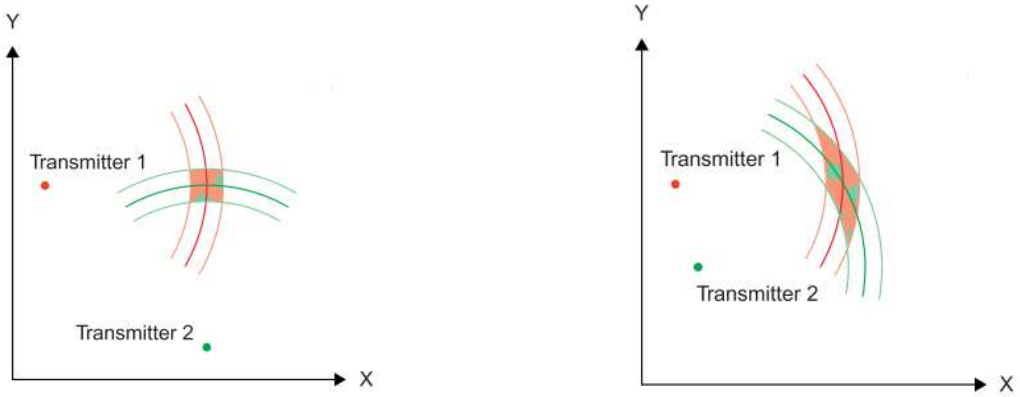
FIGURE 2.4: LoRa packet as a transmitted signal in the time domain [30]

The next section explains the concept of HDOP, and and how it affects geolocation.

2.3 Horizontal Dilution of Precision

HDOP is a unit-less ratio of the position error to the range error. This means that the position error is a product of the HDOP and the ranging errors. The ranging errors are affected by SNR, BW under the LoRa specifications and the symbol time while HDOP is affected by the locations of the transmitters relative to the receiver within a coverage area (receiver-transmitter geometry). HDOP acts as amplification factor on the range errors and therefore, there is need for optimal placement of LoRa transmitters/gateways in a coverage area in order to minimize position errors. Large HDOP values lead to higher position errors and vice versa [25]. HDOP values that are less than 1 imply that position errors are influenced mainly by the ranging errors rather than poor transmitter geometry [27]. Table 1.1 shows the ratings of HDOP values.

Navigation systems including terrestrial navigation system (TNS) employ the use of hyperbolas to attain the approximate location of a receiver [23]. Systems such as Loran and Omega used the hyperbolic location principle where three (3) or more transmitters[24] will have hyperbolas drawn from a radius equivalent to the distance between the transmitter and the receiver [23]. This is repeated for all transmitters with the point where the hyperbolas intersect being considered the approximate receiver's location. Figure 2.5a shows that when transmitters are appropriately placed the approximate location of a receiver has a smaller area of uncertainty. A poor placement scenarios, such as the one illustrated in figure 2.5b has a greater area of uncertainty. Poor placements of transmitters results in a dilution of precision, when performing a localisation in 2D this is called HDOP [9].



(A) Good HDOP due to good transmitter placement [25]

(B) Bad HDOP due to good transmitter placement [25]

FIGURE 2.5: HDOP

Within navigation is the concept of pseudorange, where a a receiver can determine the distance between itself and a transmitter through a simple calculation. The approximate distance between a transmitter and receiver is the time of flight (ToF) of a signal multiplied by the speed of light (c), $ToF \times c$. If this is repeated with multiple transmitters in a 2D or 3D space it is possible to determine the location of the receiver. However, if the transmitters are placed in a single file (one after the other). It is not easy ro determine the exact location of the receiver in 2D or 3D space. This placement of transmitters has a reduced/diluted accuracy when used to determine location of the receiver as illustrated in figure 2.5b.

The reduction in accuracy due to geometry is dilution of precision (DOP) and it exists in many forms: geometric dilution of precision (GDOP), position dilution of precision (PDOP), horizontal dilution of precision (HDOP), vertical dilution of precision (VDOP) and time dilution of precision (TDOP) [25] [24]. The relevant DOP in this research scenario is HDOP as the technology would be a terrestrial navigation system (TNS) and location is determined in latitude and longitude.

2.3.1 Deriving HDOP

If the actual locations of a transmitter and a receiver are assumed to be $(x_n, y_n)$and(x_0, y_0) in Cartesian form respectively. The Euclidean distance of a receiver (r_n) from a transmitter is shown in equation 2.11,

$$\begin{aligned} r_1 &= \sqrt{(x_0 - x_1)^2 + (y_0 - y_1)^2}, \\ r_2 &= \sqrt{(x_0 - x_2)^2 + (y_0 - y_2)^2}, \\ r_3 &= \sqrt{(x_0 - x_3)^2 + (y_0 - y_3)^2}, \\ r_n &= \sqrt{(x_0 - x_n)^2 + (y_0 - y_n)^2}. \end{aligned} \tag{2.11}$$

In reality errors make it difficult to determine the actual range between a transmitter and receiver. However, through clever assumptions it is possible to reduce the errors so a reasonable location can be determined often within 95^{th} percentile of the

actual value. Therefore, the approximate location in Cartesian may be assumed to be (x_a, y_a). The difference between the actual distance and the approximate distance between the transmitter and receiver is defined by equation 2.12,

$$\begin{aligned} r_n &= \sqrt{(x_0 - x_n)^2 + (y_0 - y_n)^2}, \\ r_{an} &= \sqrt{(x_a - x_n)^2 + (y_a - y_n)^2}, \\ x_0 &= x_a + \delta d. \end{aligned} \tag{2.12}$$

Where the r_{an}, x_a, y_a and δd are the Euclidean distance between a transmitter and an assumed initial known location, the x and y coordinates of the assumed initial location and the difference in distance between the assumed and actual location. When using the East-North-Up (ENU) reference frame and resolving for one dimension the actual location, the distance changes to the form in equation 2.13,

$$r_n = \delta d_n \sin \beta. \tag{2.13}$$

Where β is the bearing of the transmitter to the receiver. When this is repeated for multiple transmitters and a for a receiver location and the result linearised the computation takes the form of equation 2.14,

$$\begin{Bmatrix} r_1 \\ r_2 \\ r_3 \\ r_n \end{Bmatrix} = \begin{Bmatrix} sin(\beta_1) & cos(\beta_1) & 1 \\ sin(\beta_2) & cos(\beta_2) & 1 \\ sin(\beta_3) & cos(\beta_3) & 1 \\ sin(\beta_n) & cos(\beta_n) & 1 \end{Bmatrix} \begin{Bmatrix} \delta d_1 \\ \delta d_2 \\ \delta d_3 \\ \delta d_n \end{Bmatrix} + \begin{Bmatrix} N_1 \\ N_2 \\ N_3 \\ N_n \end{Bmatrix}, \tag{2.14}$$

Where N is the noise in the measurements, this equation can be further simplified into the equation 2.16, if the assignments in 2.15 are made.

$$\begin{Bmatrix} r_1 \\ r_2 \\ r_3 \\ r_n \end{Bmatrix} = \mathbf{r}, \begin{Bmatrix} sin(\beta_1) & cos(\beta_1) & 1 \\ sin(\beta_2) & cos(\beta_2) & 1 \\ sin(\beta_3) & cos(\beta_3) & 1 \\ sin(\beta_n) & cos(\beta_n) & 1 \end{Bmatrix} = \mathbf{A} \begin{pmatrix} , \\ \delta d_1 \\ \delta d_2 \\ \delta d_3 \\ \delta d_n \end{pmatrix} = \mathbf{d}, \begin{Bmatrix} N_1 \\ N_2 \\ N_3 \\ N_n \end{Bmatrix} = \mathrm{N}, \tag{2.15}$$

$$\mathbf{r} = \mathbf{Ad} + \mathbf{N}, \tag{2.16}$$

Equation 2.16 can be solved using least squares or weighted least squares. First the maximum likelihood of the vector $\mathbf{d}$ denoted as $\hat{\mathbf{d}}$ is given by equation 2.17,

$$\hat{\mathbf{d}} = argmax \rho(\frac{\mathbf{r}}{\mathbf{d}}), \tag{2.17}$$

where $\rho(\frac{\mathbf{r}}{\mathbf{d}})$ is the probability density function of $\mathbf{r}$ for fixed values of $\mathbf{d}$. Additionally, if the measurement errors N_n for n = 1, 2,...i are assumed to be to Gaussian distributed, identical with a mean of 0 and a variance σ^2, and measurements are statistically independent then equation 2.17 takes the form of equation 2.18,

$$\begin{aligned} \hat{\mathbf{d}} &= argmax \frac{1}{(2\pi\sigma)^{\frac{i}{2}}} \exp^{-\frac{1}{2\sigma^2}\|\mathbf{r}-\mathbf{Ad}\|^2}, \\ \hat{\mathbf{d}} &= argmin \|\mathbf{r} - \mathbf{Ad}\|^2, \end{aligned} \tag{2.18}$$

The solution to equation 2.18 can be attained by first differentiating the function with respect to $\hat{\mathbf{d}}$ as shown in equation 2.19. Then making $\hat{\mathbf{d}}$ subject of the formula results in a form shown by equation 2.20

$$\frac{d\|\mathbf{r}-\mathbf{A}\mathbf{d}\|^2}{d\hat{\mathbf{d}}} = 2\mathbf{A}^T\mathbf{A}\hat{\mathbf{d}} - 2\mathbf{A}^T\mathbf{r}, \tag{2.19}$$

$$\hat{\mathbf{d}} = (\mathbf{A}^T\mathbf{A})^{-1}\mathbf{A}^T\mathbf{r}, \tag{2.20}$$

Where it is assumed that the matrix inverse exists. Also, equation 2.19 is the least squares estimate because, it results in the minimum square error between the measurement vector $\mathbf{r}$ and $\mathbf{Ad}$, where the latter is the expected measurement vector based upon the estimate of $\mathbf{d}$.

Considering a more general scenario, where errors are still Gaussian distributed, with a mean of 0 and a variance σ^2. However, they are not identically distributed, the maximum likelihood estimated maybe expressed as shown in equation 2.21 and 2.23 ,

$$\hat{\mathbf{d}} = argmax \frac{1}{(2\pi)^{\frac{i}{2}}\|\sigma^2(\tau)\|^{\frac{1}{2}}} \exp -\frac{1}{2}(\mathbf{r}-\mathbf{A}\mathbf{d})^{\mathbf{T}}\sigma^2(\tau)(\mathbf{r}-\mathbf{A}\mathbf{d}), \tag{2.21}$$

Where $\sigma^2(\tau)$ is,

$$\sigma^2(\tau) = \begin{Bmatrix} \sigma_{11}^2 & 0 & 0 \\ 0 & \sigma_{22}^2 & 0 \\ 0 & 0 & \sigma_{33}^2 \end{Bmatrix}, \tag{2.22}$$

$$\hat{\mathbf{d}} = argmin(\mathbf{r}-\mathbf{A}\mathbf{d})^{\mathbf{T}}\sigma^2(\tau)(\mathbf{r}-\mathbf{A}\mathbf{d}), \tag{2.23}$$

Where $\sigma^2(\tau)$ is the covariance matrix associated with the measurement errors, and $\|\sigma^2(\tau)\|$ is the determinant of the matrix. Therefore the unweighted HDOP, has the covariance matrix equal to an identity matrix, and is therefore affected by receiver-transmitter geometry will be the square root of the trace of the of the inverse of the transpose of the geometry matrix multiplied by the geometry matrix as shown in equation 2.24. However, if the errors present in the scenario are known, then the variances of all known errors can be placed in the diagonal of the covariance matrix with the off diagonal elements being equal to zero. This means a weighted HDOP may be calculated using equation 2.25, where $\mathbf{W}$ is the weighting matrix.

$$HDOP = \sqrt{trace(\mathbf{A}^{\mathbf{T}}\mathbf{A})^{-\mathbf{1}}}, \tag{2.24}$$

$$HDOP = \sqrt{trace(\mathbf{A}^{\mathbf{T}}\mathbf{W}\mathbf{A})^{-\mathbf{1}}}. \tag{2.25}$$

2.3.2 Geolocation in LoRa

A typical low power wide area network (LPWAN) architecture is shown in figure 2.6. End nodes transmit packets via a wireless channel to a gateway. Gateways will normally be hybrid transceivers with access to WIFI, GSM or a satellite link. This allows LoRa to transmit node data to the cloud, via MQ telemetry transport (MQTT) protocol or IP for delivery to an application server such as "The Things Network"[35]. In practical applications, the actual position determination process for LoRa uses time difference of arrival (TDOA) [9]. In this method node (LoRa transceiver) will transmit a packet, which is in turn received by atleast 3 gateways and time stamped [36] [9]. The timestamped packet will be forwarded to an application server along with

data pertaining to SNR, RSSI and frequency error [9]. TDOA range estimations are limited by two major factors multipath propagation and clock accuracies [9] [36].

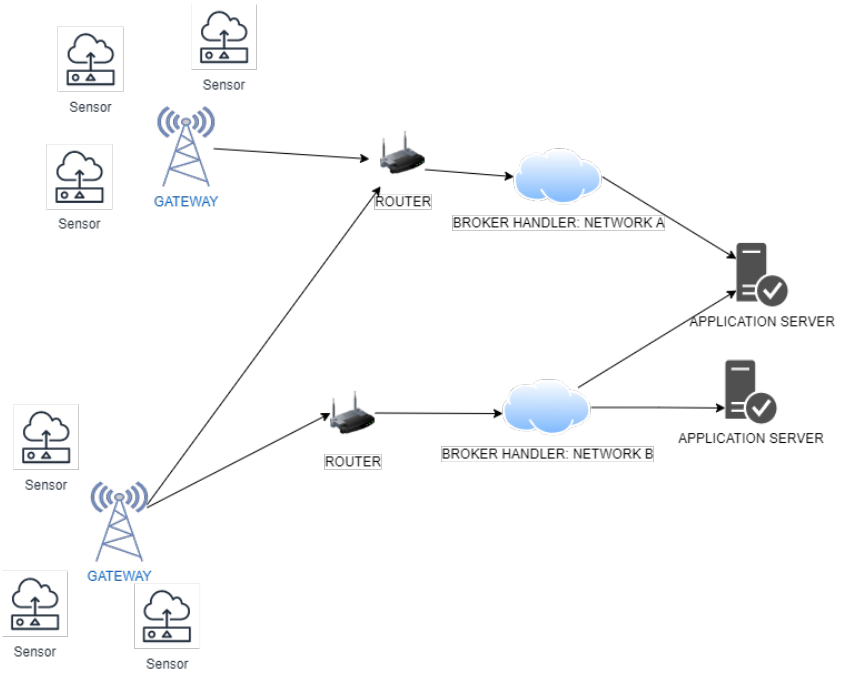


FIGURE 2.6: LPWAN Architecture [16]

The theory of maximum likelihood specifically CRLB is used to determine the minimum time of arrival variance (TOA) of the LoRa signal assuming white gaussian noise channel.

This variance in TOA can be used in a weighting matrix with the HDOP. The expression takes into account the factors which may limit accuracy in the timestamping process explained in 2.3.2, which include SNR, BW, multipath propagation and noise density to name a few. The CRLB allows us to get results which more closely approximates real world performance. Where the CRLB is a statistical measure that can determine the best possible accuracy of a location system [36].

$$CRLB = \frac{1}{E[\frac{\delta}{\delta\psi} \ln p(N|\psi)]}, \tag{2.26}$$

$$CRLB = \frac{1}{-E[\frac{\delta}{\delta\psi} \ln p(N|\psi)]}, \tag{2.27}$$

[36]

where:

- **E** is the expectation or statistical average,
- **N** is the influence of various features including multipath, SNR and RF noise,
- ψ is the desired entity.

Using the signal model in equation 2.10. The signal is discretised by sampling at Nyquist $T_s = \frac{1}{k2BW}$, where k is the oversampling ratio.

$$y[n] = \sum_{n=0}^{M-1} a_m s[n] + w[n], \tag{2.28}$$

Assuming the variance of $y[n] = \sigma^2$, and noise $w[n]$ has an average and variance N_0B, N_0. Also sampling at Nyquist, the samples maybe be assumed to be uncorrelated, the probability function of all the samples will therefore be the product of the samples and will be used to find CRLB.

$$p(y[n]) = \frac{1}{\sqrt{(2\pi\sigma^2)}} \exp^{\frac{1}{2\sigma^2}[y[n]-s[n]]^2}, \tag{2.29}$$

$$p(y;\tau) = \frac{1}{(2\pi\sigma^2)^{(\frac{N}{2})}} \exp^{\frac{-1}{2\sigma^2}\sum_{n=0}^{N-1}[y[n_i]-s[n_i\tau]]^2}, \tag{2.30}$$

Expanding the Fisher information matrix from 2.27 results in 2.31. Additionally, this model assumes the range information is dependant on the time delay of the received signal [30]. $E[\frac{\delta^2}{\delta\psi}\ln p(y|\tau)]$ therefore results in the CRLB relative to the delay.

$$E[\frac{\delta^2}{\delta\psi}\ln p(y|\tau)] = \frac{1}{\sigma^2}\sum_{n=0}^{N-1}(y[n]-s[n])\frac{\delta^2 s[n]}{\delta\tau^2} - (\frac{\delta s[n]^2}{\delta\tau})^2, \tag{2.31}$$

$$var(\tau) \geq E[\frac{\delta^2}{\delta\psi}\ln p(y|\tau)], \tag{2.32}$$

$$var(\tau) = \frac{\sigma^2}{\sum_{n=0}^{N-1}(\frac{\delta s[n]}{\delta\tau})^2}, \tag{2.33}$$

If the sampling period is assumed to be short then the summation maybe approximated using an integration operation from $t = 0 - T_s$

$$var(\tau) \geq CRLB \geq \frac{\sigma^2}{\frac{1}{T_s}\int_0^{T_s}(\frac{ds(t)}{dt})^2 dt}, \tag{2.34}$$

From [36] CRLB maybe expressed as 2.35

$$CRLB = \frac{1}{\frac{\epsilon}{\frac{N_0}{2}}\bar{F^2}}, \tag{2.35}$$

$$\bar{F^2} = \frac{\int_{-\infty}^{\infty}(s\pi F)^2|S(F)|^2 dF}{\int_{-\infty}^{\infty}|S(F)|^2 dF}, \tag{2.36}$$

[36] From [30] it is known that $\epsilon = \int_0^{T_s}|s(t)|^2dt = T_{sym}\int_{-\infty}^{\infty}|S(F)|^2$. Simplified further ϵ can be derived to be 2.37

$$\epsilon = T_{sym}BWS(F)^2, \tag{2.37}$$

$\bar{F^2}$ maybe simplified to 2.38 [30]

$$\bar{F^2} = \frac{4\pi^2(BW)^2}{3}, \tag{2.38}$$

Therefore the variance in the range for a LoRa CSS signal with a known SNR simplifies to 2.39

$$var(D) = \frac{3c^2}{8\pi^2 K T_{sym}(BW)^3 SNR}. \tag{2.39}$$

For each modulation SF, there is a minimum SNR value necessary for successful signal detection [34]. This SNR minimum maybe applied to show the possible maximum variance in position accuracy using 2.39, maximum variance is populated in table 2.1. The minimum SNR can also be used to determine the receiver sensitivity of a deployment using 2.40.

$$S_{min}dBm = -174 + 10\log(BW) + NF + SNR_{Limit}. \tag{2.40}$$

[17]

Where:

- S_{min} is the minimum receiver sensitivity,
- **BW** modulation bandwidth,
- **NF** the noise floor which is fixed at $6dB$ for SX1272 and SX1276 transceiver chips [17],
- SNR_{Limit} is the minimum detectable SNR for a given spreading factor

TABLE 2.1: SNR and TOA variance in metres

Modulation (SF)	**Minimum SNR (dB)**	**Var(D)(m)**
7	-7.5	9614.9
8	-10.0	8549.0
9	-12.5	7601.2
10	-15.0	6758.6
11	-17.5	6009.3
12	-20.0	5343.1

Tables 2.2 and 2.3 summarise the most cited work in the growing research area of LoRa navigation.

TABLE 2.2: LoRa navigation or geolocation articles

Source	Summary	Year	Citations
[37]	The authors of this article proposed three objectives: to quantify the performance of a TDOA based navigation algorithm on a public LoRa network in Netherlands for three movement types; walking, cycling and driving. Secondly, they investigate and determine the best LoRa spreading factor to use with respect to updating position accuracy frequently. Third, the researchers assess the improvements when using a tracking algorithm that takes into account road-map and the movement speed of the user. The experiment showed a 90^{th} percentile repeatable accuracy of 579 m, 490 m,324 m for walking, cycling and driving respectively, with transmission ranges of 10 km -34 km. Lastly, their experiment revealed that the SF that balances range, frequency of position updates and energy consumption was SF 8. Due to the use of a public network the authors were unable to properly account for the influence of HDOP on the ranging errors. Lastly, their work focusses specifically on the TDOA method	2018	37
[38]	The researchers of this work investigated the viability of ranging algorithms for LoRa based on TOA, TDOA, RSSI and a phased based approach (proposed by the researchers). This work determines through a combination of, presentation of observations from other authors and mathematical analysis that phase based localisation maybe the best to improve LoRa repeatable accuracy. Specifically getting it to GPS and WiFi repeatable accuracies of under 5 m. The authors cite significant signal attenuation following barrier penetration, a smooth time domain signal waveform and low resolution internal clocks as limitations for TDOA, TOA and RSSI respectively.	2018	7

TABLE 2.3: LoRa navigation or geolocation articles continued

Source	Summary	Year	Citations
[38]	The researchers of this work investigated the viability of ranging algorithms for LoRa based on TOA, TDOA, RSSI and a phased based approach (proposed by the researchers). This work determines through a combination of, presentation of observations from other authors and mathematical analysis that phase based localisation maybe the best to improve LoRa repeatable accuracy. Specifically getting it to GPS and WiFi repeatable accuracies of under 5 m. The authors cite significant signal attenuation following barrier penetration, a smooth time domain signal waveform and low resolution internal clocks as limitations for TDOA, TOA and RSSI respectively.	2018	7
[9]	This whitepaper by LoRa details the potential viability of LoRa for navigation. The document highlights key concepts such as the influence of transmitter-receiver geometry on position errors. Additionally, the authors summarise the TDOA method of localisation as well as giving documented application scenarios from animal tracking to waste tracking.	2018	3
[39]	The authors of this work proposed two TDOA based algorithms to estimate position of a stationary point. Their experiment was carried out in Denmark with four gateways encompassing an area of approximately $9km^2$. Using their algorithm they were able to achieve a repeatable accuracy of 100 m. However, the authors did not provide details of the specific SF, BW or CR used. Lastly, their work focusses specifically on the TDOA method	2017	100

A rigorous literature review shows that most of the frequently cited work in LoRa localisation or navigation focuses on either the TDOA method or RSSI method of localisation.

The next section details the taxonomy of propagations models as well as the statutory requirements of the national radio resource regulatory body, the Botswana Communications Regulatory Authority (BoCRA) and lastly metrics of interest when working with propagation models.

2.4 Taxonomy of Propagation Models

Phillips et al. proposed a taxonomy of wireless path loss and propagation models [40]. The taxonomy categories propagation models as follows:

- Theoretical/Foundation models,
- Basic models,
- Terrain models,
- Supplementary stochastic models,
- Stochastic models,
- Many Ray models,
- Active measurement models [40].

Table 2.4 and table 2.5 show the classifications of the taxonomy by [40]. Specifically, the tables contain the model name, category, the available coverage notes and the year it was first documented.

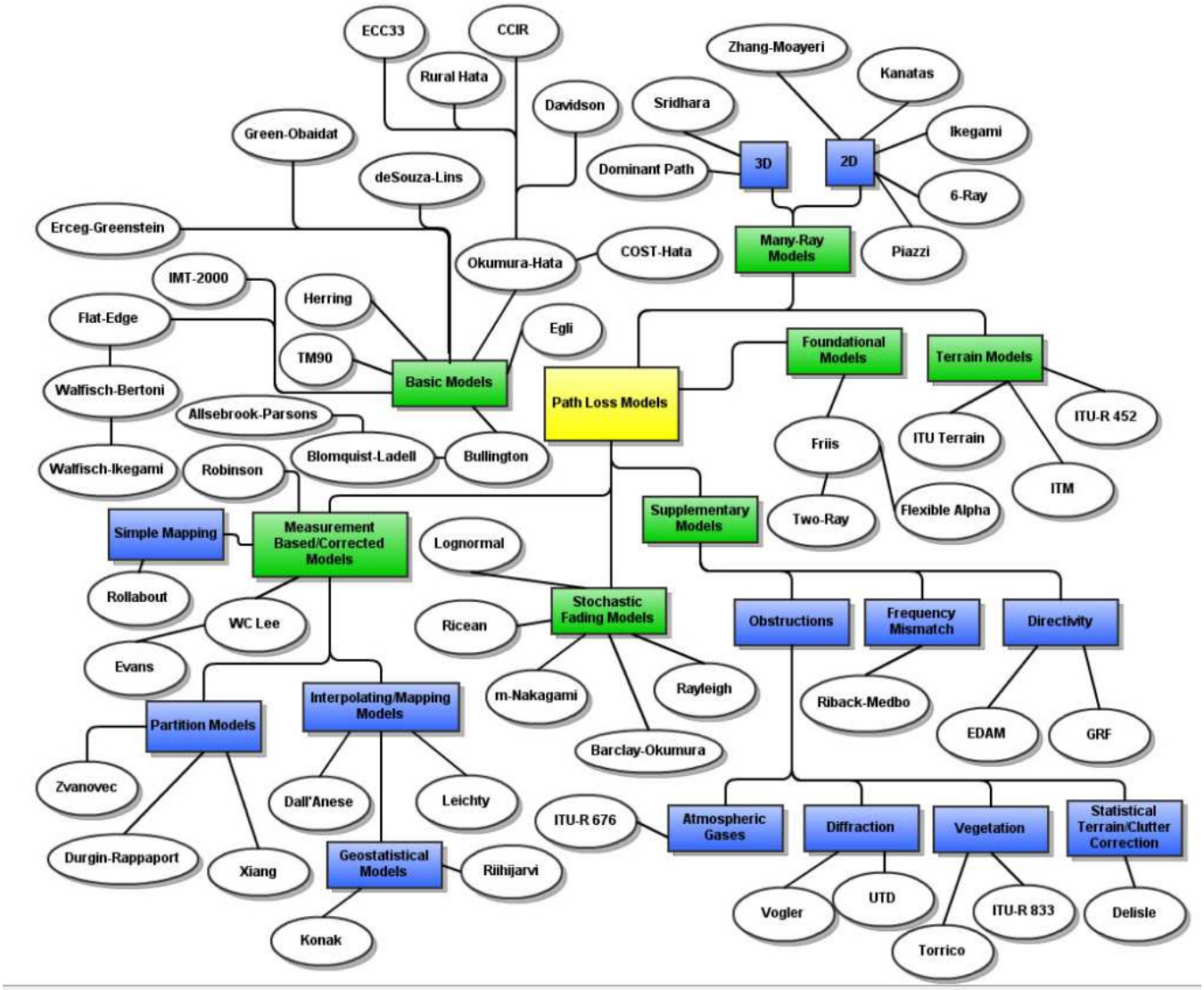


FIGURE 2.7: Phillips et al propagation model taxonomy illustrated for easy visualisation. The illustration shows the main classes of propagation models in green, the subclasses in blue and the actual model names in white. [40]

TABLE 2.4: Propagation models classification by [40]

NAME	**CATEGORY**	**COVERAGE NOTES (frequency (f) and coverage distance (d))**	**YEAR**
Friis' Freespace (Friss)	Foundation	$d < (2a^2)/\lambda$	1946
Egli	Basic	30MHz < f < 3GHz	1957
Hata-Okumura (Hata)	Basic	1Km $<$ d $<$ 10Km 150MHz $\leq$ f $\geq$ 1500MHz	1968
Edwards-Durkin (edwards)	Basic/Terrain	f $\in$ 85, 167, 441MHz	1969
Allserbrook-Parsons (allesebrook)	Basic/Terrain	$\in$ 85, 167, 441 MHz	1977
Blomquist-Ladel (blomquist)	Basic/Terrain	f $\in$ 85, 167, 441 MHZ	1977
Longley-Rice Irregular terrain model (ITM)	Terrain	1Km $\leq$ d $\geq$, 20Mhz $<$ f $<$ 20Ghz	1982
Walfisch-Bertoni (Bertoni)	Basic	N/A	1988
Flat-edge (flatedge)	Basic	N/A	1991
TM90	Basic	d $\leq$ 10miles, $h_1 \leq$ 300ft	1991
Cost-231	Basic	1Km $<$ d $<$ 20Km	1993
Walfisch-Ikagami (walfisch)	Basic	200m $<$ d $<$ 5Km, 800MHz $<$ f $<$ 2GHz, 4m $< h_b <$ 50m, 1m $< h_m <$ 3m	1993
Two-Ray/ground reflection (two ray)	foundation	N/A	1994
Hata - Davidson(davidson)	Basic	1Km $<$ d $<$ 300Km, 150MHz $<$ f $<$ 1.5GHz, 30m $< h_b <$ 1500m, 1m $< h_m <$ 20m	1997
Ericsson 9999	Basic/Terrain	150MHz $\geq$ f $\leq$ 2GHz	1997

TABLE 2.5: Continuation of propagation models classification by [40]

NAME	CATEGORY	COVERAGE NOTES	YEAR
Oda	Basic	N/A	1997
Ercog Greenstorm (ercg)	Basic	f = 1.9GHz Suburban	1998
Directional Gain reduction factor (grf)	Supplementary	f = 1.9GHz	1999
Rural Hata	Basic	f $\in$ 160, 450, 900 MHz (Rural Lithuania)	2000
ITU-Terrain (ITU)	Terrain	N/A	2001
Stanford University Interim (SUI)	Basic	2.5 < f < 2.7GHz	2001
ITU-R	Basic	1Km < d < 10Km, 1GHz < f < 2GHz, 30m < h_B < 200m, 1m < h_m < 10m	2002
Green-Obaidat (green)	Basic	N/A	2002
ECC 33	Basic	1Km < d < 10Km, 700 < f < 3000MHz, 20m < h_1 < 200m, 5m < h_1 < 10m	2003
Riback-Medbo	Supplementary	460MHz < f < 511GHz	2006
ITU-R 452	Terrain	N/A	2007

2.4.1 Statutory Regulations

LoRa operates in three (3) frequencies depending on the country/region of operation namely; 868MHz in Europe, 915MHz in the USA and Botswana and 433MHz in Asia as well as Botswana [5]. Botswana has radio bands which fall under region 1 [41]. Table 2.6 shows the legal ISM bands in Botswana.

TABLE 2.6: BOCRA documented ISM bands [41]

CENTER FREQUENCY	BANDWIDTH	UNIT
13560	13553 - 13567	Hz
27120	26957 - 27283	Hz
6780	6765-6795	Hz
40.68	40.66 - 40.70	MHz
433.92	433.05-434.79	MHz
915	902 - 928	MHz
2450	2400 - 2500	MHz
5800	5725 - 5875	MHz
24.125	24 - 24.2517	GHz
24.125	24 - 24.25	GHz
61.25	61-61.5	GHz
122.5	122-123	GHz
245	244-246	GHz

2.4.2 Propagation Metrics

This section defines the metrics commonly used by other researchers to compare theoretical path loss against actual path loss. Metrics used by researchers include the following:

RSSI: Received signal strength indicator informs the user of the power of the received signal from the source in Dbi versus the distance from the gateway. The RSSI may decline linearly depending on various attributes including topology, atmospheric conditions, presence of objects/bodies in the fransel zone.
PRR: Packet reception rate measures the number of packets received at the receiver vs what was originally transmitted at the source.
SNR: The SNR or signal to noise ratio is a ratio of the actual useful message power to noise power in a received signal.
PER: PER is the packet error rate which refers to the fraction of received packets which are erroneous vs the ones that can be recovered for information.

The next section details the propagation models which are viable for use in the 915MHz ISM band.

2.5 Propagation Models for the 915MHz ISM Band

Propagation models are classed into three categories;

- Empirical Models are based on gathered measured data in a given area [21]. These models will often be simplistic and general, as a consequence of this it will typically have a low accuracy [21] [28].
- Semi-deterministic models similarly are based on empirical measured data while also utilizing determinate aspects computed based on the application area [21]. The consequence of this is the improved accuracy relative to the empirical models.
- Deterministic models are site specific to the area. Furthermore deterministic models require significantly more types of data including geometric and geographic information [21]. These models have a very high accuracy.

All the models used in describing LoRa propagation take into account the large scale fading effects of the channel large scale fading effects . This characterization indicates the channel variations of strength over time and over frequency . Path loss is applicable in these scenarios as it is a function of distance and shadowing, caused by things such as natural formations and buildings. Furthermore, if the transmission distances are within the order of a terrestrial macro cell size ($1km^2$), the path loss is typically frequency dependent . Therefore, path loss is invariably a result of a dissipation of radiated energy by the transmitter as well as due to effects of the propagation channel [10][11]. Path loss and shadowing are phenomena which occur when signals typically travel distances of 100m and 1000m hence the term large scale fading [11].

2.5.1 Free space pathloss model

The FSPL model falls in the foundational or basic path-loss model category [40] [42]. The model predicts path-loss as a function of the square of distance less the antenna gains at the receiver and transmitter. This model is simplistic in nature and does not take into account the channel fading effects and assumes that the channel is vacuum. Equation 2.41 is the closed mathematical form of the model [42]

$$FSPL(dB) = 20(log_{10}(d) + log_{10}(f) + \frac{4\pi}{c}) - G_m - G_b. \tag{2.41}$$

Where, $FSPL$ is the loss in power in decibels, d is the distance from the transmitter to the receiver either straight line or euclidean in km, f is the frequency of operation in MHz, c is the speed of light in m/s, G_m is the gain of the transmitting antenna, and G_b is the gain of the receiver antenna.

2.5.2 COST 231- Walfish Ikagami pathloss model

The COST 231- Walfish Ikagami path-loss model is a modification of the COST231 developed by the Coorperation in Science and Technology, a European funded program [42]. This model has previously been applied to 2G and 3G technology and is applicable to the 915MHz used in region 1 for LoRa applications [40]. Table 2.5

shows the frequency, transmitter (TX) and receiver (RX) height constraints of this model.

$$PL_{los} = 42.6 + 26log_{10}(d) + 20log_{10}(f). \tag{2.42}$$

2.5.3 Ericsson 9999 pathloss model

This model was developed to predict path-loss for transmission frequencies of up to 2GHz [42]. The path loss model is able to predict path loss for different environments specifically; rural, suburban and urban environment. A closed loop form of the path-loss model is given by equation 2.43 and equation 2.44. Specific model constraints are provided in table 2.7.

$$PL_{eric999} = a_0 + a_1log_{10}(d) + a_2log_{10}(h_{te}) + a_3log_{10}(h_{te})log_{10}(d) - 0.2([log_{10}(11.75h_{re})]^2) + g(f), \tag{2.43}$$

$$g(f) = 44.49log_{10}(f) - 4.78(log_{10}(f))^2. \tag{2.44}$$

The variables a_0, a_1, a_2anda_3 are specified in table 2.7.

TABLE 2.7: Ericsson 9999 model parameters

ENVIRONMENT	**URBAN**	**SUBURBAN**	**RURAL**
a_0	36.2	43.20	45.95
a_1	30.2	68.93	100.6
a_2	12.0	12.0	12.0
a_3	0.1	0.1	0.1

Where a_n is an environmental constant unique to the type of environment, h_{te} is the height above ground of the transmitter antenna, h_{re} is the height above ground of the receiver antenna.
The next section will provide details on the systematic literature review used to determine the different applications of LoRa.

2.6 Systematic Literature Review

A systematic literature review was done to retrieve answers to the research questions. The research questions were developed after a precursory literature review and the formulation of the project objectives.The results of the systematic literature review were published in a peer reviewed journal and aspects of the study are in the following sections of this chapter. Details of the SLR search protocol is specified in table 2.8.

TABLE 2.8: Systematic Literature Review Summary

Characteristic	**Value**
Review type	Systematic literature review
Research question(s)	What is Lora and how does the PHY layer function(RQ1),What is the diversity and range of the LoRa scheme use cases?(RQ2) How is LoRa network performance measured ?
Purpose	Guide researchers and practitioners using/intending to use LoRa on the limitations and ideal use cases.
Search method	Automated and hand search, citation analysis, previously known articles,
Databases used	IJECE, IEEE Xplore, ScienceDirect, Google scholar, ACM digital library, Springer
Population	Empirical studies relating to LoRa and LoRaWAN applications, tests and use cases
Study types	Experiments, case studies, observational studies, simulation.
Inclusion criteria	(i) Refereed paper (journal or conference) (ii) Empirical study (iii) Copy of the article available in the English language
Search date	07/01/19 - present
Article dates	2010 - 2019 plus in press articles

2.6.1 Research Questions

The research questions specify the content, concepts and experimental results to be documented. By providing answers to the research questions, the research project is able to fill in knowledge gaps and add to the body of knowledge.

RQ1:What is the diversity and range of the LoRa scheme use cases?

Rationale: research question 2 will establish the different applicable use cases of LoRa technology. Furthermore it will establish the criterion used to determine the appropriateness of a given LPWAN technology in a specific area.

RQ2: How is LoRa network performance measured?

Rationale: Performance measurement in this context will specify the means by which deployment is tested (test-beds). Moreover, this research question will allude to the metrics used and the validation methods as ranked by prevalence.

2.6.2 Search Strategy

Previous articles on LPWAN technology have mainly focused on documented use case scenarios whether academic or commercial. Additionally, for most articles used in this study, care was taken to derive performance reports from OEM white-papers as well as journals, and conference articles/papers pertaining to the investigation LPWAN practical performance limitations. Lastly, novel use cases and performance experiences were solicited from Medium, which is an online repository of DIY and hobbyist practical exploits of LPWAN SDR and MAC layer manipulation.

2.6.3 Search Terminology

The following search terminology was used to ascertain journal, article and white-paper information on the subject areas.

The following steps were used to build the search terms based on existing literature and material:

1. Derive major terms from the research questions.
2. Identify synonyms and alternative spellings for major terms.
3. Using the Boolean OR and AND to incorporate and link alternative spellings and synonyms.

The search terminology development steps above resulted in the establishment of the following search strings:

LoRa OR LPWAN OR LoRaWAN Propagation Model(s) OR Performance OR Path loss AND/OR 433MHz/868MHz band LPWAN OR Low power Wide Area OR Low Power Area. SNR OR Path loss Performance OR BER OR Propagation OR PRR OR RSSI. Narrowband OR Chirp Spread Spectrum AND/OR LPWAN OR LoRa OR Long Range AND Path loss OR Propagation".

2.6.4 Search Process

The following process was used to search, filter and store material from various journals. A three (3) step process is outlined below:

Step 1

Enter search terms in google scholar/IEEE xplore/Springer/ACM/Elsivier/MDPI/Wiley Online sources/IJECE. Apply forward search via citations in search results, keep material with relevant timeline 2010-2018. Search titles of found journals for relevance. Download filtered journal with satisfactory keywords and title

Step 2

Review abstract of Step 1 filtered material. Keep document that is relevant according to contents of abstract. Use references in accepted papers to determine/find new material.

Step 3

Identify new articles relevance in accordance with Step 2, note duplicates and return to Step 1.

2.6.5 Results of the Systematic Literature Review

The following subsections detail the findings of a systematic literature review performed to understand LoRa technology, applications as well as performance metrics and test-beds used by practitioners and researchers.

RQ1:What is the diversity and range of the LoRa scheme use cases?

LoRa boasts resilience to noise, multipath fading, Doppler shift resilience as well as long range transmission rates [17]. [43] observed numerous indoor and outdoor applications. For context the largest global open source network of LoRa gateways is currently "TheThingsNetwork" [16]. "TheThingsNetwork" can also be regarded as the application layer allowing for management of data collected from the perception layer and routed through the network layer as described by [44]. Some of the most novel use cases observed in literature are provided in table 2.9.

The authors in [45] discussed that LoRa technology is limited in applications, mainly those with a tolerance to any jitters. This eliminates applications needing constant feed of multimedia. Additionally, the authors correctly point out the limitations of LoRa in so far as real-time metering is concerned as there are duty cycle limitations imposed on the ISM band usage. It is also worth noting that areas of industrial control will remain out of reach as with the lowest SF, equation 1.1 shows that the delay will be 40 ms before any control signal is received.

Nonetheless, the fact that LoRa's MAC layer can be easily modified opens the door to multiple use cases. An example of LoRa MAC layer flexibility is when authors of [46] created LoRaBink for energy efficient multi-hop transmission. Similarly, with smart encoding techniques transmission of images is possible.

TABLE 2.9: LoRa and LoRaWAN use cases [35]

Source	Application Summary	Class
[16]	UK flood network. A series of water level sensors deployed across rivers around the UK to alert residents of dangerous water levels and flood risks.	Real time monitoring
[47]	The authors documented their findings in the use of LoRa for tractical tracking systems in Thailand.	Real time covert monitoring
[48]	The researchers were able to find positive results with a mangrove monitoring. This was done through the transmission of images over the LoRa physical layer with a custom encryption technique.	Multimedia and agriculture monitoring
[49]	Carlsson et al investigated deployment of LoRa at the 868MHz frequency in three different scenarios: dense forest, open setting and high elevation. The experiment illustrates the LoRa physical layer and LoRaWAN resilience in various settings.	Performance evaluation
[50]	Juha et al were able to perform experiments on the effects of moving receivers on both land and water in urban and industrial environments. These settings are the city of Oulu in Finland as well as a dock in the same area.	Industrial monitoring

RQ2: How is LoRa network performance measured?

This research question will draw attention to how the performance of various deployments observed in literature was done with emphasis on validation, test-bed and metrics. Jaco Marais et al. authored a paper summerising the various test-beds used to test LoRa and LoRaWAN performance [51]. Network performance for LoRa is conducted on the MAC layer's ability to transfer packets reliably. Performance is measured on the following: PRR and PER, the DER and percentage loss of packets. Additionally, the physical layer's performance is often gauged based on the RSSI, SNR and the BER as well as the NEC [52].

Intra-scheme metrics of comparison

The metrics on which LoRa and the next widely available scheme (Sigfox) are to be compared are the availability of QoS, node battery life, packet latency, scalability, payload length, network coverage, global adoption, cost of deployment and the ability to be open source. These are properties derived from literature and reflect the observations of practitioners as well as researchers.
QoS: Sigfox and LoRa have very poor QoS. However, LoRa through the LoRaWAN protocol offsets this by broadcasting information to all nearby base stations in essence increasing the degrees of diversity. Sigfox will similarly transmit its message multiple times with no acknowledgements (typically three times by default) [6].
Battery life and latency: Sigfox and LoRa have end nodes consuming lower energy through the use of function states. The exception in this case being LoRa class C devices. Similarly, LoRa class C having better latency compared to class A, B as well as Sigfox [6].
Scalability and payload length: Sigfox and LoRa base stations can handle 50 thousand devices each per base station making them fairly evenly matched in this regard. More to this, LoRa and Sigfox have 243 bytes [5] and 12 bytes [6] respectively with the latter characteristic tipping the favor to LoRa.
Network coverage and range: Sigfox commands the longest range, with line of sight (LoS) communication capable of effective transmission at 40 km [6]. The second longest range with LoS range of approximately 20 km is LoRa [7].
Global adoption: According to [6] LoRa is deployed across 42 countries while Sigfox is only available in 31. Additionally, LoRa allows communication hybridization by using different communication schemes to transmit data effectively over a given distance.
Cost: The hardware cost associated with Sigfox is significantly high due to the none liberalized hardware ecosystem [6]. However, the LoRa Alliance has seen hardware development of LoRa from other organizations such as Ada-fruit and STM significantly improving availability of both enabled devices and public gateways [6] [12].
Open source: Considerable work has gone on to allowing this on the LoRa modulation scheme. The Sigfox ecosystem remains under the tight control of the creators of Sigfox. Whereas SEMTEC's LoRa continues to enjoy widespread support and experimentation of hobbyists and professionals alike [8] [13] [6].

The performance of LoRa compared to the next most popular communication scheme Sigfox is summarised in figure 2.8 .

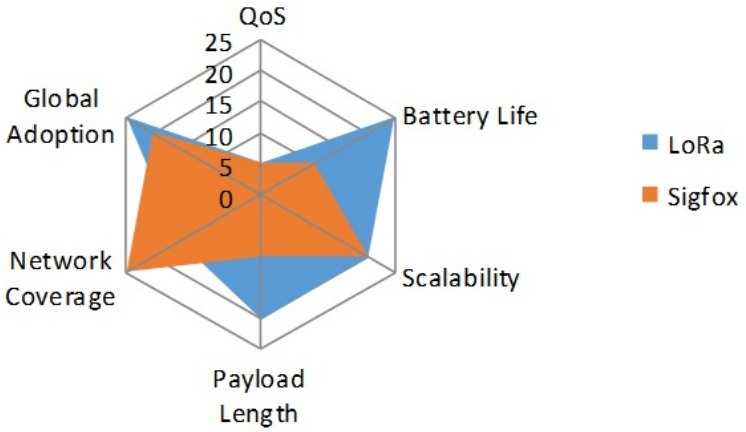


FIGURE 2.8: LoRa and Sigfox comparison

LoRa Performance metrics and test-beds

TABLE 2.10: LoRa and LoRaWAN performance metrics, validation

Source	Test-bed	Performance metrics	Validation method
[53]	Semtech SX1307 transceiver as a gateway, LoRaWAN testing done using Multitech Mdot devices in the 868MHz band	RSSI	Project monitoring
[21]	TI C110 radio module in the 433MHz band	RSSI	Dynamic analysis, simulation
[50]	Kerlink LoRa IoT station D100-1000 antenna (base station), and LoRa mote Semtech SX1272 (mobile node)	RSSI, Path-loss exponent, path-loss intercept	Project monitoring
[54]	SX1272 LoRa sheild with arduino nucleo and raspberry pi, IC880a concentrator and STMicroelectronics Nucleo-L073RZ MCU board	RSSI, SNR, PRR	Project monitoring
[55]	RN248 (RX side), RHF25008 with SX1301 chip (TX side) with a 5dBi antenna, OBCI smart everything fox board at the receiver	RSSI, PDR	Simulation, project monitoring
[32]	Netblocks XRange SX1272 LoRa RF module	PRR, δ_i, RSSI	Project monitoring and simulation

Through this SLR, the authors were able to find 13 articles to ground the study and answer the 3 research questions outlined in section 3. The main findings of this study are the following:

- LoRa technology and LPWANs have a wide array of applications with an almost equal number of potential research areas mostly into spectral access, quality of service, and MAC layer modifications,
- The main reasons for which LoRa has bloomed in IoT and research spaces is invariably true as the scheme is able to achieve very long communication distances however there is a catch. Distilling performance into two areas the MAC layer and the PHY layer. Due to the MAC layers' limitations in terms of QOS and the static nature of the protocol significant performance maybe lost as a lot of testing must be done to establish which CR, BW and SF are best suited for a particular area to maximise PRR, NEC as well as DER. With regard to the physical layer, in all instances where little or no disruption of the Fresnel zone occurs, signal propagation is observed to be high.The authors observed that it is possible to obtain relatively high levels of RSSI and still have significant PER invariably leading to inefficiency in the network implementation mainly due to poor settings at the MAC layer.
- Being an ISM based scheme, the duty cycle limitations of LoRa imposed by statutes poses significant bottlenecks in terms of accessibility as the ALOHA protocol means significant wait periods can be expected between transmissions in very RF active zones: urban and rural landscapes. This turns out to be a non-hindrance in the application area Botswana aspires for, namely agricultural monitoring, as most areas of interest have little RF traffic in the sub GHz ISM bands. However spectral measurements may need to be taken to confirm with a quantitative certainty in future.
- LoRa technology range tests/evaluations are predominantly used in the developed world. Thus the real world behaviour of LoRa is not documented in the Southern Africa although the number of gateways in the area is increasing. It is therefore the position of the authors that more field testing be done to adapt the ADR properties of the technology in Botswana and Southern Africa as a whole to ensure more efficient network deployments in agriculture and IoT novel applications.
- More work is needed to isolate appropriate pathloss and propagation models for any area. Several authors have observed the disconnect between real-world readings and traditional propagation models. This is especially true for those based on the Fresnel equation and traditional path loss model. However, in all experiments it was noted that the height above ground is critical in improving range.

2.7 Chapter Summary

Chapter 2 provided a literature review of the LoRa and the associated concepts which guide this research. Specifically concepts addressed include, LoRa,LoRaWAN, LPWAN technology comparison metrics, HDOP, geolocation in LoRa and propagation models

Chapter 3

Methodology

Chapter 3 details the methodology of the study. The chapter identifies specific objectives and gives a step by step detail of how the experiments necessary to achieve the objective are performed. Specifically, the chapter discusses the receiver sensitivity analysis, propagation model performance comparisons, gateway placement techniques and the metrics of interest with regard to navigation. The methodology employs a repeated setup methodology based on the works by [9], [27], [56] and [21]. Additionally, the simulations are based in the BIUST Palapye campus. A block diagram, figure 3.1 summarises the major components of the experimental methodology.

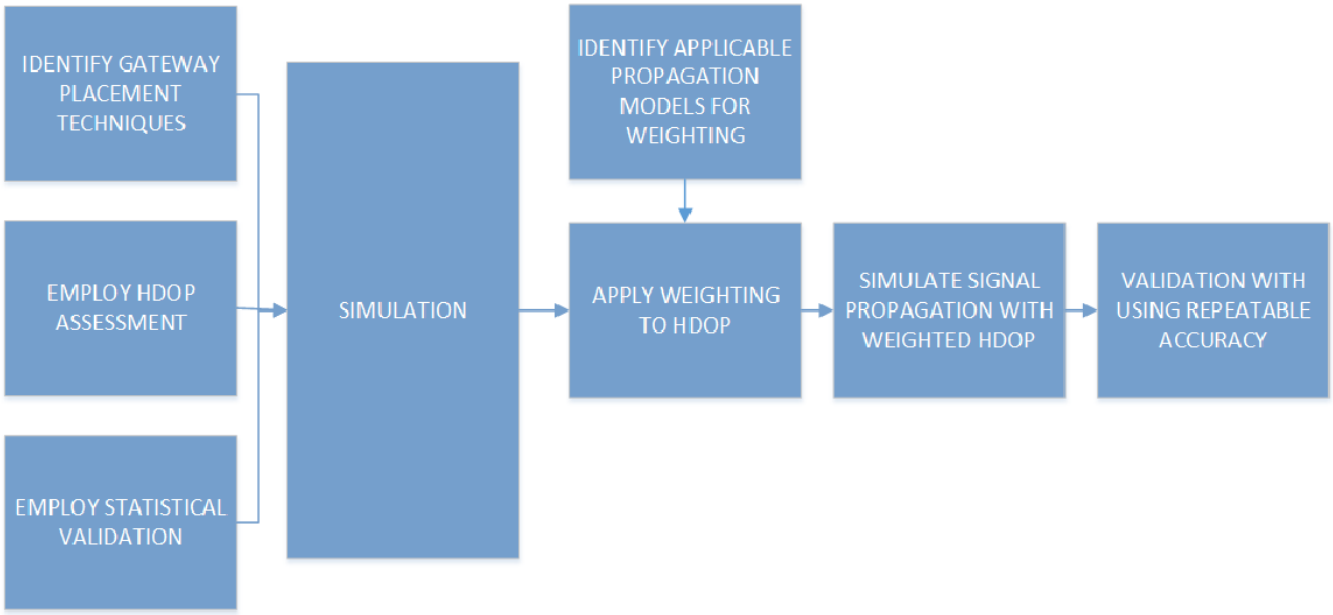


FIGURE 3.1: The proposed experimental methodology based on the work of Lebekwe et al, the LoRa alliance strategy committee, Sigweni el al and Milankovich et al.

3.1 Receiver sensitivity analysis

This section details the technique by which gateways placement will occur in the chosen geographical area. The placement technique in the context of navigation, will either amplify or not introduce any errors in the navigation process. For this reason, a well informed placement will decrease navigation errors due to poor receiver-gateway geometry.

Figure 3.2 shows the proposed area where a coverage map is to be generated, it has an approximate area of $25km^2$. The coverage area is sparsely populated with a few high rise buildings and large open spaces covered in trees and bush. This proposed coverage area is a reasonable facsimile for other potential areas where ranging maybe critical but long end node battery life and range are key deliverables such as IOL applications [9].



FIGURE 3.2: BIUST coverage area

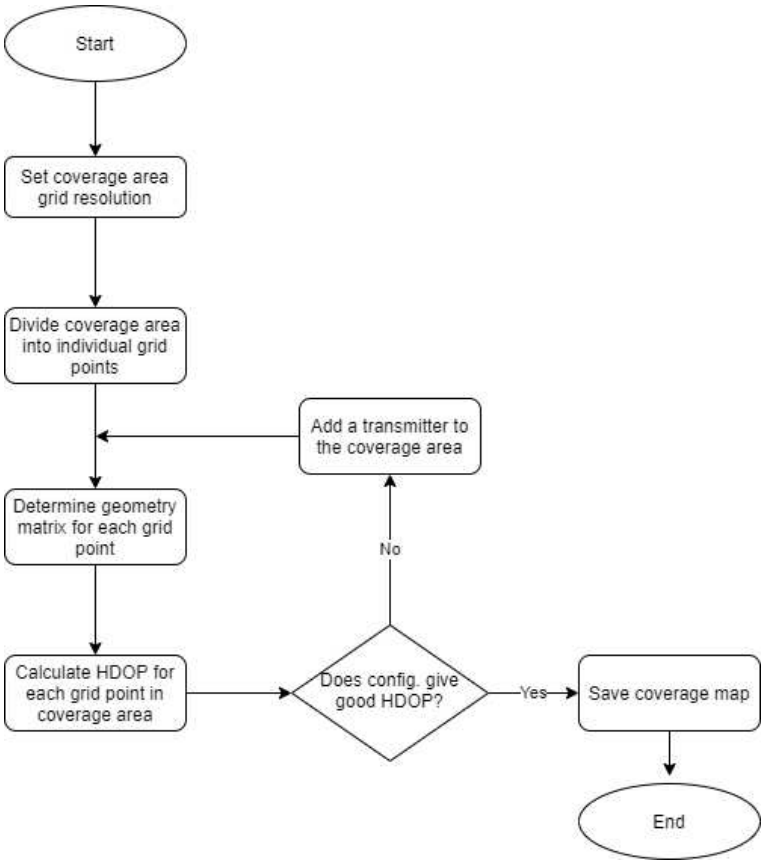


FIGURE 3.3: HDOP gateway placement algorithm

The placement of gateways in the coverage area is done at the proposed gateway sites in table 3.1, these locations are visualised in figure 3.4. Placement is performed systematically starting with 3 gateways and performing a HDOP computation, assessing the result based on the HDOP scores in table 1.1 before adding more gateways and repeating the process until most of the coverage area has a good HDOP. Figure 3.3 illustrates the steps of the process. It is also observed that the placement of gateways is more likely to result in a good HDOP when gateways are placed such that they form equilateral triangles. This means as more gateways are placed, it is important to place them at the vertices of imaginary tessellated triangle positions. The use of this procedure will result in comparatively good HDOP in the area bounded by the gateways. Using the observation of triangular tessellation results in a placement similar to figure 3.5. It is assumed that the gateways are receiving LoRa signals via LOS, and multipath effects are considered to be negligible. The SNR is assumed to be significantly above the minimum levels specified in table 2.1, and the gateways are assumed to be perfectly synced with an uncertainty of 1×10^{-6} seconds.

TABLE 3.1: Possible BIUST gateway sites coordinates

gateway Name	**BIUST**
LoRa 1	-22.575827, 27.089860
LoRa 2	-22.572183, 27.091939
LoRa 3	-22.571785, 27.125548
LoRa 4	-22.582362, 27.131265
LoRa 5	-22.588882, 27.131329
LoRa 6	-22.588869, 27.135194
LoRa 7	-22.605359, 27.154082
LoRa 8	-22.621233, 27.137303
LoRa 9	-22.634129, 27.113086
LoRa 10	-22.619672, 27.106026
LoRa 11	-22.615757, 27.107820
LoRa 12	-22.595328,27.097094

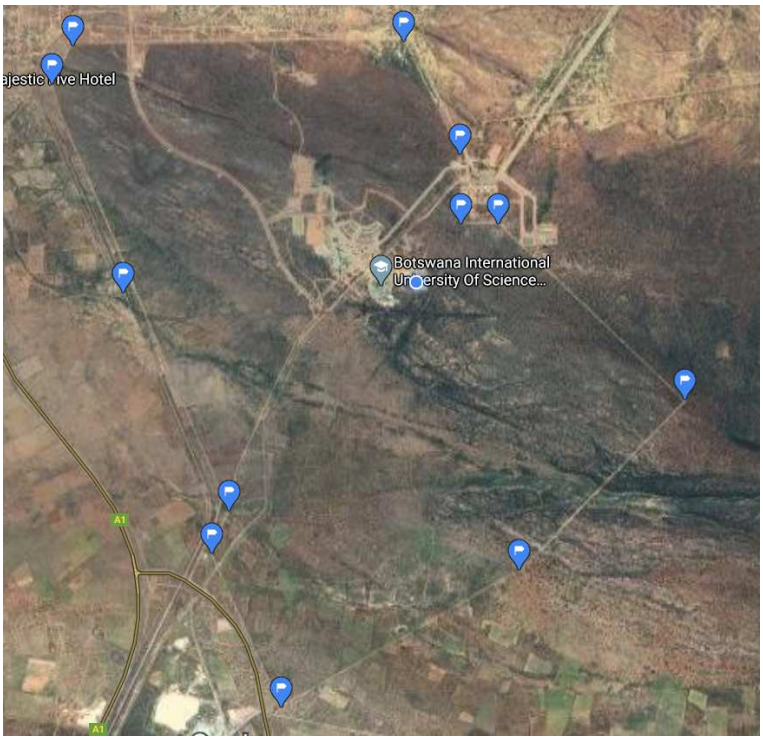


FIGURE 3.4: Possible gateway sites around the BIUST geographical area indicated by the blue mark points

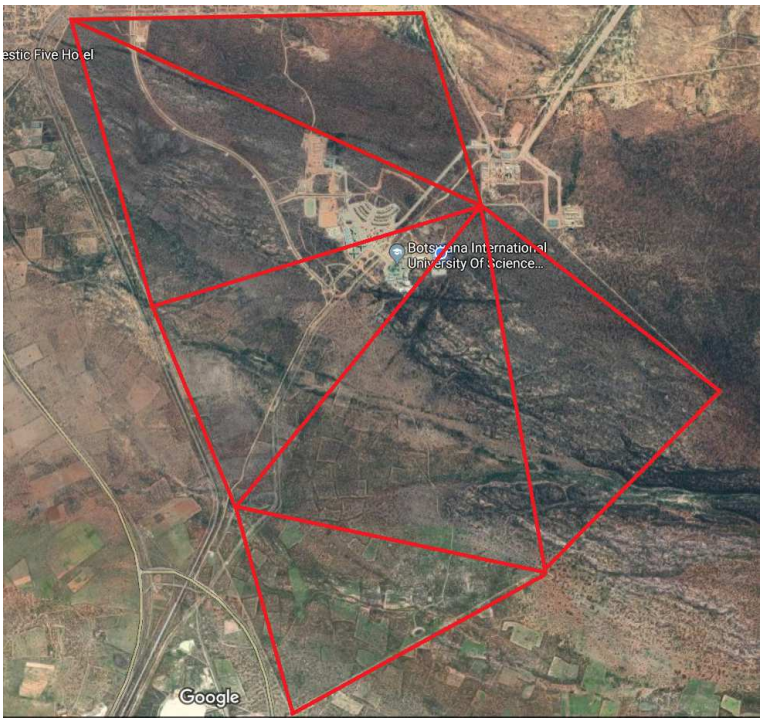


FIGURE 3.5: Triangularly tessellated gateway placement in proposed locations from 3.1

The following section details the gateway placement techniques that were used in the study as well as the justifications for their selection.

3.2 Gateway placement Techniques

The following subsections provide descriptions and justifications of the three placement techniques to be tested. These techniques are derived from LoRa literature and are tested to determine the best gateway placement technique for LoRa navigation applications.

3.2.1 Random placement

Random placement is performed to provide the authors with a benchmark placement method with HDOP as the performance metric. When performing random placement, a set of longitude and latitude coordinates equal to the number of gateways required are randomly generated using the software tool written by the author. HDOP performance of the resulting gateway configuration is then determined. Random placement places no limit on the minimum number of gateways needed to achieve the specified coverage requirement. The following steps are followed;

- the gateway placement starts with the minimum of three with the number of gateways increased by one, depending on the coverage requirements
- A set number of iterations for any random placement configuration is performed and the resulting HDOP score is determined. In this study the number of iterations were chosen to be equal to 1000 and the HDOP score was calculated out of 30 grid points. Grid points with HDOP performance of 1 or less are

considered to have good HDOP as shown in table 1.1. Each iterations' score of good HDOP grids out of 30 stored,

- and the number of gateways are increased by 1 until a certain number of gateways gateways are deployed. In this study the total number of gateways was set to 12.

The calculation will show the gateway configuration's influence on the position error in each case. The HDOP score generated from the placement is the number of grid points with a good HDOP score out of 30 in the coverage area. This placement by nature is not does not take into account gateway geometry and the expectation is in most deployments it will fail to meet the coverage requirement that the authors specified. However, given that random chance is at play it is expected for there to be outliers in both very good coverage and very poor coverage.

3.2.2 Naive placement

A naive placement technique of LoRa gateways was observed in literature in the work of [57], [58], [59] and [60]. The summaries of the articles and their methods are given by table 3.2. None of the studies were explicit in the manner by which gateways were placed in the coverage area. However, each study placed gateways in a manner such that there were no overlaps in their physical locations. Additionally, their placements guarantee that moving nodes are able to get LOS communication are they move across their grids or coverage area.

TABLE 3.2: LoRa naive deployment articles

Source	Summary	Year	Citations
[60]	The article proposes an analysis of gateway placement, spreading factor assignment, and power allocation in LoRa network planning. Emphasis is in the spreading factor assignments and power allocation to maximise network lifetime. Additionally a placement strategy is proposed in the work, however it is unsuitable for a ranging application.	2019	6
[58]	This article investigates heterogeneous network deployments and Spreading Factor (SF) allocation strategies. The researchers of this study determine the performance of homogeneous networks (i.e. when all the nodes select the same LoRa configuration) and heterogeneous networks (i.e. when each node selects its LoRa configuration according to its link budget or their needs) for large scale deployments (up to 10000 nodes per gateway). They further developed a LoRa Module, based on improved WSNet simulator, including a spectrum usage abstraction, the co-channel rejection due to the quasi-orthogonality of SFs and the gateway capture effect. Their study gives performance comparisons in terms of reliability, network capacity and power consumption for homogeneous and heterogeneous deployments as a function of the number of nodes and the traffic intensity.	2018	7
[59]	This article analyses the efficiency of large LoRa networks, specifically those with a minimum of 10000 moving nodes transmitting to the gateway. The article compares the existing adaptive data rate (ADR) and EXpLoRa-AIR of LoRa versus a new algorithm AD MAIORA with the moving nodes having homogeneous configurations (spreading factor(SF), frequency (F_c), bandwidth (BW), coding rate (C/R))	2018	5
[57]	This article investigates the effects of network densification through the addition of multiple gateways and node configurations. The researchers start with 3 gateways and 1000 nodes and increase the gateway numbers until 9 gateways assessing the effect of the different SF on the PDR and ratio of covered nodes with increased redundancy.	2019	0

When deploying naive placement of gateways it is assumed that the standard coverage is equal to the radius of a single gateway. In this scenario, and based on literature,the transmitted signal from a Lora gateway meets the SNR requirements

and that there is no packet loss and LOS exist over a distance of 1 km [61]. Assuming omni-directional gateway transmission, the area that a signal can be reliably detected is assumed to be a circle with the gateway at its centre, is equal to πr_{km}^2. Therefore the number of gateways required to cover a known area can be calculated by equation 3.2. In this scenario equation 3.2 showed that a minimum of 7.9 gateways would be required to service the coverage area, this figure was rounded up to the nearest whole number. The required gateways are placed in the coverage area as evenly as possible and not overlap. Once placement is done, HDOP is calculated to determine the score of the deployment out of 30. The result is compared to the imaginary triangular tessellation placement and random gateway placement.

$$A_{tx} = \pi r^2, \tag{3.1}$$

$$N_{tx} = \frac{A_c}{A_{tx}}. \tag{3.2}$$

where A_{tx} A and r are the gateway coverage area in square kilometres and its transmission range in kilometres respectively. The number of gateways needed to service the geographical area is given by N_{tx} and is calculated using equation 3.2.

3.2.3 Placement with imaginary triangular tessellation

Figure 3.6 shows the proposed gateway sites in the BIUST geographical area with gateways placed at the vertices of a triangle. Specifically, gateway A, B and C are placed at the vertices of one of the imaginary triangles. Additionally, the omni-directional/radial transmission of each gateway is shown in the colour of the gateway letter.

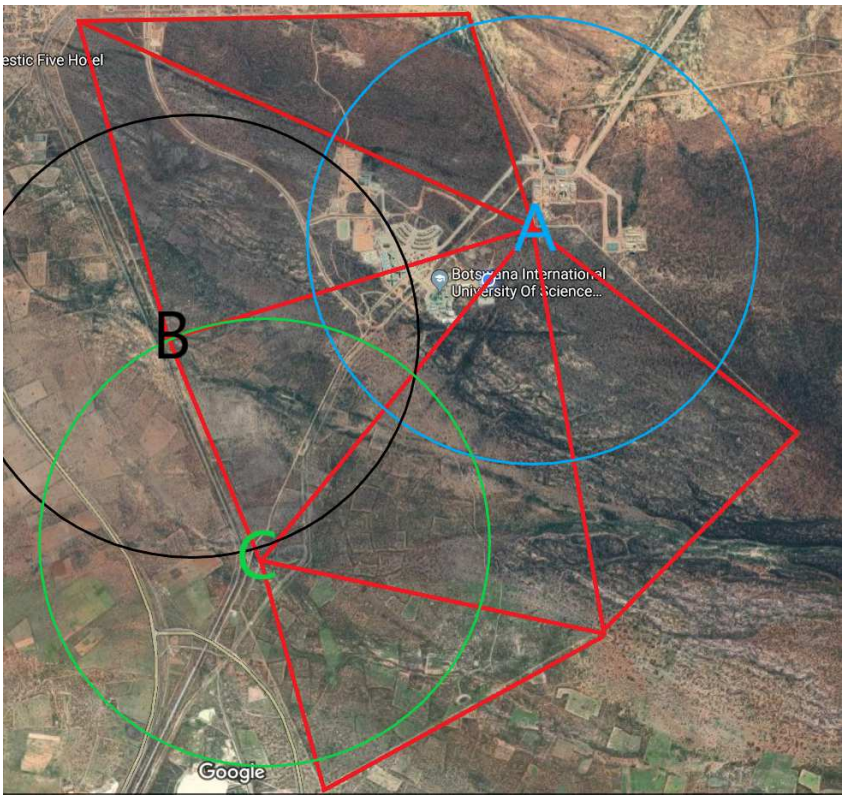


FIGURE 3.6: Placed gateways

Ideal placement of the gateways or gateways in a desired coverage area is illustrated in figure 3.7. This method of placement utilises triangular tessellation to optimally place gateways to maximise coverage in the coverage area with the minimum number of gateways. This relies on the use of polygon triangulation [62] and is a variant of the art gallery problem proposed by Victor Klee in 1973 [63].

However, unlike typical WSN sensor deployments a LoRa navigation placement setup requires that a moving gateway or node be placed within range of at least three gateways for sufficient ranging. Being within range means that the gateways are within the maximum/minimum transmission range of each other, as illustrated in figure 3.7 with A,B,C and A,C,D. Using the maximum or minimum range will generate the minimum number of of gateways or maximum numbers respectively. The overlapping areas between gateways A,B,C and A,C,D are over determined meaning that there are more equations to solve than the number of unknown variables. A moving node will therefore have high location accuracy due to a good HDOP within the zones of overlap.

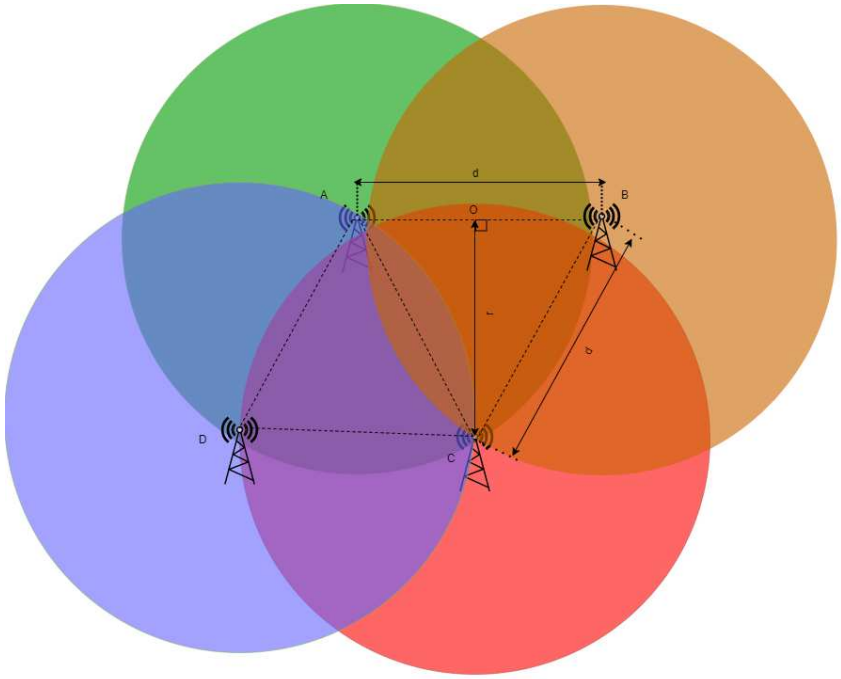


FIGURE 3.7: HDOP guided method, placed gateways

Optimally, d represents the distance within which a signal is detectable. This means that the received signal within this area meets the SNR requirements shown in table 2.1. Three gateways will therefore have distances d between them with the angle CAB, ABC and BCA being 60°. The perpendicular distance between a gateway (C) and two gateways (AB), a distance d from each other, is r. The variables d and r are specified in equations 3.4 and 3.3 respectively. The overdetermined solution therefore exists in an area calculated using equation 3.5. Assuming good HDOP in the coverage area, the required number of gateways may be approximated by equation 3.6.

$$r = \frac{\sqrt{3}}{2}d, \tag{3.3}$$

$$d = \frac{2}{\sqrt{3}}r, \tag{3.4}$$

$$A_o = \frac{\sqrt{3}}{4}d^2, \tag{3.5}$$

$$N_{tx} = \frac{4A_c}{d^2\sqrt{3}} - 1. \tag{3.6}$$

An assessment of the placement methods is then performed where imaginary triangular tessellation placement, is compared to the random gateway placement and a naive gateway placement with HDOP being the metric of assessment. It is worth noting that the placement method illustrated in figure 3.7 is idealised. In reality, a coverage area may not be perfectly symmetrical or a regular shape and so triangular tessellation is performed. The arrangement of gateways will be made as close to points representing the vertices of equilateral triangles as possible. An example of this is shown in figure 3.5. The next section details the statistical tests used to validate the different placement techniques specified in section 3.2.

3.3 Statistical Tests: Statistical significance and Effect size

The following subsections will provide explanations and descriptions of the statistical significance test and effect size respectively. In addition, justifications are given as to the choice of test in each case are provided. A brief description of the sample sizes of the simulation data is also provided.

3.3.1 Statistical significance

A statistical significance test determines the likelihood that the differences in results from 2 or more treatments are due to factors inherent in the individual methods or are due to chance. The measure of statistical significance is performed with a confidence limit [64] exceeding or being below a P value normally 5%. A 5% confidence level means that there is a 5% chance that the differences in performance are due to random chance. In the context of the three placement methods, gateway placement using imaginary triangular tessellation or guided HDOP guided placement, random placement and naive placement are compared. Specifically, the extent to which the main placement method achieves good HDOP in the coverage area, using the minimum number of gateways. This performance is compared to random gateway placement in a coverage map and placing gateways with no overlaps (naive placement) is determined. The determination is done using the HDOP coverage scores of each method; scores are the number of grid points with good HDOP out of 30 in the coverage area.

3.3.2 Effect size

The effect size is a measure of the difference in central tendency of results. The higher the effect size score the more likely that the difference between central tendency measures means one method is better/worse than the other. The interpretation is subjective and can lead to the wrong statistical inferences if not done correctly [65]. An effect size score ranks the difference in central tendency depending on the class of the measure (d, r or η^2) [66]. An η^2 score below 0.06 (exclusive) is considered small and is not acceptable. While and score between 0.06-0.11 (inclusive) is intermediate and acceptable, above 0.140 to 0.200 (inclusive) is a large effect size

TABLE 3.3: Simulation data characteristics

Property	**Random Placement**	**Naive placement**	**HDOP guided placement**
Sample size	1000	50	50
Median	9	14	21

and is acceptable. Acceptable scores of effect size mean the observed differences are large and conclusions maybe drawn of how effective or well a treatment/method performs while the converse is true for non acceptable effect sizes [64] [65].

3.3.3 Simulation Data

The simulation results generated using Matlab were observed to be highly skewed and not normally distributed. Simulation data summaries are illustrated in the box and whisker graphs in figure. 4.15. Table 3.3 shows the sample sizes and central tendencies of the three methods being tested. For results which do not exhibit normal distribution tendencies, statistical significance is determined using non-parametric tests such as the Wilcox Signed rank test if the data contains paired samples. Non-parametric tests are less susceptible to the skewing effect that outliers have on data [65] This study's authors determined that a Mann Whitney U Test was used as a the primary assessment for statistical significance and a Z statistic test was used to confirm the result. Secondly, in all three combinations of the tests an effect size was calculated to determine the significance of the differences in the measures of central tendency in this case median due to the skewed nature of the results.

Sigweni et al. proposed the use of blind analysis to assess effort estimation techniques and eliminate bias in the the assessment [65]. Key concepts outlined by the authors are the use of the blind analysis algorithm for two researchers; one researcher to label data separately, removing labels about the true identity of the technique while another researcher selects appropriate tests to determine statistical significance and effect size of the technique. Additionally, their work proposes the use of a random technique for benchmarking [67] [65] as some studies have noted that some reputable techniques sometimes fail to surpass random chance in their predictions. The work of the researchers highlights the importance of determining as accurately as possible the effectiveness of different techniques using quantitative methods, something which is done in the social sciences and medicine. The authors of this paper sought to use the same or similar techniques to quantify the performance of the placement methods, however the Mann U Whitney, Z score and η^2 measures were best suited for independent non normally distributed results [64].

The following section details the means by which empirical pathloss models will be assessed and used in our chosen geolocation application.

3.4 Empirical propagation model performance

The empirical models simulated in the study are this FSPL, COST 231-Walfish Ikagami and Ericsson 9999 path-loss models. These models fit constraints which are observed in real life deployments reviewed in the SLR with the search protocol in table 2.8. The list of applications that have used LoRa are given in table 2.9 [35]. Table 3.4 shows the proposed terrestrial navigation use case applied and described for this research..

TABLE 3.4: Use case table for terrestrial navigation/positioning

Item	**Description**
Usecase Name	LoRa navigation
Usecase Description	An actor wishes to determine the location of a LoRa gateway in a bounded geographical area (BIUST)
Actor	Organisation/Agent
Pre conditions	Object or Article or Animal being tracked has a class A LoRa transceiver module
Normal flow	1. A class A LoRa transceiver transmits a packet to at least 3 gateways in the geographical area, 2. Determine if RSSI meets minimum requirement for given SF, 3. Time synced gateways transmit packet time of arrival to application server, 4. Application server calculates proximity of transceiver relative to gateways and provides position fix.
Alternative flow	1. Step 1 and 2 are executed as before, 2. If SNR is below threshold packet is rejected and a notification is sent to application server. 3. System 'waits and listens' for new packet(s).
Post condition	Actor location determined or displayed.

3.4.1 Performance comparison

The work by [35] researched the performance metrics for LoRa deployments. [35] found that LoRa has gained widespread use in LPWAN applications due to the long ranges that LoRa signals can propagate using relatively little transmission power. When determining how deployments were evaluated. The authors of that work determined that monitoring of RSSI, SNR, PRR and path-loss were the primary metrics [68], [54], [45]. Table 2.10 shows the documented deployments and the performance metrics. In a positioning application, shown in table 3.4, a deployment with good HDOP will lead to TOA variance being the major source of error for position fixes. Specifically, the SNR in the TOA variance in equation 2.39 will determine the position uncertainty. The path-loss models show the power loss over a given transmission distance, which can be used to determine P_r, SNR and TOA variance. In the simulation the path-loss models will give the power loss over distance and the SNR. The simulation data for the path-loss models is listed in table B.1.

TABLE 3.5: Transmission characteristics 1

Transmission frequency (MHz)	**Transmission power (dbm)**	**gateway Gain(dB)**	**Receiver gain(dB)**	**Noise (dB)**
915	13.979	5	10	17.5*

TABLE 3.6: Transmission characteristics 2

Transmission frequency (MHz)	**SF**	**BW (KHz)**
915	7	125

*Noise is man-made noise in a quiet site for 900MHz[69] and noise figure [17]

3.4.2 Deployment of the gateways in the coverage area

Gateway placement is simulated with different gateway separations, SF,and pathloss models. The gateway deployment was done to achieve a 20 m repeatable accuracy over the chosen geographical area. The 20 m repeatable accuracy was chosen here to determine if LoRa can compete with other navigation systems such as eLoran and the theoretical accuracies for TDOA based navigation by LoRa of 20 m - 200 m [9]. First the gateways were arranged to form equilateral triangles of sides equal to 1000 m, 400 m and 200 m. This would make LoRa a valuable candidate in the navigation receiver proposed by [70]. Once the locations of the gateways in a geographical area are known, the geographical area is then divided into grid points of equal size. At each grid point the SNR is determined from the overall received signal and the system noise, N_{oise} given by:

$$N_{oise} = KTB. \tag{3.7}$$

where K is the Boltzmann constant equal to $1.38 \times 10^{-23} J/K$, T is the temperature in Kelvin, and B is the bandwidth of the system in Hz.

In our study the system noise is assumed to be the dominant noise. The overall received signal is determined by the difference of the transmitted power and the power lost along the propagation path. Power lost along the propagation path was estimated using Ericsson 9999, COST 231-Walfish Ikagami pathloss model, ECC-33 pathloss model and FSPL. The signal strength of sample gateways determined using the Ericsson9999, COST 231-Walfish Ikagami pathloss pathloss model and FSPL models and different SFs' for the 1500 m, 1000 m and 400 m gateway separation are illustrated in figures C.1 to C.27 in appendix C. In all illustrations, the magenta dots represent gateways, while the white border line demarcates the bounds of the coverage area.

3.5 Chapter Summary

Chapter 3 detailed the methodology used to address the project objectives, generate the quantitative data needed to run simulations, procedure and assumptions used to create the models and simulation as well as the quantitative techniques to analyse the results of the simulation. This was performed by identifying the most appropriate method of determining the performance of the propagation models identified in chapter 2 to address objective 1. Additionally, we determine the metrics which are best suited to measure performance in a navigation application, to address objective 2. In conducting the work, modifications had to be made to address the experimental needs of this research, where the specific innovations in this regard where the use of the HDOP scoring and statistical analysis to assess the placement techniques. The use of repeatable accuracy to assess LoRa's suitability to terrestrial navigation was also novel at the time of researching. Chapter 3 explains the necessity of first determining a placement technique appropriate for a navigation application based on LoRa and the metrics of interest in that regard. To facilitate this, a triangular tessellation method is proposed and its performance is compared against two other common methods, namely the random and naive placement methods for the LoRa gateways. The chapter then details the nature of the generated simulation data to apply propagation models to while implementing the placement techniques most suited for navigation. Lastly, methods of analysis are discussed in detail to analyse the results. These are the statistical significance tests, effect size and practical significance.

Chapter 4

Results and Analysis

This chapter presents the results of the simulations conducted during the research process. Specifically the receiver sensitivity map over the study area, a statistical analysis of the result to validate the use of HDOP method when placing gateways. As well as an analysis of the performance of path-loss models in the use-case scenario used in the research project.

4.1 Receiver Sensitivity analysis

Three methods were used to place gateways on the selected coverage area, BIUST main campus. The methods are a random placement, naive placement and guided HDOP method. Using the methods receiver sensitivity maps were drawn up with HDOP being used as the performance metric. In each receiver sensitivity map the BIUST main campus is demarcated using a white line. While gateways are illustrated using magenta circles. Lastly, contours with black or orange colours are regions with very poor HDOP, the colorbar beside every map shows the HDOP value of any other colour on the contour map with the exception of black.

4.1.1 Random gateway placement

The random placement of gateways in the coverage area was used a benchmark to determine how much better or worse the HDOP guided method is for gateway placement in a geographical area. A growing window method is employed, initially 3 gateways are placed in randomly generated coordinates, the simulation runs a thousand times then 1 other gateway is added as outlined in figure 3.3. The algorithm in figure 3.3 is used except the placement occurs until most of the map has been covered.

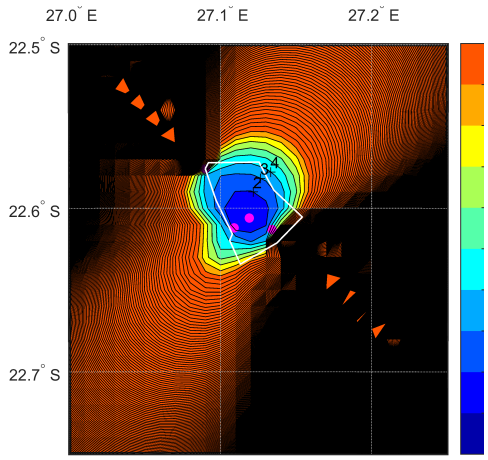


FIGURE 4.1: 4 Randomly placed gateways

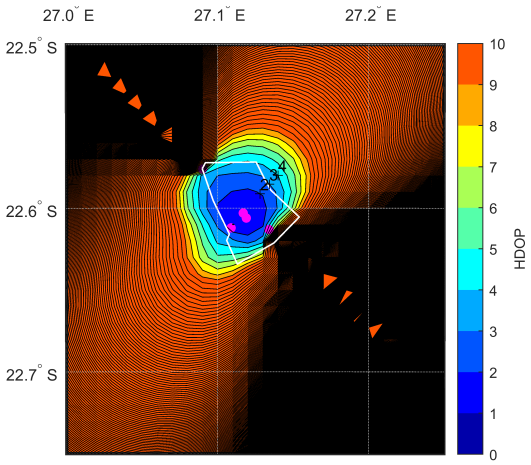


FIGURE 4.2: 5 Randomly placed gateways

Figure 4.1 and figure 4.2 show the sensitivity map created using unweighted HDOP as a metric for measuring coverage. As expected the HDOP within the coverage area is greater than 1 suggesting that there is bad HDOP caused primarily by poor geometry. In this configuration there is an amplification of positioning errors by poor geometry.

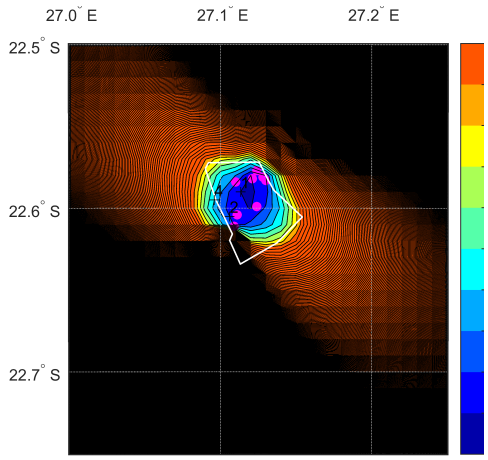


FIGURE 4.3: 8 Randmoly placed gateways

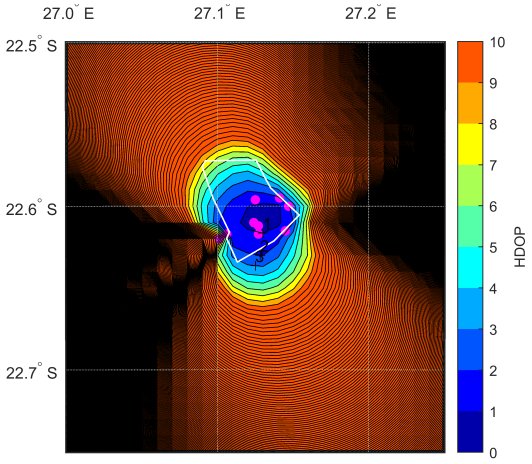


FIGURE 4.4: 9 Randomly placed gateways

Figure 4.3 and figure 4.4 show the sensitivity map created using unweighted HDOP. As the number of gateways increases the likelihood of attaining good HDOP increases. This observation is visible on the sensitivity map where the deep blue areas show areas with an HDOP value of 1 or less, good HDOP. These areas benefit from no error amplification due to poor gateway geometry. The same observation applies in figure 4.5.

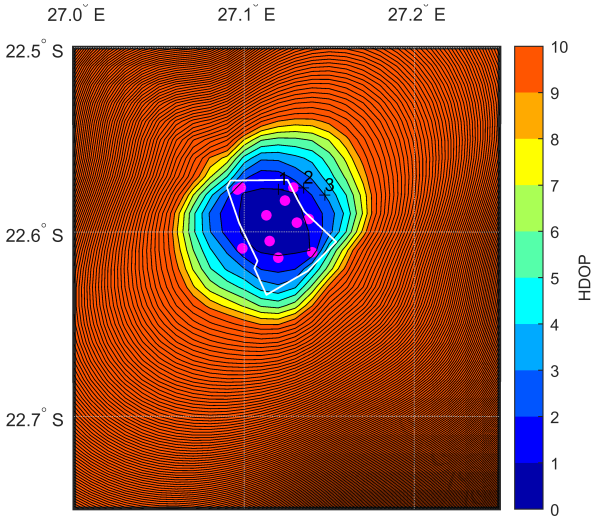


FIGURE 4.5: 11 Randomly placed gateways

4.1.2 Naive gateway placement

The assumptions outlined in section 3 guided the placement of gateways. Naive placement requires that the gateways simply not overlap. Additionally, the placement process does not necessarily use the procedure in 3.3 HDOP in figure 4.6 and figure 4.7 is less than and equal to 1 in many areas. Specifically, figure 4.6, has 53% of the coverage area having good HDOP and therefore not having any positioning

error amplification. Figure 4.7 has 47% of the coverage area having good HDOP or good coverage.

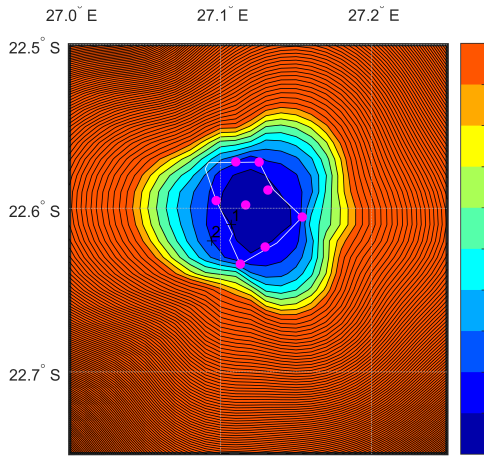


FIGURE 4.6: 8 Naively placed gateways arrangement 1

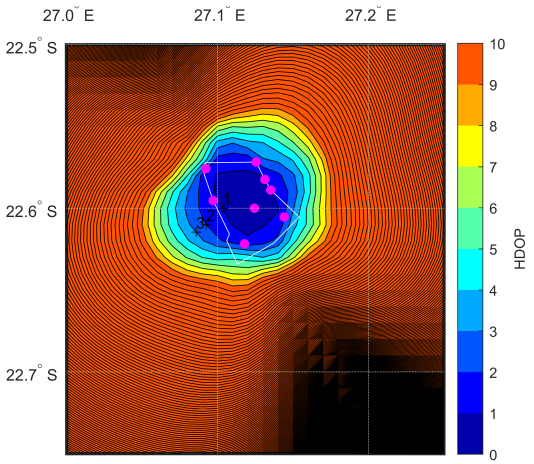


FIGURE 4.7: 8 Naively placed gateways arrangement 2

Figure 4.8 and figure 4.9 have good HDOP in 47% and 50% respectively. Ultimately, the maximum coverage area with good HDOP is 53%.

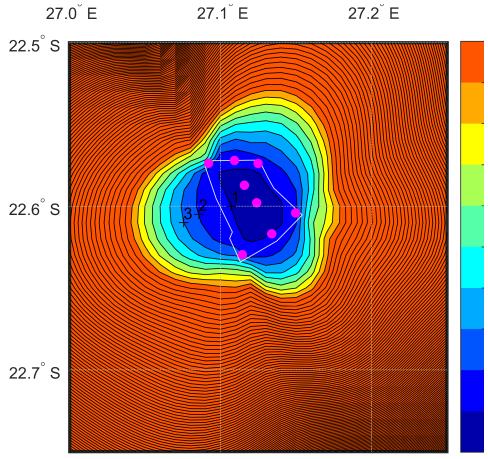


FIGURE 4.8: 8 Naively placed gateways arrangement 3

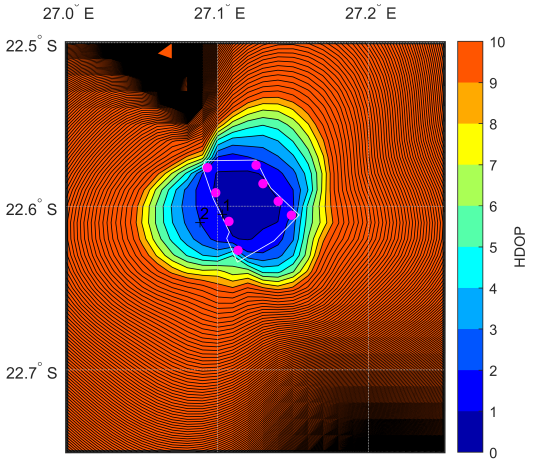


FIGURE 4.9: 8 Naively placed gateways arrangement 4

4.1.3 Guided HDOP gateway placement

The guided HDOP placement method uses the triangular tessellation, as well as the HDOP scores to place gateways. The observations made were that within the tessellated triangle regions HDOP tended to be better than the surrounding areas.

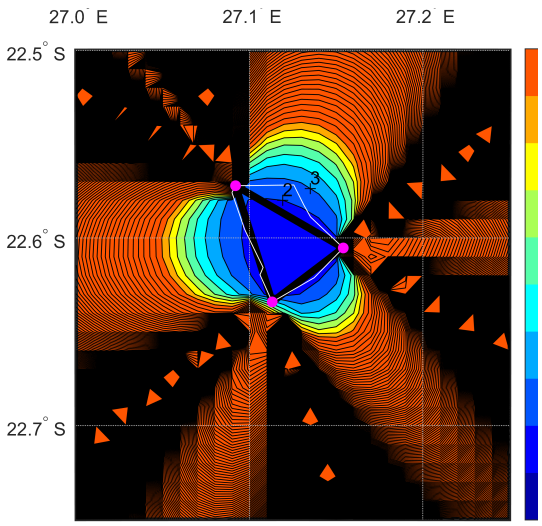


FIGURE 4.10: 3 HDOP guided gateway placements

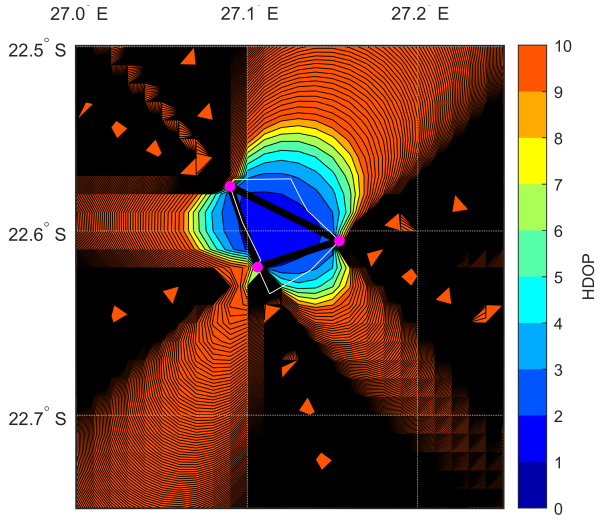


FIGURE 4.11: Unweighted HDOP map with HDOP guided placed gateways

Figure 4.10 and figure 4.11 both have 3 gateways in the coverage area and within the confines of the imaginary triangle formed by the gateways HDOP is 2, much better than the outside of the triangle's parameter.

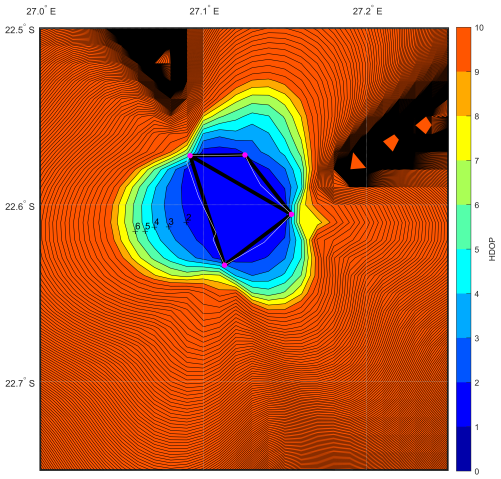


FIGURE 4.12: 4 HDOP guided gateway placements

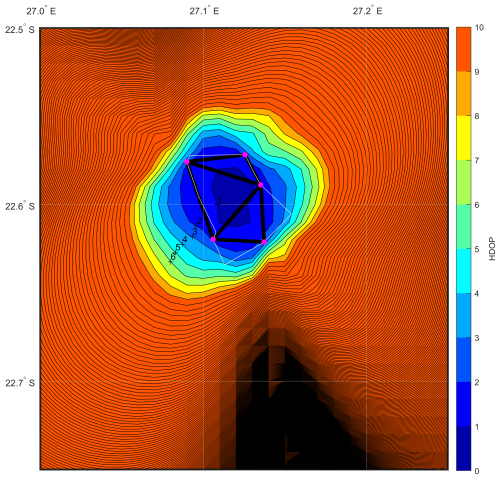


FIGURE 4.13: 5 HDOP guided gateway placements

Figure 4.12 and figure 4.13 both use the procedure in 3.3. Within the confines of the imaginary tessellated triangles shown in the figures HDOP is significantly better than the rest of the coverage area. In figure 4.13, the first instance of HDOP less then or equal to 1 is achieved, and this only occurs within the imaginary tessellated triangle zones.

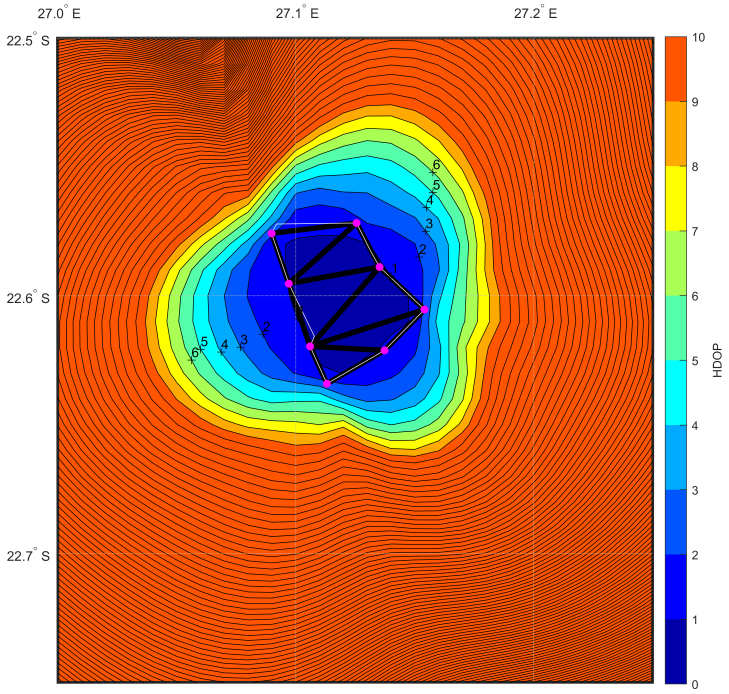


FIGURE 4.14: 8 HDOP guided placed gateways

When adding more gateways, HDOP continues to improve (becomes 1), within the confines of the outlined imaginary triangles. These changes in HDOP are visualised in figures 4.12 and 4.13. The good geometry in this placement means in 70% of the coverage area, there will be no amplification of ranging errors due to poor geometry of the gateway placements. Rather ranging errors will be a result of TOA variance which is affected by SNR.

4.2 Statistical Analysis of Placement methods

Figure 4.15 illustrates the spread of the HDOP scores of the placement methods. Specifically, the results of random placements (1), are seen to be almost normal with approximately 50% of the scores being between 13 and 7. However, it is also observable that the random placement technique generates a number of outliers. These figures are beyond the whisker plot in the same graph. By comparison the naive placement technique (2) has most 50% of the scores being between 15 and 14. HDOP guided placement has outliers below 20 and 50% of the HDOP scores being between 20 and 21. Unfortunately, the 50th percentile blue block is so small it is simply not visible in the current scale. Additionally, the whisker plot shows that 75% of the scores are below 21 and above 18. This means the average performance of the method is greater than the other two methods. The visual results warrant further statistical analysis to determine, effect size, statistical significance and practical significance. Table 4.1, table 4.2 and table 4.3 show the results from the Mann U Whitney tests; specifically the P values, a Z statistic and η^2.

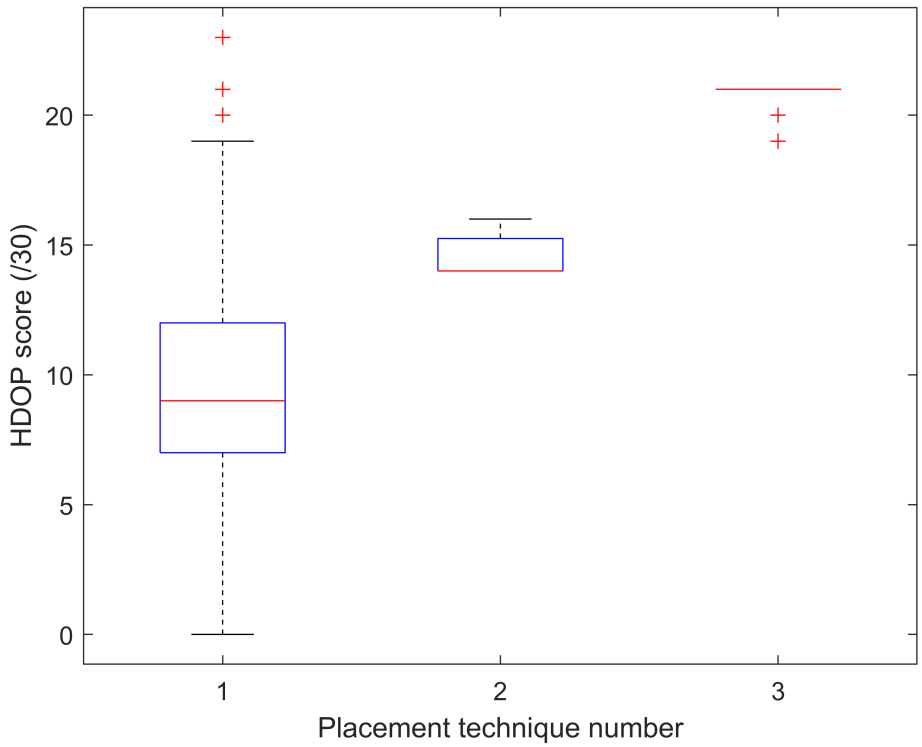


FIGURE 4.15: Box and Whisker plot for random placement (1), naive placement (2) and HDOP guided placement (3)

4.2.1 Statistical tests:Naive placement VS Random Placement

Table 4.1 has the the statistical significance and effect size of the naive method vs the random placement method. The P value proves that there is a statistical significance as the 5% threshold is higher than the calculated P value of 2.6682e-23. A secondary statistical significance figure, Z score of 9.9444 also shows statistical significance since the figure is greater than 1.645 [64]. Differences in the central tendencies of the two methods have an η^2 score of 0.094 showing that the difference is large. This implies the naive method is statistically better than random placement when deploying gateways in a coverage area.

Practically, random placement on average will result in only 30with the minimum most gateways while naive placement provides coverage of 46.7%. The difference in coverage is approximately 1166.5 of the coverage area. Naive placement can therefore be ranked above random placement. Figure 4.16 illustrates the results of the random placement method. Initially, only three gateways are randomly placed on the coverage map and this increased until the minimum 8. The centre and right images of figure 4.16 show some of the best and worst placements with 8 gateways.

TABLE 4.1: Mann-Whitney U Test Result: Naive placement VS Random Placement

Property	**Naive placement VS Random Placement**
Z statistic	9.9444
P value	2.6682e-23
η^2	0.094

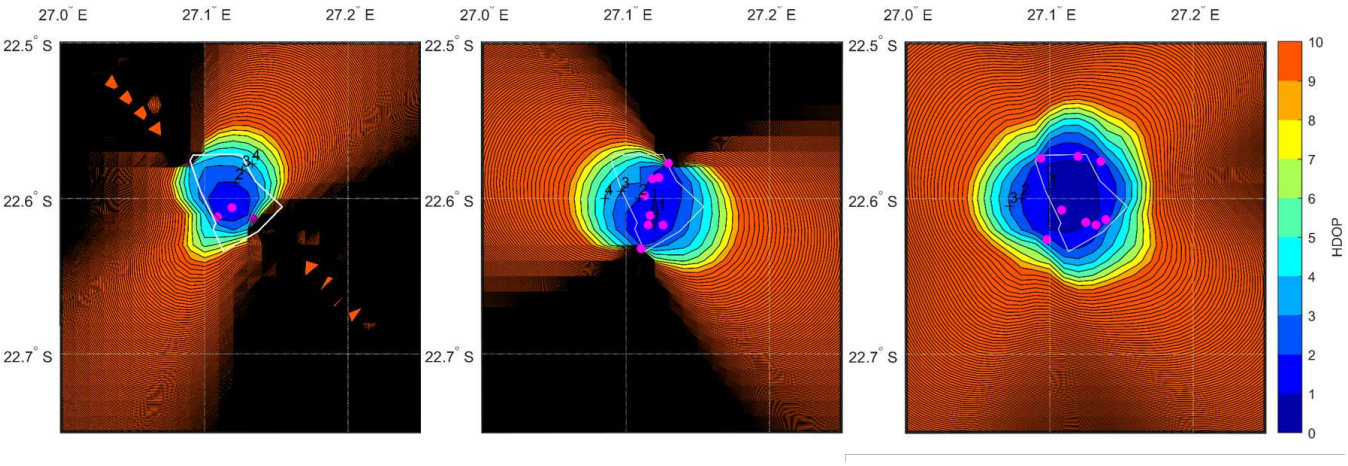


FIGURE 4.16: Random placement coverage results

4.2.2 Statistical tests:HDOP guided placement VS Random Placement

From table 4.2 the differences between the two placement methods (HDOP guided placement and random placement) is shown to have a statistical significance. This is confirmed by the P value of 1.6859e-34. Using the Z statistic statistical significance is also confirmed with a Z score of 12.2497 which is greater than the 1.645 threshold. With regard to the difference in central tendency η^2 is 0.143 which a strong effect size. The statistical results show that the HDOP guided method is at-least statistically better than random placement.

The practical significance of the results is that on average the HDOP guided method provides good HDOP coverage in 70% of the coverage area with the minimum number of gateways. In terms of area this is 1000 more hectares of coverage area compared to random placement. HDOP guided method therefore ranks above the random placement method. Figure 4.17 illustrates the visual results of the naive placement method over the coverage map. The figure shows the different configurations of non overlapping gateways in the coverage area and the resulting HDOP.

TABLE 4.2: Mann-Whitney U Test Result: HDOP guided placement VS Random Placement

Property	**HDOP guided placement VS Random Placement**
Z statistic	12.2497
P value	1.6859e-34
η^2	0.143

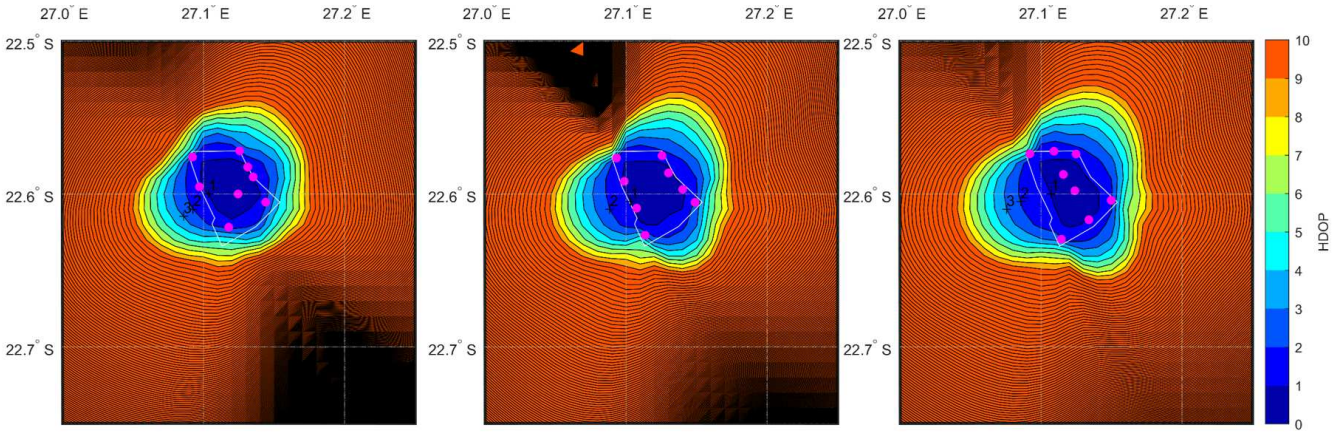


FIGURE 4.17: Naive placement coverage results

4.2.3 Statistical tests:HDOP guided placement VS Naive Placement

In table 4.2 the differences between the two methods (HDOP guided placement and naive placement) are shown to be statistically significant by the P value of 1.7420×10^{-21}. However, this is not confirmed by the Z statistic of -9.5194. In this scenario the secondary statistical significance test assumes that the two methods samples are normally distributed so the result of the Mann U Whitney test is more significant than the secondary Z statistic. Moreover, literature shows that the Z-statistics assumes that large enough sample sizes will eventually mimic a normal distribution. However, the naive and tessellation technique have relatively small sample sizes compared to either technique and random placement. Statistical significance will nonetheless be inconclusive as the two tests do not convey the same conclusions. The effect size of the central tendencies of the tests show an intermediate difference which is acceptable. Therefore while the statistical significance is inconclusive the effect size is large enough that the tessellation technique maybe considered better than naive placement.

Practical significance also shows that the HDOP guided method will on average provide good HDOP scores in more portions of the coverage area. Average coverage of the naive placement method is 46.7% while the HDOP guided method has an average coverage of 70%. Area wise, HDOP guided method provides coverage in approximately 583.35 hectares of the coverage area with the minimum number of gateways. Figure 4.18 illustrates the visual results of the HDOP guided method with the imaginary tessellated triangles outlined on the coverage map. The figure shows the improvement of HDOP from the first 3 gateways, skipping to 5 and finally 8 gateways.

TABLE 4.3: Mann-Whitney U Test Result: HDOP guided placement VS Naive Placement

Property	**HDOP guided placement VS Naive Placement**
Z statistic	-9.5194
P value	1.7420e-21
η^2	0.0864

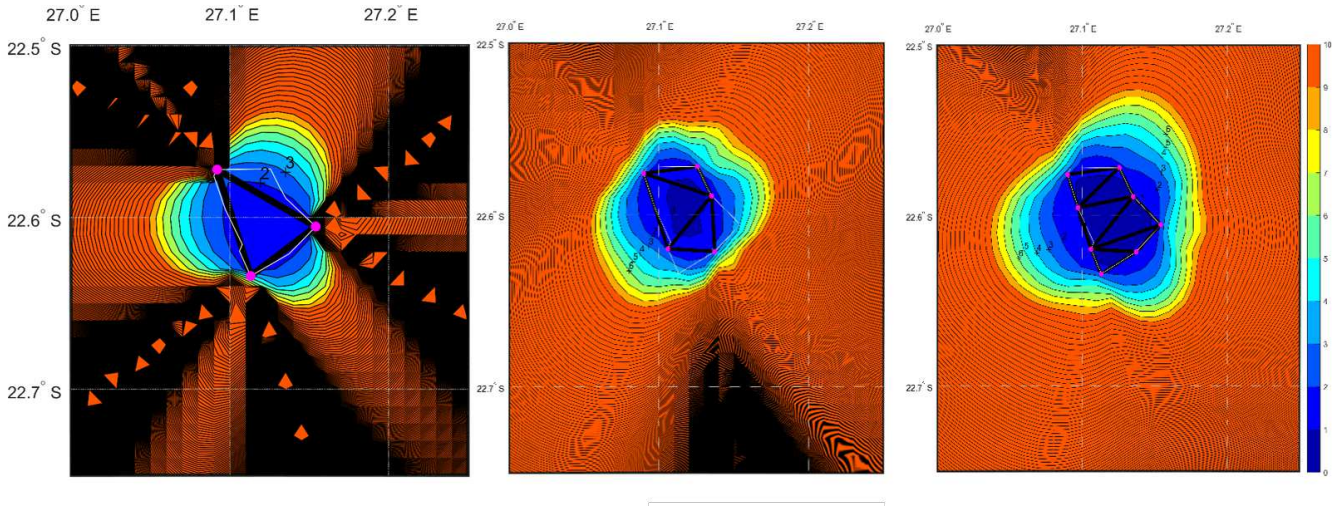


FIGURE 4.18: HDOP guided placement coverage results

4.3 Propagation Model Ranking

The models simulated to visualise the possible path-loss of a LoRa terrestrial navigation system over a range of 25km the transmission characteristics shown in table 3.5 and table 3.6. Figure 4.19 illustrates the path-loss of the FSPL, Ericsson 9999 and COST 231-WI models. The simulation shows the manner by which losses will likely be experienced in a LOS application of LoRa in using 915MHz for transmission. In any given situation there is a minimum sensitivity of SNR that a receiver may detect successfully and the losses in figure 4.19 for the Ericsson 9999 models are greater than the calculated minimum sensitivity for the SF 7. Minimum receiver sensitivity was calculated using equation 2.40.

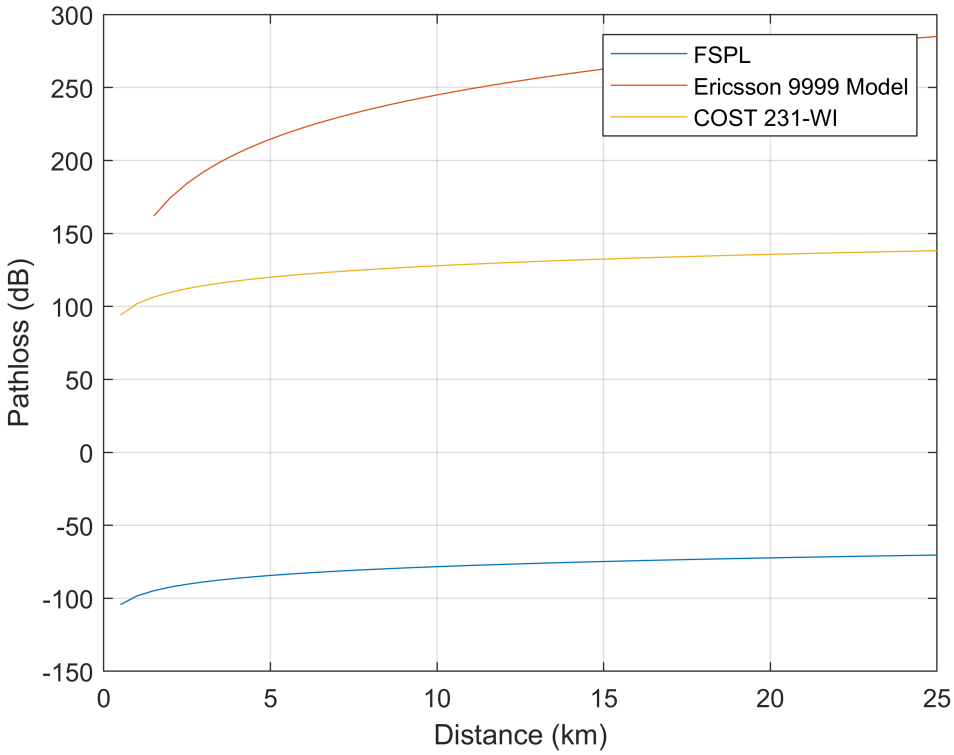


FIGURE 4.19: LoRa path-loss model performance

Figures 4.20, 4.21 and 4.22 show the simulated SNR values for COST-WI, Ericsson 9999 and FSPL models. When analysing the results, they suggest that while a packet could be successfully detected by a receiver upto approximately 5km away according to the COST-WI the SNR is far too low for a ranging application using SF7. Similarly, the FSPL model suggests that ranging could occur up-to 10km with successful detection occurring beyond 25km. While, the Ericsson 9999 results suggest that successful detection will occur below 1km but ranging will not be possible. The latter two models show results which do-not reconcile with known performances of LoRa in deployments documented by [35] and listed in table 2.9. This contradiction implies that the Ericsson 9999 models may not be appropriate for LoRa network planning in the 915MHz frequency. However, this conclusion is not absolute as the simulation results have not been validated by a practical experiment.

Similarly, the results from FSPL and COST-WI while more consistent with practical observations are not absolute, because practical validation has not been done. However,these two models maybe more adept at portraying SNR performance in a LOS application deployed in a rural area at a frequency of 915MHz.

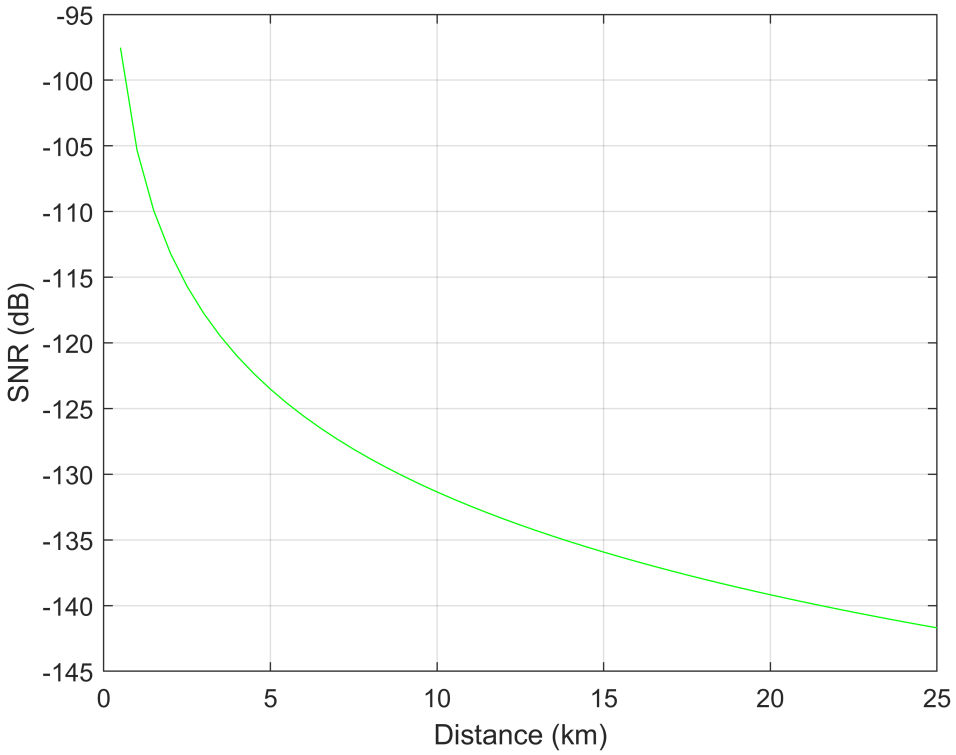


FIGURE 4.20: COST WI SNR graph

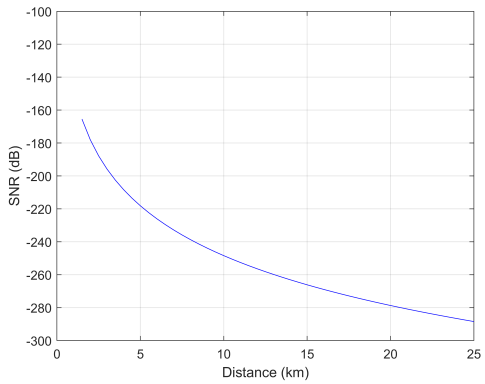


FIGURE 4.21: Ericsson 9999 SNR graph

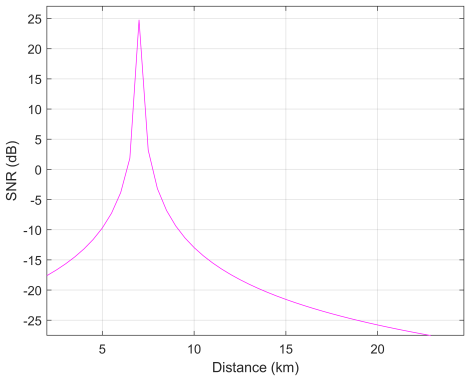


FIGURE 4.22: Free Space Path Loss SNR graph

4.3.1 Coverage area Repeatable accuracy

This subsection presents the results of the simulations determining the repeatable accuracy of the three propagation models used in the weighting matrix. The repeatable accuracy is determined to be within the 90^{th} percentile.

4.3.2 Repeatable accuracy summery

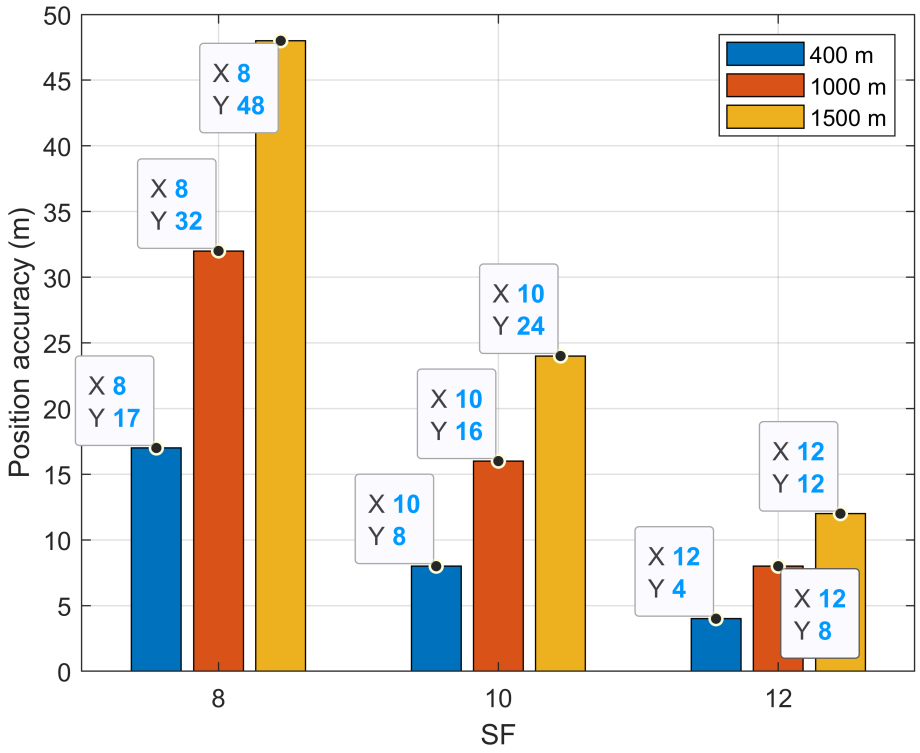


FIGURE 4.23: FSPL repeatable accuracy: 400 m, 1000 m, 1500 m gateway separation at SF 8,10,12 and BW 125kHz

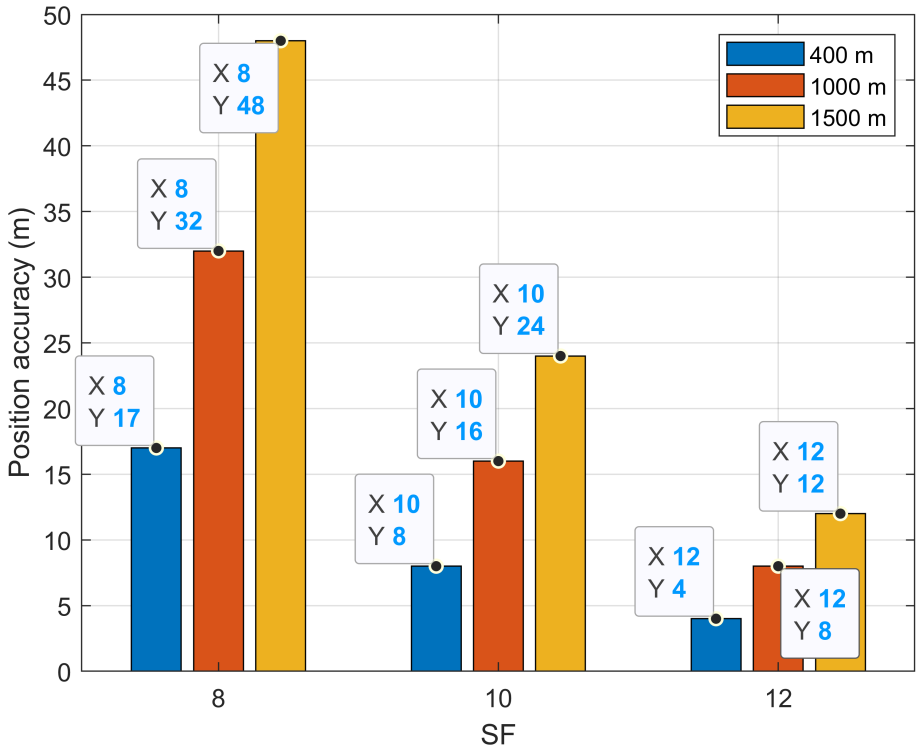


FIGURE 4.24: COST 231 WI repeatable accuracy: 400 m, 1000 m, 1500 m gateway separation at SF 8,10,12 and BW 125kHz

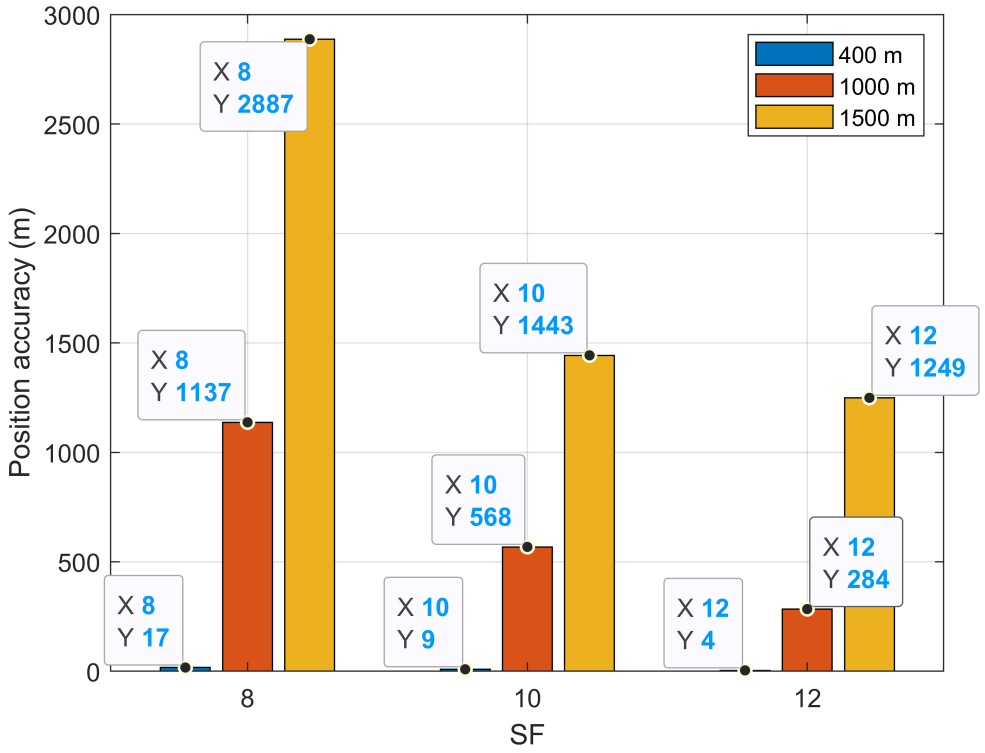


FIGURE 4.25: Ericsson 9999 repeatable accuracy: 400 m, 1000 m, 1500 m gateway separation at SF 8,10,12 and BW 125kHz

The results illustrate that in general an increased SF improves the repeatable accuracy improves significantly. Figures 4.23, 4.24 and 4.25 illustrate the changes in repeatable accuracy as spreading factor is increased for gateways spaced 400 m, 1000 m and 1500 m when using the free space path-loss model, COST 231 WI and Ericsson 9999 models respectively. In each configuration/gateway separation, the moving node was made to move across the grid created using the procedure outlined in section 3 and at each grid point, which was a movement of 0.01 deg in the latitude and longitudes of the coverage area. After each move the SNR at all the gateways was determined. This was then used to determine the repeatable accuracy based on SF, SNR, and distance using equation 2.39. In these simulations, we kept the BW of the system constant and used the same path-loss model to determine the signal strengths at different distances from the gateways using equations outlined in chapter 2.

We observed that at a SF of 8, the best repeatable accuracy in the 1500 m separation was over 2000 m, this is an unacceptable result. Increasing the spreading factor to 10, and finally 12 led to an accuracy of 1249 m, this value of repeatable accuracy was the best, but still fell short of the 20 m target. A contour plot of the repeatable accuracy of the coverage area for the different path-loss models are illustrated in figures C.28 to C.54 for SF 8,10 and 12.

For the 1500 m separation the FSPL results had a repeatable accuracy of 48 m, 24 m and 12 m for a SF of 8, 10 and 12 respectively. These results while within range of the set thresholds are from a simplistic model. Comparatively, The COST 231 WI model has repeatable accuracies of 48 m, 24 m and 12 m for SFs of 8, 10 and 12

respectively. These figures are similar to those of the FSPL this maybe due to the similarities in some of the models' assumptions. Finally, the Ericsson 9999 model, designed primarily for 3G networks and with extensive use in research, provided a repeatable accuracy of 2887 m, 1443 m and 1249 m for SFs of 8, 10 and 12 respectively. The results of the three models are summarised using bar-charts illustrated in figures 4.23, 4.24 and 4.23 for the FSPL, COST 231 WI and Ericsson 9999 respectively. The best repeatable accuracies are generally observed with higher SF which is was expected from theoretical analysis, and in real world experiments such as those outlined in table 2.2. Additionally, the results from the FSPL and COST 231 WI meet the thresholds which would make LoRa a competitive navigation technology comparable to more established terrestrial navigation technologies or become a SoOP in Botswana.

For the 1000 m separation the FSPL results had a repeatable accuracy of 32 m, 16 m and 8 m for SF of 8, 10 and 12 respectively. These results show that the effect of reducing the distance between gateways, namely that the smaller distance means there is a lower path-loss and hence a better SNR given that the system noise remains relatively constant. Comparatively, The COST 231 WI model has repeatable accuracies of 32 m, 16 m and 8 m for SFs of 8, 10 and 12 respectively. These figures are similar to those of the FSPL this maybe due to the similarities in some of the models' assumptions. In a similar manner, Finally, the Ericsson 9999 model, designed primarily for 3G networks and with extensive use in research, provided a repeatable accuracy of 1137 m, 568 m and 284 m for SFs of 8, 10 and 12 respectively. When consulting prior research the Ericsson 9999 results are very similar to the practical results recorded by the authors of [37]. The results of the three models are summarised using bar-charts illustrated in figures 4.23, 4.24 and 4.23 for the FSPL, COST 231 WI and Ericsson 9999 respectively.

The best repeatable accuracies are generally observed with higher SF which is was expected from theoretical analysis, and in real world experiments such as those outlined in table 2.2 and table 2.3. Additionally, the results from the FSPL and COST 231 WI all show significant improvements in the repeatable accuracies observed computationally in all the models. The changes are improved by the reduced path-loss due to the smaller distances between gateways which increases both the SNR of the received signal as well as the increased number of gateways per square kilometre. The former, in combination with the ideal placement technique from the previous subsection yields improved repeatable accuracy and additional improvements when the SF is increased. It is worth noting however, that this increases the signal symbol time. This generally means that energy expended by the node will increase. However, the energy consumption is not in the scope of this thesis.

Finally, in the 400 m separation the FSPL results had a repeatable accuracy of 17 m, 8 m and 4 m for SF of 8, 10 and 12 respectively. These results while within range of the set thresholds are from a simplistic model. Comparatively, The COST 231 WI model has repeatable accuracies of 17 m, 8 m and 4 m for SFs of 8, 10 and 12 respectively. These figures are similar to those of the FSPL this maybe due to the similarities in some of the models' assumptions. Finally, the Ericsson 9999 model, designed primarily for 3G networks and with extensive use in research, provided a repeatable accuracy of 17 m, 9 m and 4 m for SFs of 8, 10 and 12 respectively. The results of the three models are summarised using bar-charts illustrated in figures 4.23, 4.24 and 4.23 for the FSPL, COST 231 WI and Ericsson 9999 respectively. The

latter values of repeatable accuracy are comparable to accuracies of most popular navigation systems including but not limited to Loran, GPS and WiFi.

4.4 Chapter Summary

This chapter provided the results of the receiver sensitivity map using unweighted HDOP in the BIUST coverage area of 2500 hectares, a statistical analysis of methods an analysis of eligible path-loss models as well as repeated accuracy contour plots using the three curated propagation models.

Additionally, a statistical analysis was performed on the guided HDOP method which uses triangular tessellation to place gateways. The guided HDOP method results were compared to placements which use randomly generated coordinates and naive placement. These methods were assessed for statistical significance, effect size and practical significance. It was determined that the HDOP guided method provided results with a statistical significance as determined by the Mann U Whitney test and a Z test compared to random placement and naive placement. Also the HDOP guided method was determined to have a high effect size when compared to random and naive placement as well as a high practical significance.

Finally, a simulation and analysis of eligible path-loss models for LoRa deployments in a rural area with LOS characteristics for 915MHz transmission with a SF of 7 and BW of 125kHz. The results showed that in general, an increase in the SF improved the propagation such that regardless of the node distance there was always an improvement in repeatable accuracy until we were able to attain a 20 m repeatable accuracy with a 1000 m spacing using both the FSPL and COST 231 models, while the Ericsson 9999 model showed that a spacing of atleast 400 m would be needed to attain such values. In both instances, it is important for a practical experiment to take place to help in determining the accuracy of all models and help refine the model and techniques.

Chapter 5

Conclusion

This chapter provides the conclusion drawn from the research project with regard to the original project objectives. More generally, a review of the research findings is performed, research contributions are provided as well as potential future work in the area on LoRa navigation.

5.1 Receiver sensitivity grid

This research proposed an application area which could be used to investigate LoRa. Terrestrial navigation was determined to be an ideal application due to its relevance in security, agriculture, tourism and logistics, these are all key economic and research areas in Botswana. Also, the geographical area used for the application is the BIUST Palapye campus in Botswana. This area was determined to be a good approximation of a rural deployment area (almost anywhere in Botswana) for terrestrial navigation or animal tracking as the land is mostly flat, it has vegetation and few buildings or obstructions increasing the likelihood of a LOS transmission.

5.1.1 Placement technique

Through the use of a statistical analysis consisting of a statistical significance test and effect size the three placement methods were assessed for a ranging application. The results show that the HDOP guided method was superior to the naive and random placement method. Additionally, the practical significance was assessed using the difference in average coverage area of the methods.

5.2 Propagation model performance

Simulations of four eligible propagation models were conducted for FSPL, ECC-33, Ericsson 9999 and COST 231-WI models. The results from FSPL and COST-WI while more consistent with practical observations are not absolute, because practical validation has not been done. ECC-33 and the Ericsson 9999 suggest that LoRa would not be suitable for a ranging application due to an inability to meet the minimum SNR for ranging in SF7. However,the former two models may be more adept at portraying SNR performance in a LOS application deployed in a rural area at a frequency of 915MHz. Further practical experimentation is necessary to determine which propagation models are best at predicting path-loss and SNR for LoRa in the BIUST coverage area or a similar area.

5.3 Research Contributions

This research project has resulted in the publication of a systematic literature review in a SCOPUS indexed journal.

5.4 Future Work

The results of this work demonstrate that LoRa is a viable technology for terrestrial navigation applications. Future work on LoRa navigation could focus on using LoRa signals as a SoOP, where LoRa would work in conjunction with other major navigation technologies.

5.5 Chapter Summary

The objectives originally set in chapter 1 were accomplished in this research. Specifically, it was determined that HDOP was the best metric for creating a receiver sensitivity map when LoRa is to be employed for ranging applications. This metric is relevant and has in the past been used for navigation systems such as Loran, DGPS and Omega to mention but a few. Moreover, empirical propagations suited to model LoRa propagation were found and subsequently used in the modelling of LoRa in a navigation application. With repeatable accuracy (key metric) being observed with each model to determine, which one most closely performed in a manner similar to what some attempted applications have found. Furthermore, research showed that for ranging, the deployment or placement of gateways is critical. This led to a statistical analysis and practical significance assessment for three candidate placement methods also sourced from literature: a stochastic or random placement method, a naive placement method and HDOP guided method. The assessments showed that:

- a deterministic method is statistically more effective at ensuring greater coverage in an area for the same number of gateways,
- the HDOP guided method which is based on polygon triangulation is better than a naive method at ensuring better coverage.

Practically, the research showed that for the same number of gateways the HDOP guided method provided 583.35 hectares more coverage than naive placement. Additionally, a review of path-loss models was performed and four eligible models were identified and simulated for the 915MHz band. The simulations of FSPL and COST-WI showed that LoRa could operate in a ranging application. This is because the distances over which the models predicted path-loss and later SNR were consistent with observations of long range applications of LoRa. In the absence of practical validation these results are not absolute, which is a limitation of the study. In conclusion, the research was able to meet the proposed research objectives and contributed a systematic literature review to the body of research.

Appendix A

Appendix A

A.1 Effect Size

TABLE A.1: Interpretation of effect sizes [66]

d	r^*	η^2	**Interpretation sensu Cohen (1988)**	**Interpretation sensu Hattie (2009)**
<0	<0	-	Adverse Effect	
0.0	0.00	0.000	No Effect	Developmental effects
0.1	0.05	0.003	Small Effect	Teacher effects
0.2	0.10	0.010		
0.3	0.15	0.022		
0.4	0.20	0.039		Zone of desired effects
0.5	0.24	0.060	Intermediate Effect	
0.6	0.29	0.083		
0.7	0.33	0.110		
0.8	0.37	0.140	Large Effect	
0.9	0.41	0.168		
> 1.0	0.45	0.200		

$$\eta^2 = \frac{Z^2}{n-1}. \tag{A.1}$$

A.2 Statistical significance

n_2	α	n_1																	
		3	4	5	6	7	8	9	10	11	12	13	14	15	16	17	18	19	20
3	.05	0	0	1	2	2	3	4	4	5	5	6	7	7	8	9	9	10	11
	.01	--	0	0	0	0	0	1	1	1	2	2	2	3	3	4	4	4	5
4	.05	0	1	2	3	4	5	6	7	8	9	10	11	12	14	15	16	17	18
	.01	--	--	0	1	1	2	3	3	4	5	5	6	7	7	8	9	9	10
5	.05	1	2	4	5	6	8	9	11	12	13	15	16	18	19	20	22	23	25
	.01	--	0	1	2	3	4	5	6	7	8	9	10	11	12	13	14	15	16
6	.05	2	3	5	7	8	10	12	14	16	17	19	21	23	25	26	28	30	32
	.01	--	1	2	3	4	6	7	8	9	11	12	13	15	16	18	19	20	22
7	.05	2	4	6	8	11	13	15	17	19	21	24	26	28	30	33	35	37	39
	.01	0	1	3	4	6	7	9	11	12	14	16	17	19	21	23	24	26	28
8	.05	3	5	8	10	13	15	18	20	23	26	28	31	33	36	39	41	44	47
	.01	0	2	4	6	7	9	11	13	15	17	20	22	24	26	28	30	32	34
9	.05	4	6	9	12	15	18	21	24	27	30	33	36	39	42	45	48	51	54
	.01	1	3	5	7	9	11	14	16	18	21	23	26	28	31	33	36	38	40
10	.05	4	7	11	14	17	20	24	27	31	34	37	41	44	48	51	55	58	62
	.01	1	3	6	8	11	13	16	19	22	24	27	30	33	36	38	41	44	47
11	.05	5	8	12	16	19	23	27	31	34	38	42	46	50	54	57	61	65	69
	.01	1	4	7	9	12	15	18	22	25	28	31	34	37	41	44	47	50	53
12	.05	5	9	13	17	21	26	30	34	38	42	47	51	55	60	64	68	72	77
	.01	2	5	8	11	14	17	21	24	28	31	35	38	42	46	49	53	56	60
13	.05	6	10	15	19	24	28	33	37	42	47	51	56	61	65	70	75	80	84
	.01	2	5	9	12	16	20	23	27	31	35	39	43	47	51	55	59	63	67
14	.05	7	11	16	21	26	31	36	41	46	51	56	61	66	71	77	82	87	92
	.01	2	6	10	13	17	22	26	30	34	38	43	47	51	56	60	65	69	73
15	.05	7	12	18	23	28	33	39	44	50	55	61	66	72	77	83	88	94	100
	.01	3	7	11	15	19	24	28	33	37	42	47	51	56	61	66	70	75	80
16	.05	8	14	19	25	30	36	42	48	54	60	65	71	77	83	89	95	101	107
	.01	3	7	12	16	21	26	31	36	41	46	51	56	61	66	71	76	82	87
17	.05	9	15	20	26	33	39	45	51	57	64	70	77	83	89	96	102	109	115
	.01	4	8	13	18	23	28	33	38	44	49	55	60	66	71	77	82	88	93
18	.05	9	16	22	28	35	41	48	55	61	68	75	82	88	95	102	109	116	123
	.01	4	9	14	19	24	30	36	41	47	53	59	65	70	76	82	88	94	100
19	.05	10	17	23	30	37	44	51	58	65	72	80	87	94	101	109	116	123	130
	.01	4	9	15	20	26	32	38	44	50	56	63	69	75	82	88	94	101	107
20	.05	11	18	25	32	39	47	54	62	69	77	84	92	100	107	115	123	130	138
	.01	5	10	16	22	28	34	40	47	53	60	67	73	80	87	93	100	107	114

FIGURE A.1: Mann Whitney U one tailed test critical values [71]

A.3 Statistical Significance Formulae

$$T_1 = n_1 n_2 + \frac{n_1(n_1+1)}{2} + R_1, \tag{A.2}$$

[71]

$$E[T_1] = \frac{1}{2} n_1 (n_1 + n_2 + 1). \tag{A.3}$$

[72]

Where the variables used:

- T_i test statistic from sample i,

- n_i number of elements in sample i,
- R_i sum of ranks in sample i,
- $E(T_1)$ expected value of the test statistic.

$$Z = \frac{|T_i - E(T_i)|}{\frac{\sqrt{n_1 n_2 (n_1 + n_2 + 1)}}{12}}, \tag{A.4}$$

[72]

$$\eta^2 = \frac{Z^2}{N - 1}. \tag{A.5}$$

[72]

Where the variables used mean:

- Z is the test statistic used to test significance for samples which are large,
- N is the total number of elements of the samples.

Appendix B

Appendix B

B.1 Pathloss Table

TABLE B.1: Gateway and transmitter heights above ground

Gateway Height above ground (m)	Transmitter Height above ground (m)	Distance (km)
5	2	0.5
5	2	1.0
5	2	1.5
5	2	2.0
5	2	2.5
5	2	3.0
5	2	3.5
5	2	4.0
5	2	4.5
5	2	5.0
5	2	5.5
5	2	6.0
5	2	6.5
5	2	7.0
5	2	7.5
5	2	8.0
5	2	8.5
5	2	9.0
5	2	9.5
5	2	10.0
5	2	10.5
5	2	11.0
5	2	11.5
5	2	12.0
5	2	12.5
5	2	13.0

TABLE B.2: Gateway and transmitter heights above ground

Gateway Height above ground (m)	**Transmitter Height above ground (m)**	**Distance (km)**
5	2	13.5
5	2	14.0
5	2	14.5
5	2	15.0
5	2	15.5
5	2	16.0
5	2	16.5
5	2	17.0
5	2	17.5
5	2	18.0
5	2	18.5
5	2	19.0
5	2	19.5
5	2	20.0
5	2	20.5
5	2	21.0
5	2	21.5
5	2	22.0
5	2	22.5
5	2	23.0
5	2	23.5
5	2	24.0
5	2	24.5
5	2	25.0

Appendix C

Appendix C

C.1 LoRa Deployments Signal Strength

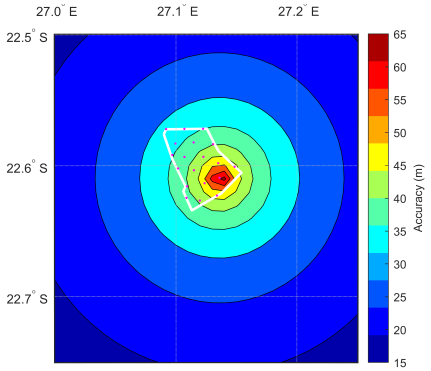


FIGURE C.1: FSPL Signal Strength: 1500 m gateway separation at SF12

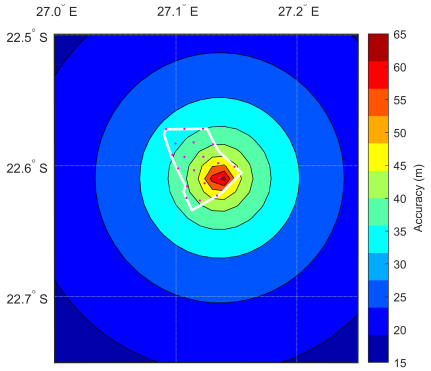


FIGURE C.2: FSPL Signal Strength: 1500 m gateway separation at SF10

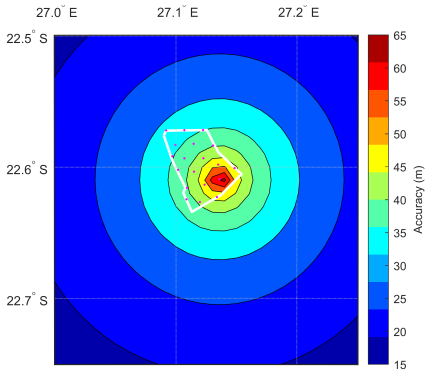


FIGURE C.3: FSPL Signal Strength: 1500 m gateway separation at SF8

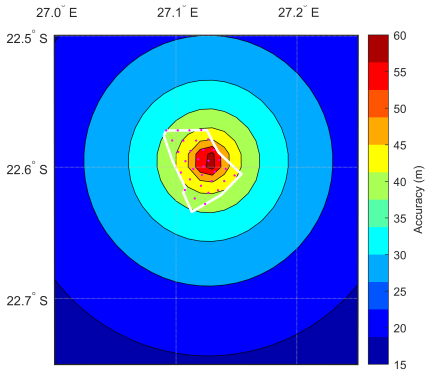


FIGURE C.4: FSPL Signal Strength: 1000 m gateway separation at SF12

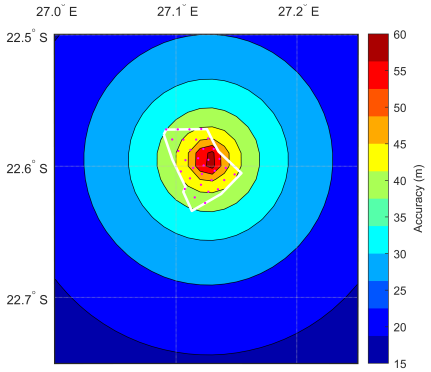


FIGURE C.5: FSPL Signal Strength: 1000 m gateway separation at SF10

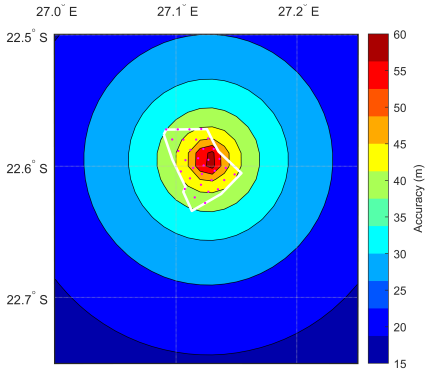


FIGURE C.6: FSPL Signal Strength: 1000 m gateway separation at SF8

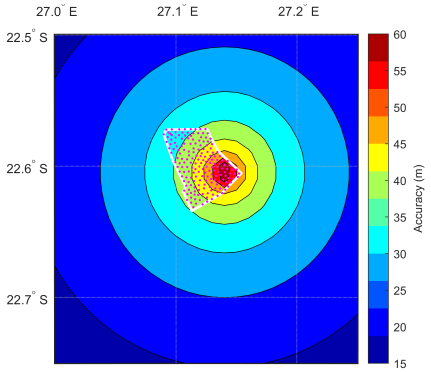


FIGURE C.7: FSPL Signal Strength: 400 m gateway separation at SF12

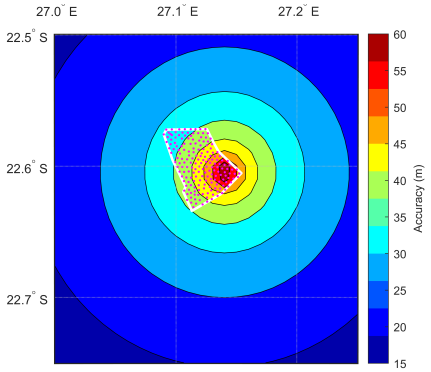


FIGURE C.8: FSPL Signal Strength: 400 m gateway separation at SF10

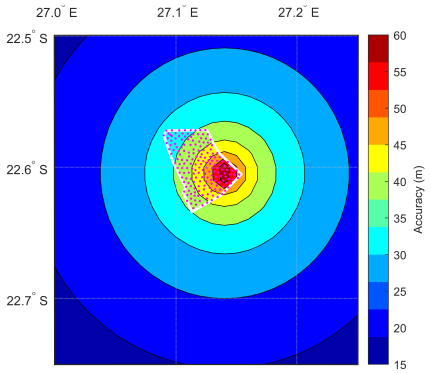


FIGURE C.9: FSPL Signal Strength: 400 m gateway separation at SF8

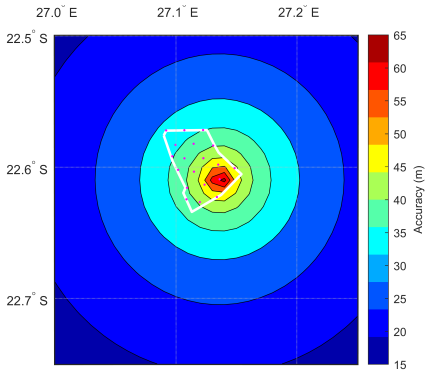


FIGURE C.10: COST 231 Signal Strength: 1500 m gateway separation at SF12

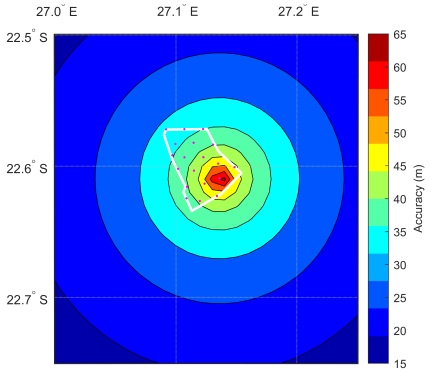


FIGURE C.11: COST 231 Signal Strength: 1500 m gateway separation at SF10

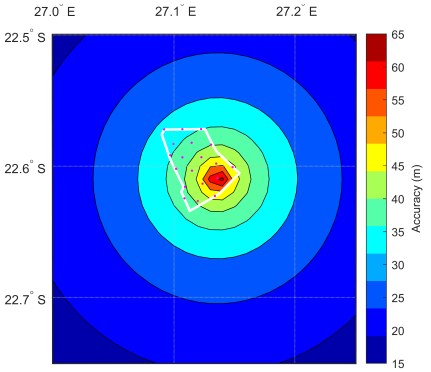


FIGURE C.12: COST 231 Signal Strength: 1500 m gateway separation at SF8

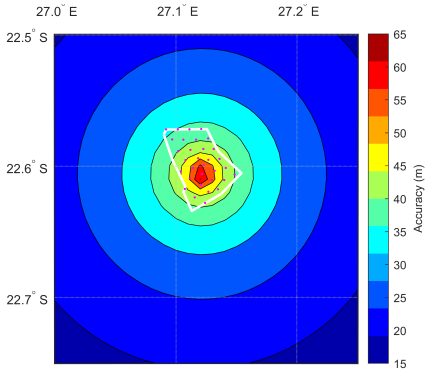


FIGURE C.13: COST 231 Signal Strength: 1000 m gateway separation at SF12

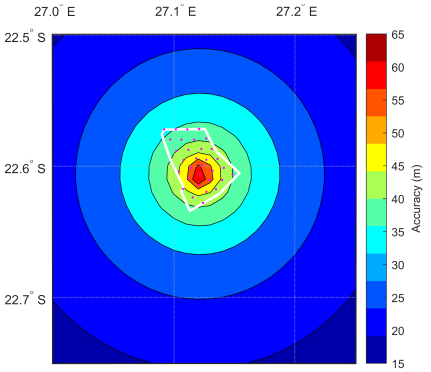


FIGURE C.14: COST 231 Signal Strength: 1000 m gateway separation at SF10

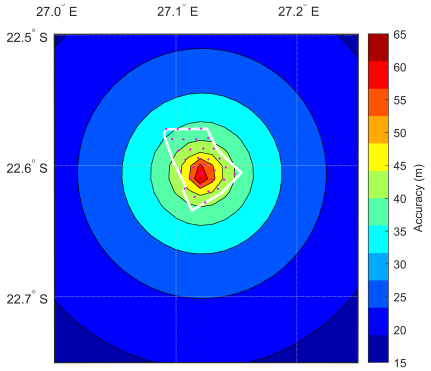


FIGURE C.15: COST 231 Signal Strength: 1000 m gateway separation at SF8

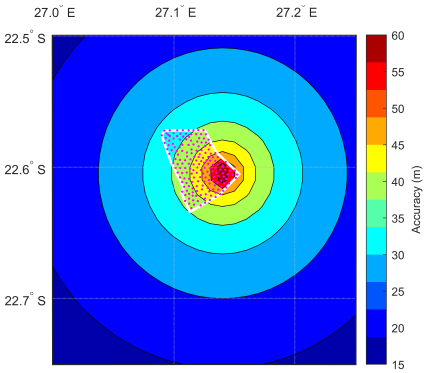


FIGURE C.16: COST231 Signal Strength: 400 m gateway separation at SF12

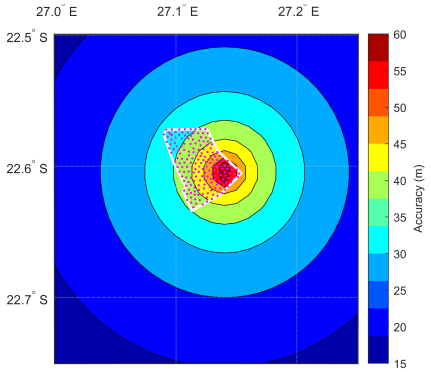


FIGURE C.17: COST 231 Signal Strength: 400 m gateway separation at SF10

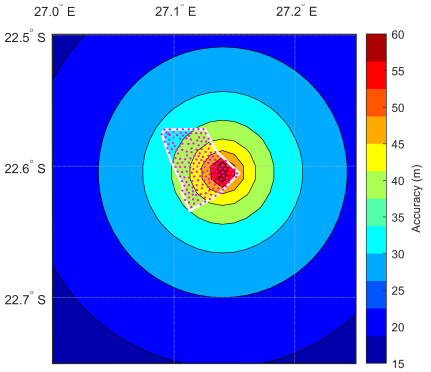


FIGURE C.18: COST 231 Signal Strength: 400 m gateway separation at SF8

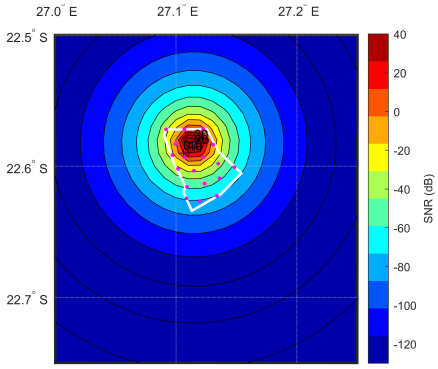


FIGURE C.19: ERICSSON 9999 Signal Strength: 1500 m gateway separation at SF12

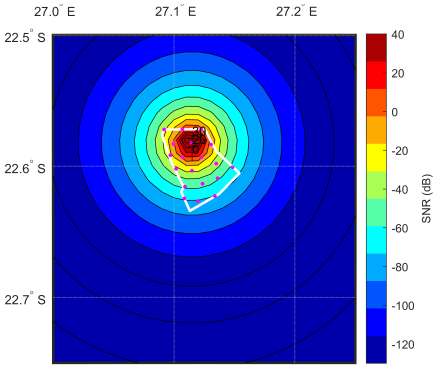


FIGURE C.20: ERICSSON 9999 Signal Strength: 1500 m gateway separation at SF10

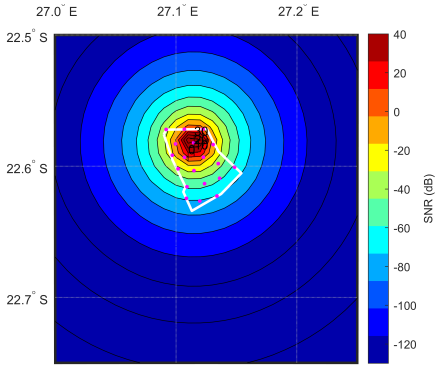


FIGURE C.21: ER-ICSSON 9999 Signal Strength: 1500 m gateway separation at SF8

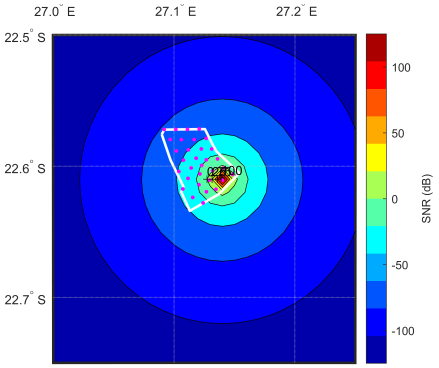


FIGURE C.22: ER-ICSSON 9999 Signal Strength: 1000 m gateway separation at SF12

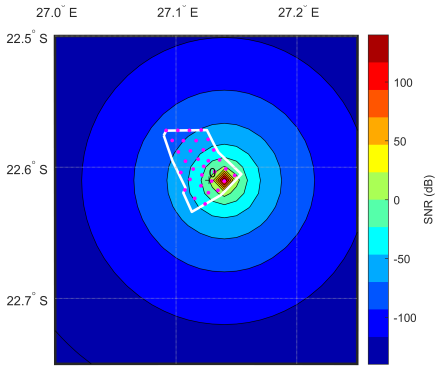


FIGURE C.23: ER-ICSSON 9999 Signal Strength: 1000 m gateway separation at SF10

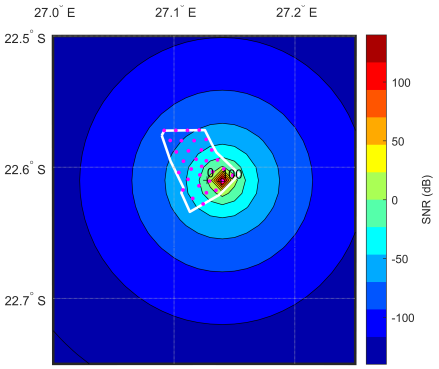


FIGURE C.24: ER-ICSSON 9999 Signal Strength: 1000 m gateway separation at SF8

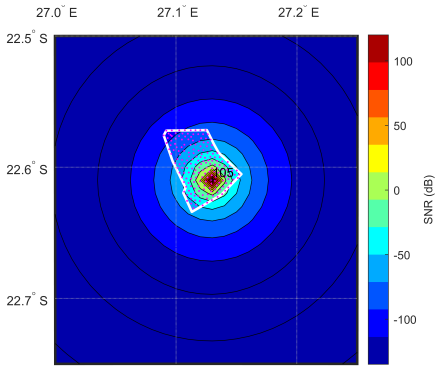


FIGURE C.25: ERICSSON 9999 Signal Strength: 400 m gateway separation at SF12

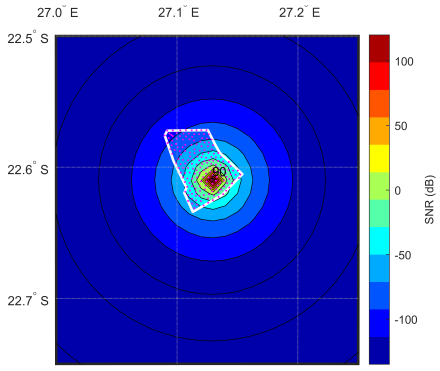


FIGURE C.26: ERICSSON 9999 Signal Strength: 400 m gateway separation at SF10

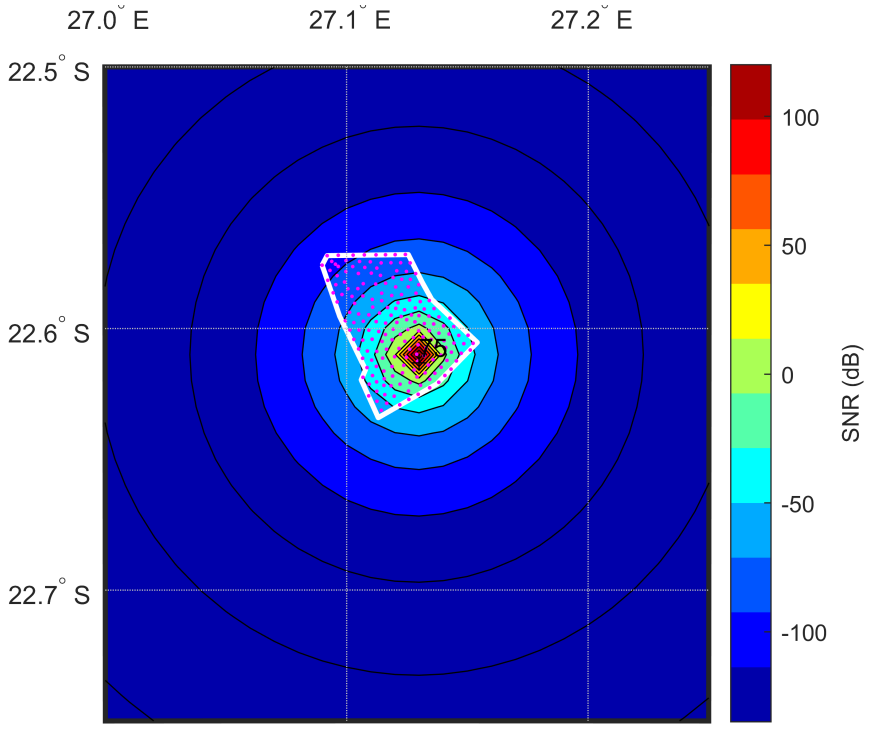


FIGURE C.27: ERICSSON 9999 Signal Strength: 400 m gateway separation at SF8

C.2 FSPL Repeatable Accuracy in the coverage area

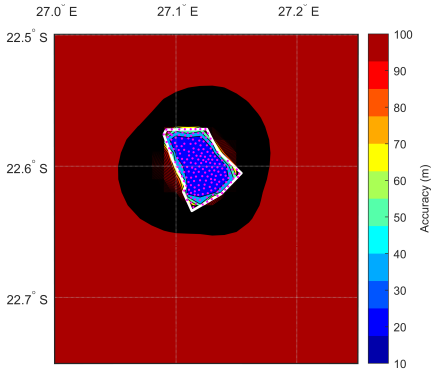


FIGURE C.28: FSPL Signal Strength: 400 m gateway separation at SF8 BW 125kHz

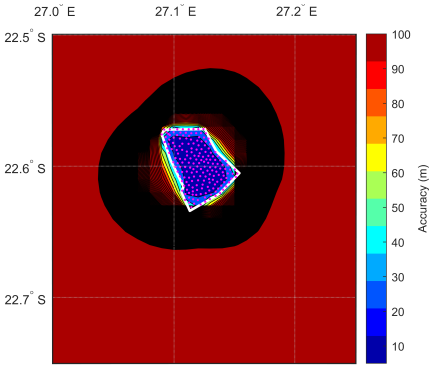


FIGURE C.29: FSPL Signal Strength: 400 m gateway separation at SF10 BW 125kHz

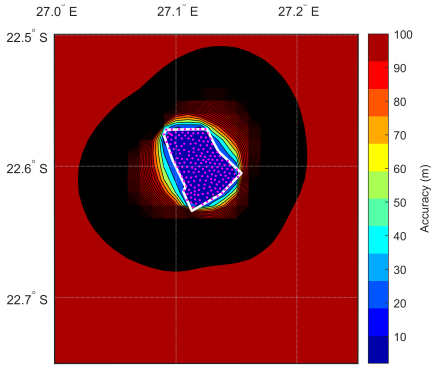


FIGURE C.30: FSPL Signal Strength: 400 m gateway separation at SF12 BW 125kHz

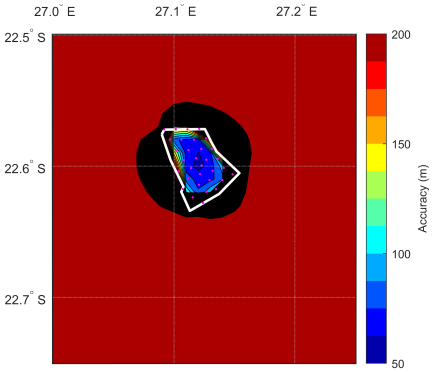


FIGURE C.31: FSPL repeatable accuracy: 1000 m gateway separation at SF8 BW 125kHz

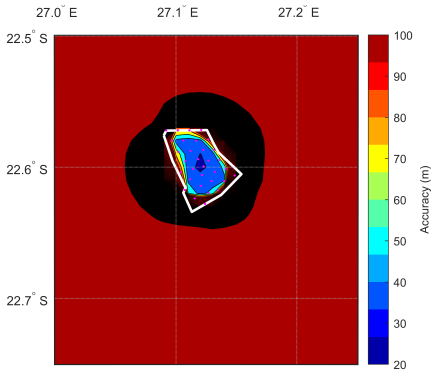


FIGURE C.32: FSPL repeatable accuracy: 1000 m gateway separation at SF10 BW 125kHz

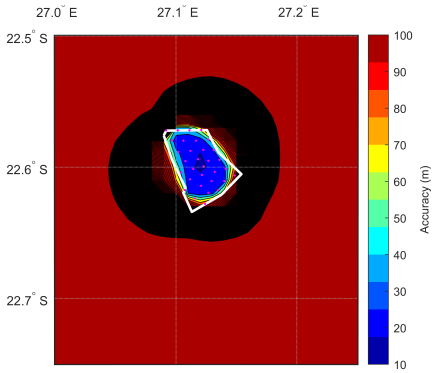


FIGURE C.33: FSPL repeatable accuracy: 1000 m gateway separation at SF12 BW 125kHz

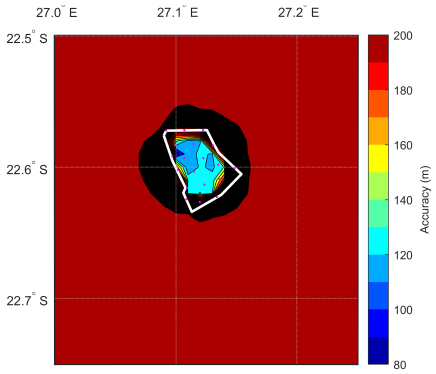


FIGURE C.34: FSPL repeatable accuracy: 1500 m gateway separation at SF8 BW 125kHz

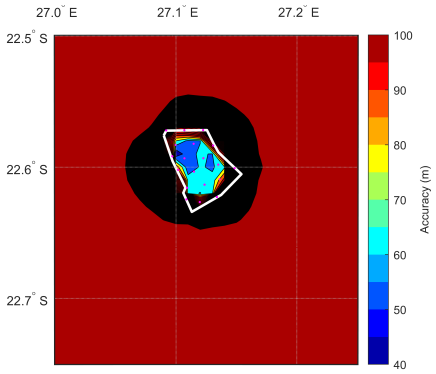


FIGURE C.35: FSPL repeatable accuracy: 1500 m gateway separation at SF10 BW 125kHz

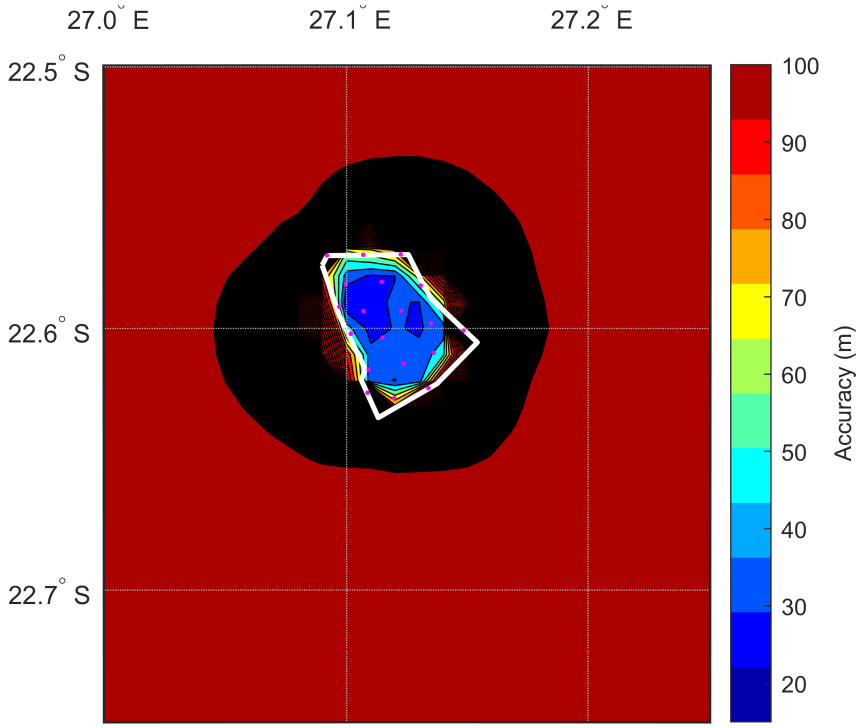


FIGURE C.36: FSPL repeatable accuracy: 1500 m gateway separation at SF12 BW 125kHz

C.3 COST 231 WI Repeatable Accuracy in the coverage area

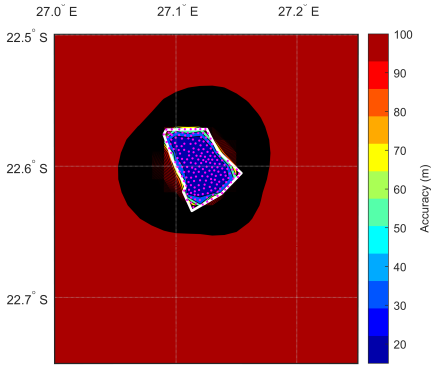


FIGURE C.37: COST 231 WI repeatable accuracy: 400 m gateway separation at SF10 BW 125kHz

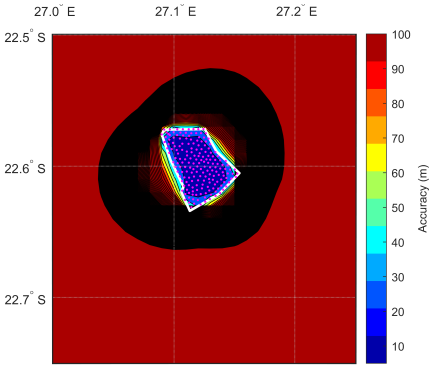


FIGURE C.38: COST 231 WI repeatable accuracy: 400 m gateway separation at SF12 BW 125kHz

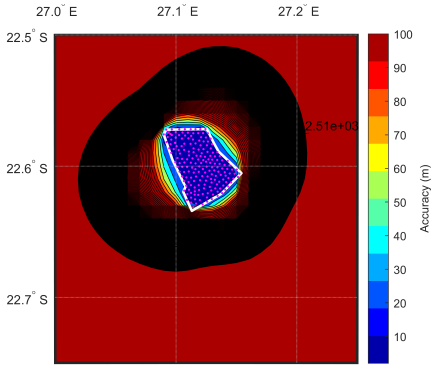


FIGURE C.39: COST 231 WI repeatable accuracy: 400 m gateway separation at SF12 BW 125kHz

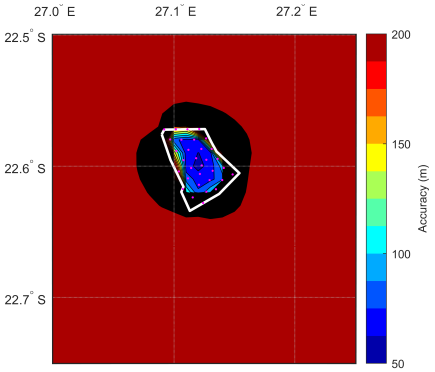


FIGURE C.40: COST 231 WI repeatable accuracy: 1000 m gateway separation at SF8 BW 125kHz

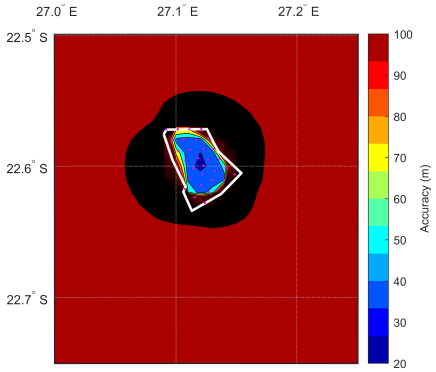


FIGURE C.41: COST 231 WI repeatable accuracy: 1000 m gateway separation at SF10 BW 125kHz

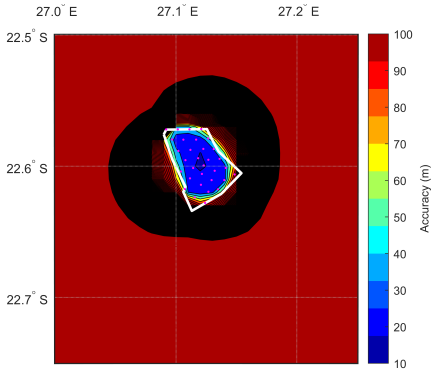


FIGURE C.42: COST 231 WI repeatable accuracy: 1000 m gateway separation at SF12 BW 125kHz

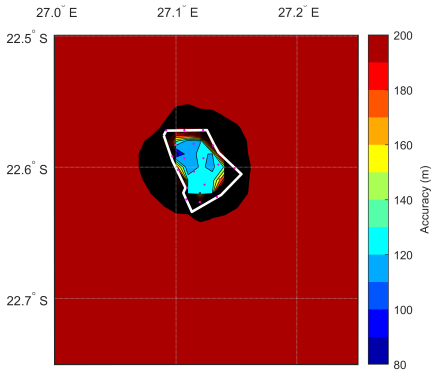


FIGURE C.43: COST 231 WI repeatable accuracy: 1500 m gateway separation at SF8 BW 125kHz

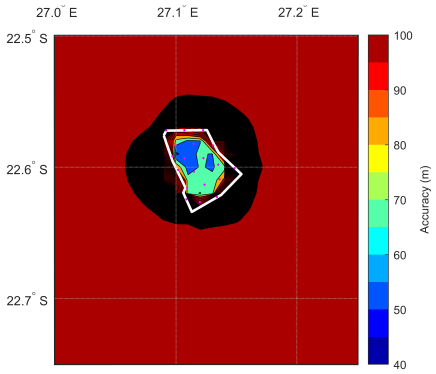


FIGURE C.44: COST 231 WI repeatable accuracy: 1500 m gateway separation at SF10 BW 125kHz

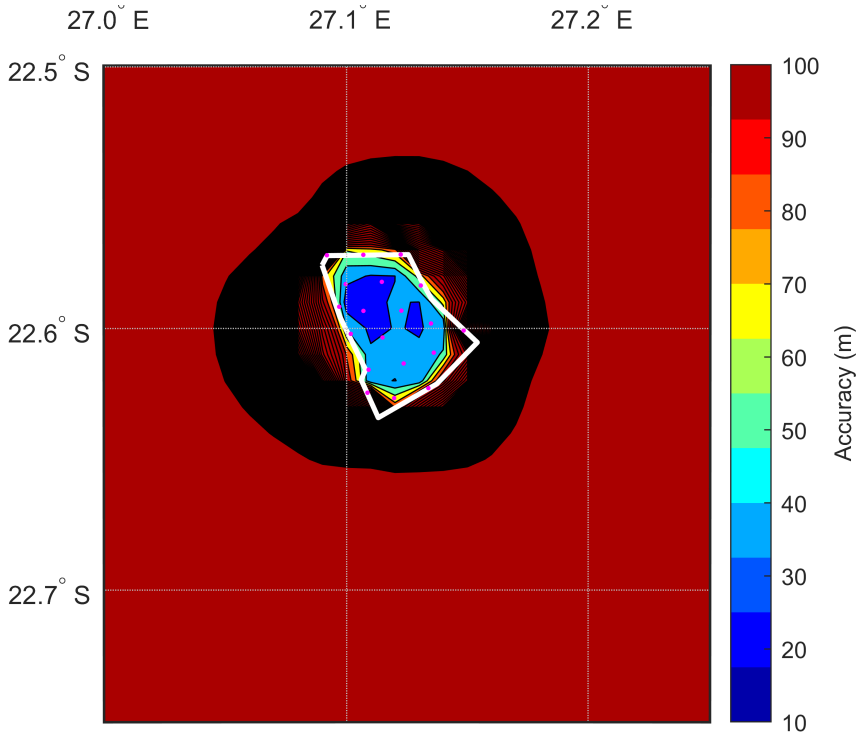


FIGURE C.45: COST 231 WI repeatable accuracy: 1500 m gateway separation at SF12 BW 125kHz

C.4 Ericsson 9999 Repeatable Accuracy in the coverage area

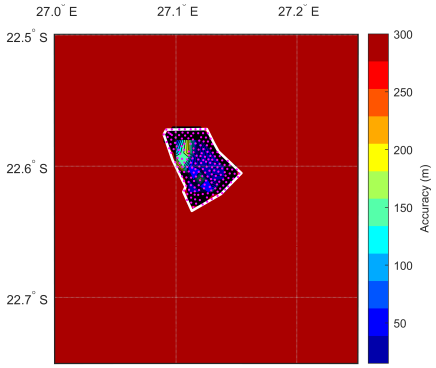


FIGURE C.46: Ericsson 9999 repeatable accuracy: 400 m gateway separation at SF8 BW 125kHz

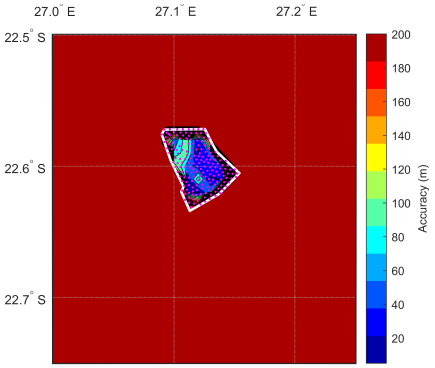


FIGURE C.47: Ericsson 9999 repeatable accuracy: 400 m gateway separation at SF10 BW 125kHz

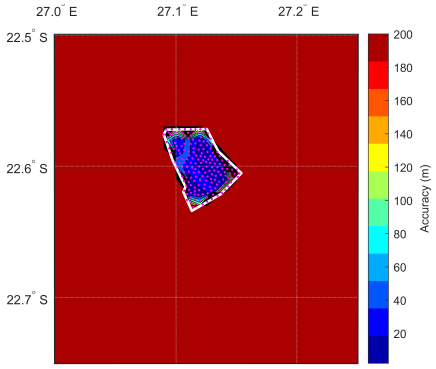


FIGURE C.48: Ericsson 9999 repeatable accuracy: 400 m gateway separation at SF12 BW 125kHz

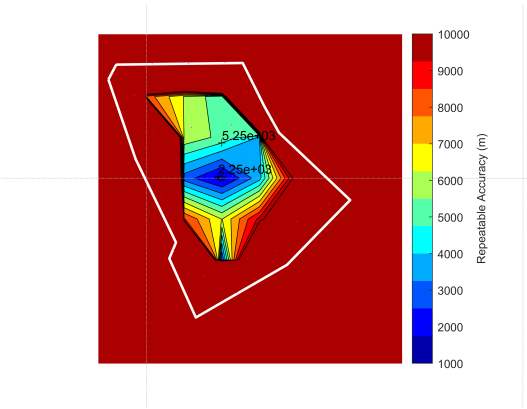


FIGURE C.49: Ericsson 9999 repeatable accuracy: 1000 m gateway separation at SF8 BW 125kHz

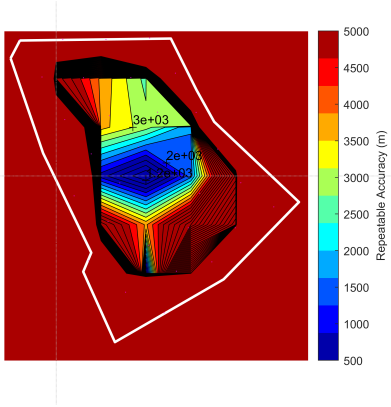


FIGURE C.50: Ericsson 9999 repeatable accuracy: 1000 m gateway separation at SF10 BW 125kHz

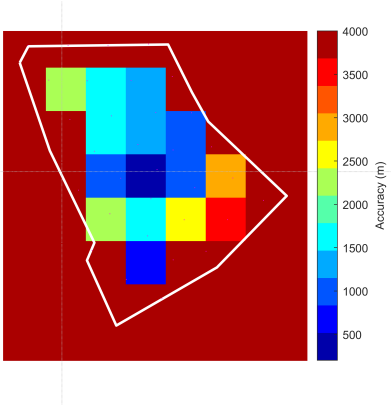


FIGURE C.51: Ericsson 9999 repeatable accuracy: 1000 m gateway separation at SF12 BW 125kHz

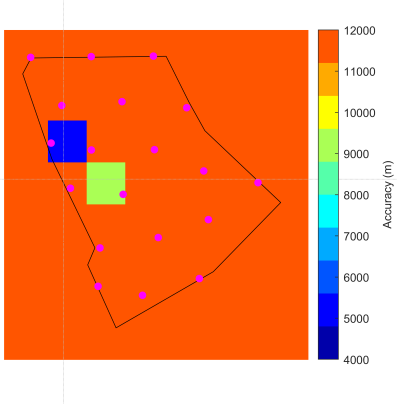


FIGURE C.52: Ericsson 9999 repeatable accuracy: 1500 m gateway separation at SF8 BW 125kHz

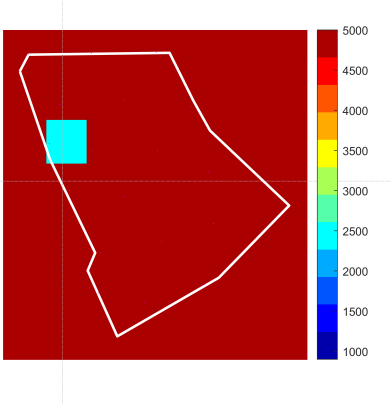


FIGURE C.53: Ericsson 9999 repeatable accuracy: 1500 m gateway separation at SF10 BW 125kHz

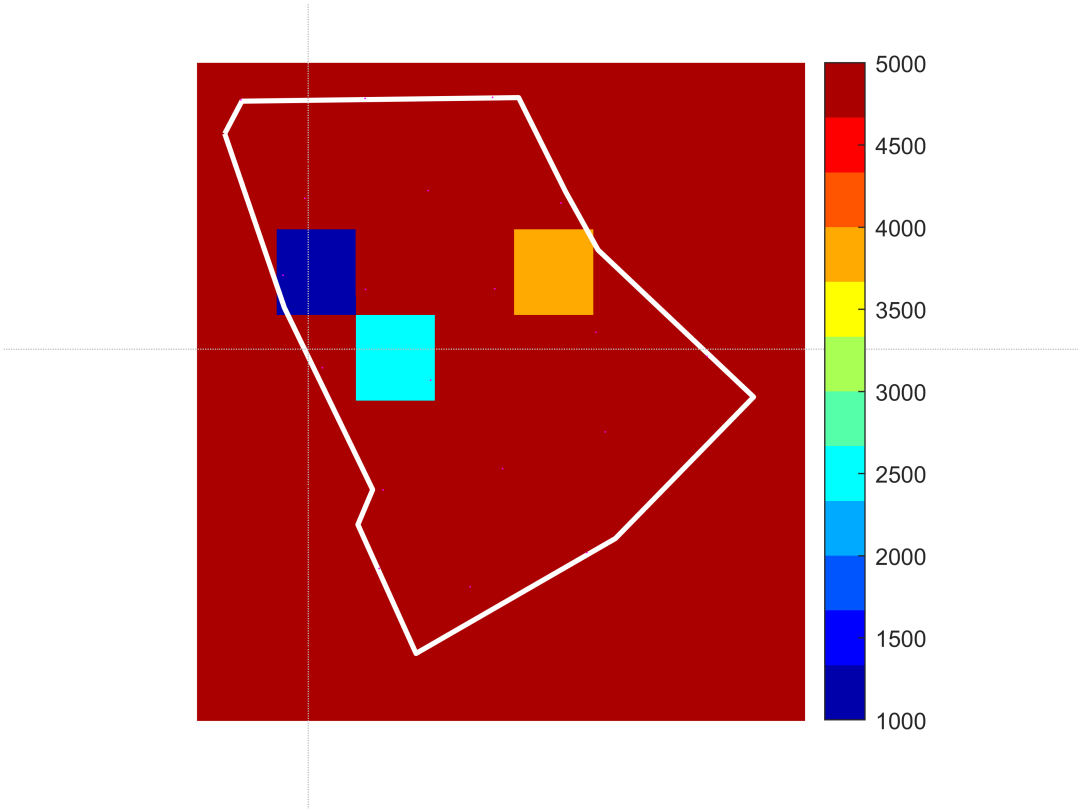


FIGURE C.54: Ericsson 9999 repeatable accuracy: 1500 m gateway separation at SF12 BW 125kHz

Bibliography

[1] "Prnet," Jan 2021. [Online]. Available: https://en.wikipedia.org/wiki/PRNET

[2] S. K. Sarkar, T. G. Basavaraju, and C. Puttamadappa, *Ad hoc mobile wireless networks: principles, protocols and applications*. Auerbach publications, 2007.

[3] M. Bor and U. Roedig, "LoRa transmission parameter selection," *Proceedings - 2017 13th International Conference on Distributed Computing in Sensor Systems, DCOSS 2017*, vol. 2018-Janua, pp. 27–34, 2018.

[4] L. Alliance, "LoRa Specification," p. 82, 2015.

[5] LoRaAlliance and LoRa Alliance, "LoRaWAN 1.1 Specification," *LoRa Alliance*, no. 1.1, p. 101, 2017. [Online]. Available: https://lora-alliance.org/resource-hub/lorawantm-specification-v11

[6] K. Mekki, E. Bajic, F. Chaxel, and F. Meyer, "A comparative study of lpwan technologies for large-scale iot deployment," *ICT express*, vol. 5, no. 1, pp. 1–7, 2019.

[7] T. Lassen, "Long-range RF communication: Why narrowband is the de facto standard," *WHITE Pap. Texas Instruments*, p. 8, 2014.

[8] P. P. Ray, "A survey on Internet of Things architectures," *J. King Saud Univ. - Comput. Inf. Sci.*, vol. 30, no. 3, pp. 291–319, 2018.

[9] LoRa Alliance Strategy Committee, "LoRaWAN Geolocation Whitepaper," no. January, p. 15, 2018. [Online]. Available: https://docs.wixstatic.com/ugd/eccc1a{_}d43b3b29dfff4ec2b00f349ced4225c4.pdf

[10] D. Tse and V. Pramod, "Fundamentals of wireless communication," *Fundamentals of Wireless Communication*, vol. 9780521845, pp. 1–564, 2005.

[11] A. Goldsmith, *Wireless communications*. Cambridge university press, 2005.

[12] R. S. Sinha, Y. Wei, and S. H. Hwang, "A survey on LPWA technology: LoRa and NB-IoT," *ICT Express*, vol. 3, no. 1, pp. 14–21, 2017.

[13] R. HICKEY, "IOT / M2M PLATFORMS LPWAN : Choice Overload and Confusion," pp. 2–5, 2018. [Online]. Available: https://www.lightreading.com/iot/m2m-platforms/lpwan-choice-overload-and-confusion/a/d-id/718233

[14] GSMA. (2016, Mar) Mobile iot low power wide area connectivity gsma industry paper. [Online]. Available: https://www.gsma.com/iot//wp-content/uploads/2016/03/Mobile-IoT-Low-Power-Wide-Area-Connectivity-GSMA-Industry-Paper.pdf

[15] K.-H. Ke, Q.-W. Liang, G.-J. Zeng, J.-H. Lin, and H.-C. Lee, "A lora wireless mesh networking module for campus-scale monitoring: demo abstract," in *Proceedings of the 16th ACM/IEEE International Conference on Information Processing in Sensor Networks*, 2017, pp. 259–260.

[16] N. Blenn and F. Kuipers, "Lorawan in the wild: Measurements from the things network," *arXiv preprint arXiv:1706.03086*, 2017.

[17] Semtech, "LoRa^{TM}Modulation Basics Semtech," Tech. Rep. May, 2015.

[18] O. Kennedy, E. Chukwu, O. Shobayo, E. Noma-Osaghae, I. Okokpujie, and M. Odusami, "Comparative analysis of the performance of various active queue management techniques to varying wireless network conditions," *International Journal of Electrical and Computer Engineering (IJECE)*, vol. 9, no. 1, p. 359, 2019.

[19] B. Sklar, *Digital Communications Fundamentals and Applications 2nd Edition*, 2nd ed. Prentice Hall, 2001, no. 1132.

[20] I. A. Hieder, "Compared to wireless deployment in areas with different environments," *International Journal of Electrical and Computer Engineering*, vol. 9, no. 2, pp. 934–940, 2019.

[21] Á. Milánkovich, K. Lendvai, S. Imre, S. Szabó, Á. Milánkovich, K. Lendvai, S. Imre, S. Szabó, and R. Propagation, "Radio Propagation Modeling on 433 MHz To cite this version : HAL Id : hal-01543157," *Springer*, pp. 384–395, 2017.

[22] A. Saltelli, M. Ratto, T. Andres, F. Campolongo, J. Cariboni, D. Gatelli, M. Saisana, and S. Tarantola, *Global sensitivity analysis: the primer*. John Wiley & Sons, 2008.

[23] H. Tong and H. Xu, "Horizontal dilution of precision analysis for Loran C/ Beidou integrated navigation system," *3rd International Symposium on Electronic Commerce and Security, ISECS 2010*, no. 2, pp. 167–170, 2010.

[24] M. Tahsin, S. Sultana, T. Reza, and M. Hossam-E-Haider, "Analysis of DOP and its preciseness in GNSS position estimation," *2nd International Conference on Electrical Engineering and Information and Communication Technology, iCEEiCT 2015*, no. May, pp. 21–23, 2015.

[25] R. B. Langley, "Dilution of Precision," *GPS World*, vol. 10, no. May, pp. 52–59, 1999.

[26] C. J. Hegarty, *Understanding GPS / GNSS*, 3rd ed., 2017.

[27] C. K. Lebekwe, A. Yahya, and I. Astin, "An Improved Accuracy Model Employing an e-Navigation System," *2018 9th IEEE Annual Ubiquitous Computing, Electronics and Mobile Communication Conference, UEMCON 2018*, pp. 152–158, 2018.

[28] J. Fischer, M. Grossmann, W. Felber, M. Landmann, and A. Heuberger, "A measurement-based path loss model for wireless links in mobile ad-hoc networks (MANET) operating in the VHF and UHF band," *Proceedings of the 2012 IEEE-APS Topical Conference on Antennas and Propagation in Wireless Communications, APWC'12*, pp. 349–352, 2012.

[29] D. Tse and V. Pramod, "Fundamentals of wireless communication," *Fundamentals of Wireless Communication*, vol. 9780521845, pp. 1–564, 2005.

[30] D. Ming, "M . Sc . Thesis Investigation on Time-of-Arrival Estimation for the LoRa Network," 2019.

[31] L. Vangelista, "Frequency Shift Chirp Modulation: The LoRa Modulation," *IEEE Signal Processing Letters*, vol. 24, no. 12, pp. 1818–1821, 2017.

[32] M. Bor and U. Roedig, "LoRa transmission parameter selection," *Proc. - 2017 13th Int. Conf. Distrib. Comput. Sens. Syst. DCOSS 2017*, vol. 5, pp. 27–34.

[33] LoRa Alliance Technical Committee, "LoRaWAN 1.1 Specification," LoRa Alliance, Inc., Beaverton, Tech. Rep. 2010, 2017.

[34] R. Lie, "LoRa/LoRaWAN tutorial 17: LoRa Packet Format, Time on Air and Adaptive Data Rate," 2018. [Online]. Available: https://www.mobilefish.com/developer/lorawan/lorawan{_}quickguide{_}tutorial.html

[35] L. Kolobe, B. Sigweni, and C. K. Lebekwe, "Systematic literature survey: Applications of LoRa communication," *International Journal of Electrical and Computer Engineering*, vol. 10, no. 3, pp. 3176–3183, 2020.

[36] Bensky Alan, *Wireless positioning technologies and applications*, 2nd ed. Artech House, 2016.

[37] N. Podevijn, D. Plets, J. Trogh, L. Martens, P. Suanet, K. Hendrikse, and W. Joseph, "TDoA-Based Outdoor Positioning with Tracking Algorithm in a Public LoRa Network," *Wireless Communications and Mobile Computing*, vol. 2018, 2018.

[38] C. Gu, L. Jiang, and R. Tan, "LoRa-based localization: Opportunities and challenges," *arXiv*, 2018.

[39] B. C. Fargas and M. N. Petersen, "GPS-free geolocation using LoRa in low-power WANs," *GIoTS 2017 - Global Internet of Things Summit, Proceedings*, 2017.

[40] C. Phillips, D. Sicker, and D. Grunwald, "A Survey of Wireless Path Loss Prediction and Coverage Mapping Methods," *IEEE Communications Surveys & Tutorials*, vol. 15, no. 1, pp. 255–270, 2013.

[41] B. C. R. A. (BOCRA), "Annex F-Botswana National Frequency Allotment Plan," vol. 91, pp. 399–404, 2016.

[42] O. O. Erunkulu, A. M. Zungeru, C. K. Lebekwe, and J. M. Chuma, "Cellular Communications Coverage Prediction Techniques: A Survey and Comparison," *IEEE Access*, vol. 8, pp. 113 052–113 077, 2020.

[43] J. M. Marais, R. Malekian, and A. M. Abu-Mahfouz, "LoRa and LoRaWAN testbeds: A review," *2017 IEEE AFRICON: Science, Technology and Innovation for Africa, AFRICON 2017*, pp. 1496–1501, 2017.

[44] A. Rghioui and A. Oumnad, "Internet of things: Surveys for measuring human activities from everywhere," *International Journal of Electrical and Computer Engineering*, vol. 7, no. 5, pp. 2474–2482, 2017.

[45] F. Adelantado, X. Vilajosana, P. Tuset-Peiro, B. Martinez, J. Melia-Segui, and T. Watteyne, "Understanding the Limits of LoRaWAN," *IEEE Communications Magazine*, vol. 55, no. 9, pp. 34–40, 2017.

[46] M. C. Bor, J. Vidler, and U. Roedig, "LoRa for the Internet of Things," *Proceedings of the 2016 International Conference on Embedded Wireless Systems and Networks*, pp. 361–366, 2016.

[47] W. San-Um, P. Lekbunyasin, M. Kodyoo, W. Wongsuwan, J. Makfak, and J. Kerdsri, "A long-range low-power wireless sensor network based on U-LoRa technology for tactical troops tracking systems," in *Proceedings - ACDT 2017: 3rd Asian Conference on Defence Technology: Advance Research Collaboration on Defence Technology*, 2017, pp. 32–35.

[48] A. I. Akram H. Jebril , Aduwati Sali and M. F. A. Rasid, "Overcoming Limitations of LoRa Physical Layer in image transmission," *MDPI, Sensors*, vol. 18, no. 3257, pp. 1–22, 2018.

[49] O. Galinina, S. Andreev, S. Balandin, and Y. Koucheryavy, "Measuring a Lora Network: Performance, Possibilities and Limitations," *Springer Nature (Switzerland)*, no. September, pp. 116–128, 2018.

[50] J. Petäjäjärvi, K. Mikhaylov, A. Roivainen, T. Hänninen, and M. Pettissalo, "On the coverage of LPWANs: Range evaluation and channel attenuation model for LoRa technology," *2015 14th Int. Conf. ITS Telecommun. ITST 2015*, pp. 55–59, 2016.

[51] J. M. Marais, R. Malekian, and A. M. Abu-Mahfouz, "LoRa and LoRaWAN testbeds: A review," *2017 IEEE AFRICON: Science, Technology and Innovation for Africa, AFRICON 2017*, pp. 1496–1501, 2017.

[52] M. H. Habaebi, I. J. Chowdhury, M. R. Islam, and N. A. B. Zainal, "Effects of shadowing on LoRa LPWAN radio links," *International Journal of Electrical and Computer Engineering*, vol. 7, no. 6, pp. 2970–2976, 2017.

[53] A. J. Wixted, P. Kinnaird, H. Larijani, A. Tait, A. Ahmadinia, and N. Strachan, "Evaluation of LoRa and LoRaWAN for wireless sensor networks," *Proc. IEEE Sensors*, vol. 0, pp. 5–7, 2017.

[54] A. Carlsson, I. Kuzminykh, R. Franksson, and A. Liljegren, "Measuring a LoRa Network: Performance, Possibilities and Limitations," in *Springer Nature (Switzerland)*. Springer International Publishing, 2018, no. September, pp. E1–E1.

[55] R. Sanchez-Iborra, J. Sanchez-Gomez, J. Ballesta-Viñas, M. D. Cano, and A. F. Skarmeta, "Performance evaluation of lora considering scenario conditions," *Sensors (Switzerland)*, vol. 18, no. 3, 2018.

[56] B. Sigweni and M. Shepperd, "Using blind analysis for software engineering experiments," *ACM International Conference Proceeding Series*, vol. 27-29-Apri, 2015.

[57] M. N. Ochoa, A. Guizar, M. Maman, and A. Duda, "Toward a Self-Deployment of LoRa Networks: Link and Topology Adaptation," *International Conference on Wireless and Mobile Computing, Networking and Communications*, vol. 2019-Octob, 2019.

[58] F. Cuomo, M. Campo, E. Bassetti, L. Cartella, F. Sole, and G. Bianchi, "Adaptive mitigation of the air-time pressure in lora multi-gateway architectures," *24th European Wireless 2018 "Wireless Futures in the Era of Network Programmability", EW 2018*, pp. 56–61, 2018.

[59] M. N. Ochoa, L. Suraty, M. Maman, and A. Duda, "Large Scale LoRa Networks: From Homogeneous to Heterogeneous Deployments," *International Conference on Wireless and Mobile Computing, Networking and Communications*, vol. 2018-Octob, pp. 192–199, 2018.

[60] B. Ousat and M. Ghaderi, "LoRa network planning: Gateway placement and device configuration," *Proceedings - 2019 IEEE International Congress on Internet of Things, ICIOT 2019 - Part of the 2019 IEEE World Congress on Services*, pp. 25–32, 2019.

[61] N. Vatcharatiansakul, P. Tuwanut, and C. Pornavalai, "Experimental performance evaluation of LoRaWAN: A case study in Bangkok," in *Proceedings of the 2017 14th International Joint Conference on Computer Science and Software Engineering, JCSSE 2017*, 2017, pp. 7–10.

[62] M. Younis and K. Akkaya, "Strategies and techniques for node placement in wireless sensor networks: A survey," *Ad Hoc Networks*, vol. 6, no. 4, pp. 621–655, 2008.

[63] M. Aigner and G. M. Ziegler, *Proofs from THE BOOK Sixth Edition*, 2018.

[64] R. Bevans, "Statistical tests: which one should you use?" 2020. [Online]. Available: https://www.scribbr.com/statistics/statistical-tests/

[65] B. Sigweni and M. Shepperd, "Using blind analysis for software engineering experiments," in *Proceedings of the 19th International Conference on Evaluation and Assessment in Software Engineering*, 2015, pp. 1–6.

[66] W. Lenhard and A. Lenhard, "Calculation of effect sizes. bibergau, germany: Psychometrica," 2015.

[67] M. Shepperd and S. MacDonell, "Evaluating prediction systems in software project estimation," *Information and Software Technology*, vol. 54, no. 8, pp. 820–827, 2012.

[68] K. Mikhaylov and J. Petäjäjärvi, "Analysis of Capacity and Scalability of the LoRa Low Power Wide Area Network Technology," *Univ. Oulu, Cent. Wirel. Commun. Finl.*, pp. 119–124, 2016.

[69] Q. Itu-r and W. Gaussian, "REPORT ITU-R P.2089 The analysis of radio noise data," *In Practice*, pp. 1–6, 2006.

[70] P. S. Gregory Johnson, "Feasibility Study of R-Mode combining MF DGNSS , AIS , and eLoran Transmissions," pp. 1–48, 2014.

[71] W. W. LaMorte, "Nonparametric tests," 2017. [Online]. Available: https://sphweb.bumc.bu.edu/otlt/mph-modules/bs/bs704_nonparametric/bs704_nonparametric4.html

[72] J. Zeltzer. (2017, feb) Hypothesis testing. [Online]. Available: http://www.zstatistics.com/about